Na Duong (northern Vietnam)-an exceptional window into Eocene ecosystems from Southeast Asia

Madelaine Böhme, Manuela Aiglstorfer, Pierre-Olivier Antoine, Erwin Appel, Philipe Havlik, Grégoire Métais, Laq The Phuc, Simon Schneider, Fabian Setzer, Ralf Tappert, et al.

Bayerische Staatssammlung für Paläontologie und Geologie

- Zitteliana A 53, 120 – 167
- München, 31.12.2013
- Manuscript received 17.12.2013; revision accepted 19.01.2014
- ISSN 1612 - 412X

Na Duong (northern Vietnam) – an exceptional window into Eocene ecosystems from Southeast Asia

Madelaine Böhme[1, 2*], Manuela Aiglstorfer[1, 2], Pierre-Olivier Antoine[3], Erwin Appel[1], Philipe Havlik[1, 2], Grégoire Métais[4], Laq The Phuc[5], Simon Schneider[6], Fabian Setzer[1], Ralf Tappert[7], Dang Ngoc Tran[8], Dieter Uhl[2, 9] & Jérôme Prieto[1,10]

[1]Department of Geoscience, Eberhard Karls University, Sigwartstr. 10, D-72076, Tübingen, Germany
[2]Senckenberg Centre for Human Evolution and Palaeoenvironment (HEP), Sigwartstr. 10, D-Tübingen, Germany
[3]Institut des Sciences de l'Évolution, UMR-CNRS 5554, CC064, Université Montpellier 2, Place Eugène Bataillon, F-34095 Montpellier, France
[4]CR2P, Paléobiodiversité et Paléoenvironnements, UMR 7207 (CNRS, MNHN, UPMC), 8 rue Buffon, CP 38, F-75231 Paris Cedex 05, France
[5]Geological Museum, 6 Pham Ngu Lao Str., Hanoi, Vietnam
[6]CASP, University of Cambridge, West Building, 181A Huntingdon Road, Cambridge CB3 0DH, UK
[7]Institut für Mineralogie und Petrographie, Universität Innsbruck, Innrain 52f, A-6020, Innsbruck, Austria
[8]Department of Geology and Minerals of Vietnam (DGMV), 6 Pham Ngu Lao Str., Hanoi, Vietnam
[9]Senckenberg Forschungsinstitut, Senckenberganlage 25, D-60325 Frankfurt am Main, Germany
[10]Bayerische Staatssammlung für Paläontologie und Geologie, Richard-Wagner-Str. 10, D-80333 Munich, Germany

**Author for correspondence and reprint requests: E-mail:* m.boehme@ifg.uni-tuebingen.de

Abstract

Today, the continental ecosystems of Southeast Asia represent a global biodiversity hotspot. From a deep-time perspective, however, very little is known about the formation of this hotspot. In particular, the evolutionary and biogeographic roots of numerous terrestrial biota are unknown, and ecosystemic information, especially for the Paleogene, is unavailable. The Na Duong Basin in northern Vietnam has yielded a remarkable diversity of Paleogene vertebrate, invertebrate, and plant fossils, and is thus one of the few localities in Southeast Asia allowing for multi-focused investigation of this period. We present stratigraphic, paleontologic, and paleoecologic results from the 220 m thick Na Duong section derived from magnetostratigraphy, biochronology, vertebrate, invertebrate, and plant taxonomy, and biomarker analysis. Only the upper 40 m of the section show the original magnetization, prohibiting any further magnetostratigraphic interpretation. The affinities of two newly described mammal species, *Bakalovia orientalis* nov. sp. (Anthracotheriidae) and *Epiaceratherium naduongense* nov. sp. (Rhinocerotidae), suggest an Eocene, late Bartonian to Priabonian age (39–35 Ma). High biodiversity is recorded for unionid mussels (five species), freshwater fishes (nine taxa, including *Planktophaga minuta* nov. gen. et sp.), turtles (five to six taxa), and crocodiles (three taxa), and long-term stability of Southeast Asian unionid and fish faunas is demonstrated. Fossil leaves, wood and resin document azonal and zonal vegetation; dipterocarp trees were identified from resin exudate spectroscopy. In-situ tree-stump horizons allow for calculation of tree density (600 specimens/ha) and maximum canopy height (35m); both values resemble those of recent Southeast Asian peat swamp forests. Environment changed abruptly from a swamp forest to a tropical to warm sub-tropical lake of fluctuating water depth. The strong biogeographic link between the Eocene mammal faunas from Na Duong and Europe highlights the importance of Southeast Asia as a source region for trans-continental mammal dispersal along the northern Tethys margin.

Key words: Eocene, Southeast Asia, mammals, transcontinental migration, ecosystems, crocodiles, fishes, mollusks, Dipterocarpaceae, biogeography

Zusammenfassung

Heutige kontinentale Ökosysteme Südost Asiens sind ein Hotspot der globalen Biodiversität, über dessen geohistorische Entstehung jedoch sehr wenig bekannt ist. So sind die evolutionären und biogeographischen Wurzeln der meisten terrestrischen Lebensformen unbekannt und Daten zu Ökosystemen, speziell aus dem Paläogen, fehlen. Das Becken von Na Duong im nördlichen Vietnam beherbergt bemerkenswert diverse Biota fossiler Pflanzen, Mollusken und Wirbeltiere und stellt für das Paläogen eine der wenigen Regionen Südost Asiens dar, welche einen multi-disziplinären Untersuchungsansatz erlauben. Auf der Grundlage von Paläomagnetik, Biochronologie, Wirbeltier-, Mollusken- und Pflanzen-Taxonomie, sowie der Analyse von Biomarkern präsentieren wir hier unsere stratigraphischen, palä-

ontologischen und paläo-ökologischen Ergebnisse eines 220 m mächtigen Profils der Braunkohlengrube Na Duong. Nur die hangenden 40 m der Sektion zeigen die ursprüngliche Magnetisierung, wodurch eine magnetostratigraphische Interpretation verhindert wird. Die Verwandschaftsverhältnisse von zwei neu beschriebenen Säugetierarten, *Bakalovia orientalis* nov. sp. (Anthracotheriidae) und *Epiaceratherium naduongense* nov. sp. (Rhinocerotidae), verweisen auf ein eozänes Alter (oberes Bartonium bis Priabonium, 39-35 Ma). Starke biogeographische Bezüge beider Säugetiere aus Na Duong zu europäischen Arten unterstreichen die Bedeutung Südost Asiens als eine Quellregion paläogener transkontinentaler Säugetier Ausbreitungen entlang des nördlichen Randes der Tethys. Hohe Diversitäten werden für unionide Muscheln (fünf Arten), Süßwasserfische (9 Taxa, darunter *Planktophaga minuta* nov. gen. et sp.), Schildkröten (fünf bis sechs Taxa) und Krokodile (drei Taxa) belegt, wobei eine taxonomische Langzeit-Stabilität der Unioniden- und Fisch-Faunen Südost Asiens belegt wird. Fossile Blätter, Hölzer und Harze dokumentieren die azonale und zonale Vegetation, letztere repräsentiert durch spektroskopisch an Harzen belegte Zweiflügelfrucht-Gewächse (Dipterocarpaceae). In-situ Baumstubben-Horizonte erlauben die Berechnung der Baum-Dichte (600 per ha) und der maximalen Kronendach-Höhe (35 m), welches in guter Übereinstimmung zu heutigen südostasiatischen Sumpfwäldern steht. Die Umwelt veränderte sich abrupt von einem Sumpfwald zu einem tropisch bis warm-subtropischen See mit fluktuierender Wassertiefe.

Schlüsselwörter: Eozän, Südost Asien, Säugetiere, transkontinentale Migration, Ökosysteme, Krokodile, Fische, Mollusken, Dipterocarpaceae, Biogeographie

1. Introduction

During the Paleogene, the Asian continent experienced a dramatic tectonic and geographic reorganization that was triggered by the collision of India and Asia and the resulting uplift of the Tibetan Plateau (Hall 2002; Wang et al. 2008; Clark 2011). This continental-scale reconfiguration significantly contributed to changes in global climate (Ramstein et al. 1997; Harris 2006; Kent & Muttoni 2008; Meng et al. 2012) and had a sustained impact on Asian biodiversity (Bossuyt & Milinkovitch 2001; Raxworthy et al. 2002; Dutta et al. 2011). The dramatic environmental changes likely affected ecosystems throughout most of Asia, but so far this has been difficult to document, due primarily to a lack of knowledge of Paleogene ecosystems especially from the southern part of Asia.

At global scale, the late Paleogene interval, and in particular the Eocene–Oligocene transition, is marked by a deep reorganisation of terrestrial ecosystems related to climatic and biogeographic factors (e.g., Prothero 1994). Across the Holarctic region (Europe, North America, and Asia), different patterns of faunal turnover are documented. In Europe, the major faunal turnover, termed the 'Grande Coupure' by Stehlin (1909), severely affected vertebrate faunas between the biochrones MP20 and MP21 (e.g., BiochroM'97 1997). The 'Grande Coupure' implies the sudden extinction of European endemic taxa, correlating with the first appearance of Arctic (Heissig 2003) and Asian immigrants. The latter probably entered Europe via land bridges between the Western European Island and the Asian mainland that were created by Alpine tectonics in Southeast Europe (Heissig 1979). In North America, faunal changes among vertebrates show a contrasting, transitional pattern with a significant turnover at the Middle Eocene–Late Eocene transition (Prothero & Heaton 1996). Although Asia is a vast landmass, the Late Eocene and the Eocene–Oligocene transition are documented only in a few areas. One of these regions is the Mongolian Plateau, where the successive mammalian faunas document a turnover intermediate in scale between those observed in Europe and North America (Meng & McKenna 1998). In southern and Southeast Asia, however, the Eocene–Oligocene transition is only recorded in comparably short mammal-bearing sections, which provide a series of "snapshots" on either side of the stage boundary rather than a continuous faunal succession. Consequently, it remains difficult to assess how severely faunas and ecosystems in this region were affected by changing environments. Moreover, age calibration is crucial to understand the pattern of biotic changes, but the ages of the few late Paleogene faunas from Southeast Asia (e.g., Naduo and Gongkang Formations in the Bose Basin, Wang et al. 2007) remain controversial. Besides documentation of changes at regional scale, the late Paleogene faunas and ecosystems from Southeast Asia are highly significant for large-scale paleobiogeographic reconstructions. Several Eocene localities in southeast Europe have yielded mammal species of Southeast Asian affinities, indicating that this area may have been an important source region of Asian immigrants, which replaced most of the European Eocene endemics after the 'Grande Coupure' (Heissig 1979; Baciu & Hartenberger 2001).

The Na Duong Basin in northern Vietnam (~20 km SE of Lang Son, the capital of Lang Son Province, Fig. 1) is one of the very few sections in South Asia allowing for integrated investigation of the Eocene–Oligocene interval. Since it represents a hitherto unstudied territory, it offers the opportunity to reveal a wide array of primary data. Preliminary research has shown that the late Paleogene Na Duong Basin yields a high diversity of exceptionally well-preserved fossils in such different groups as mollusks, fishes, and reptiles (Böhme et al. 2011; Schneider et al. 2013).

The 45 km^2 large Na Duong Basin (for geological maps, see Wysocka 2009; Böhme et al. 2011), situated near the boundary between the Indochina and Southern China microplates, is part of the Cao Bang-

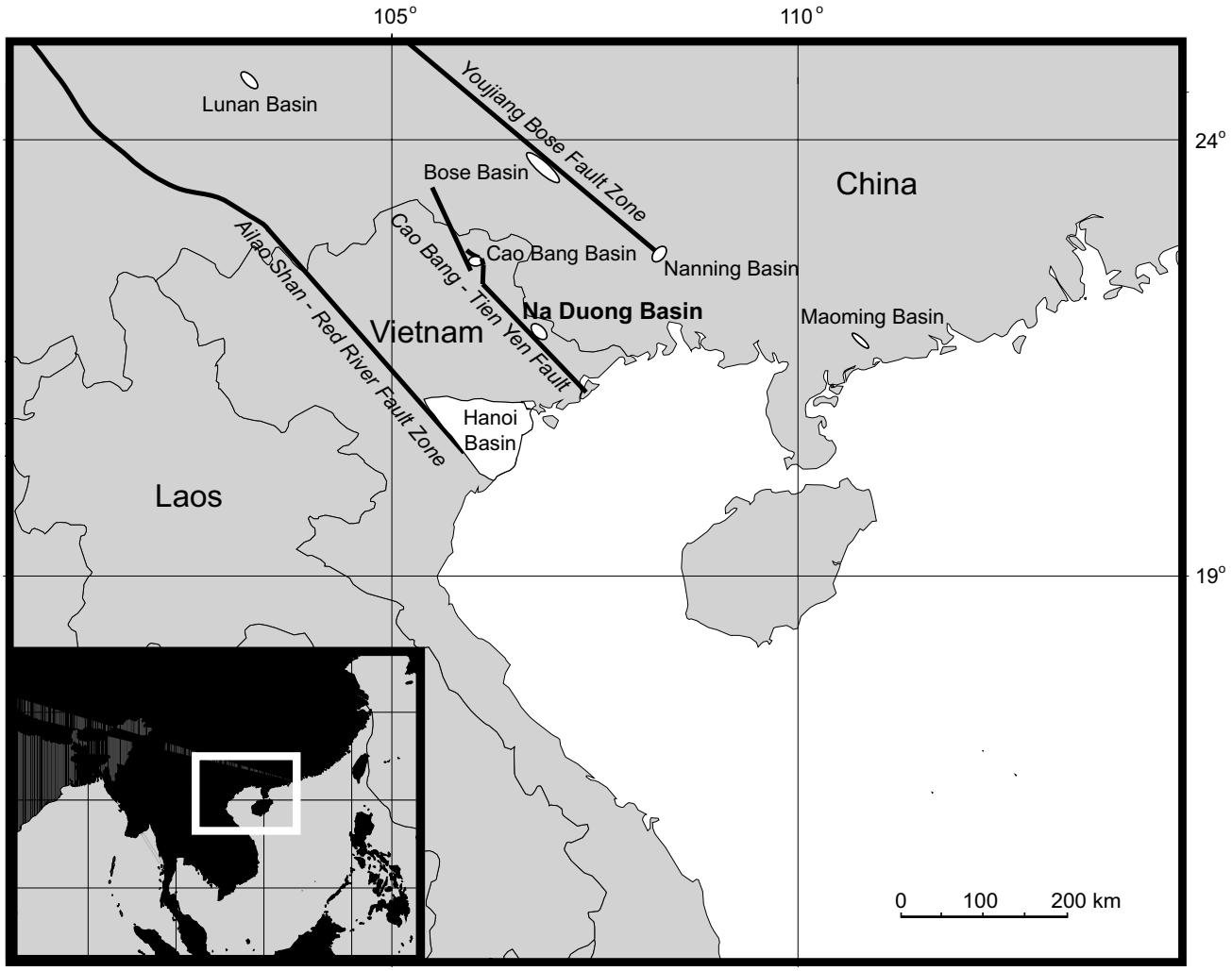

Figure 1: Map of northern Southeast Asia. Major fault systems and major Paleogene on-shore basins in northern Vietnam and southeastern China are indicated (after Pubellier et al. 2003; Wysocka 2009; Böhme et al. 2011).

Tien Yen fault system (CBTY; Pubellier et al. 2003), paralleling the Ailao Shan-Red River Fault Zone, which is situated at 160 km distance to the South (Fig. 1). Similar to numerous other pull-apart basins on the southern Chinese microplate, the Na Duong Basin formed during the Paleogene resulting from strike-slip motion along the CBTY fault (Pubellier et al. 2003; Böhme et al. 2011). Drill cores revealed a more than 570 m thick sedimentary succession infilling the basin (Wysocka 2009), which is subdivided into the lower, coal-bearing Na Duong Formation and the overlying Rhin Chua Formation (Thuy 2001). Large parts of both formations are perfectly exposed in the large, active, opencast coalmine of Na Duong (N 21°42.2', E 106°58.6').

We present results of a detailed study of paleontology, paleomagnetics, and biomarkers, which provides insight into (1) the stratigraphy of the basin; (2) the taxonomic and ecologic paleodiversity of plants, mollusks, fishes, reptiles, and mammals; (3) the paleoclimate and ecosystem surrounding these biota; and (4) the paleobiogeographic affinities of the fauna, with a particular focus on large mammals.

2. Material and Methods

2.1 Field work and collection references

Permissions for fieldwork conducted in cooperation with the Geological Museum at Hanoi were granted by the Department of Geology and Minerals of Vietnam (DGMV). The vertebrate fossils collected at Na Duong are temporarily stored in the paleontological collections of the University of Tübingen (Germany). Specimen numbers are provided in the text. The following collection acronyms are used: GPIT – Paläontologische Sammlung der Universität Tübingen, Germany; IVPP – Institute for Vertebrate Paleontology Beijing, China.

2.2 Paleomagnetic sampling and measurements

In total, 247 oriented samples were taken in roughly equidistant intervals of ca. 1 m along two partly overlapping profiles (see Fig. 2). In some parts,

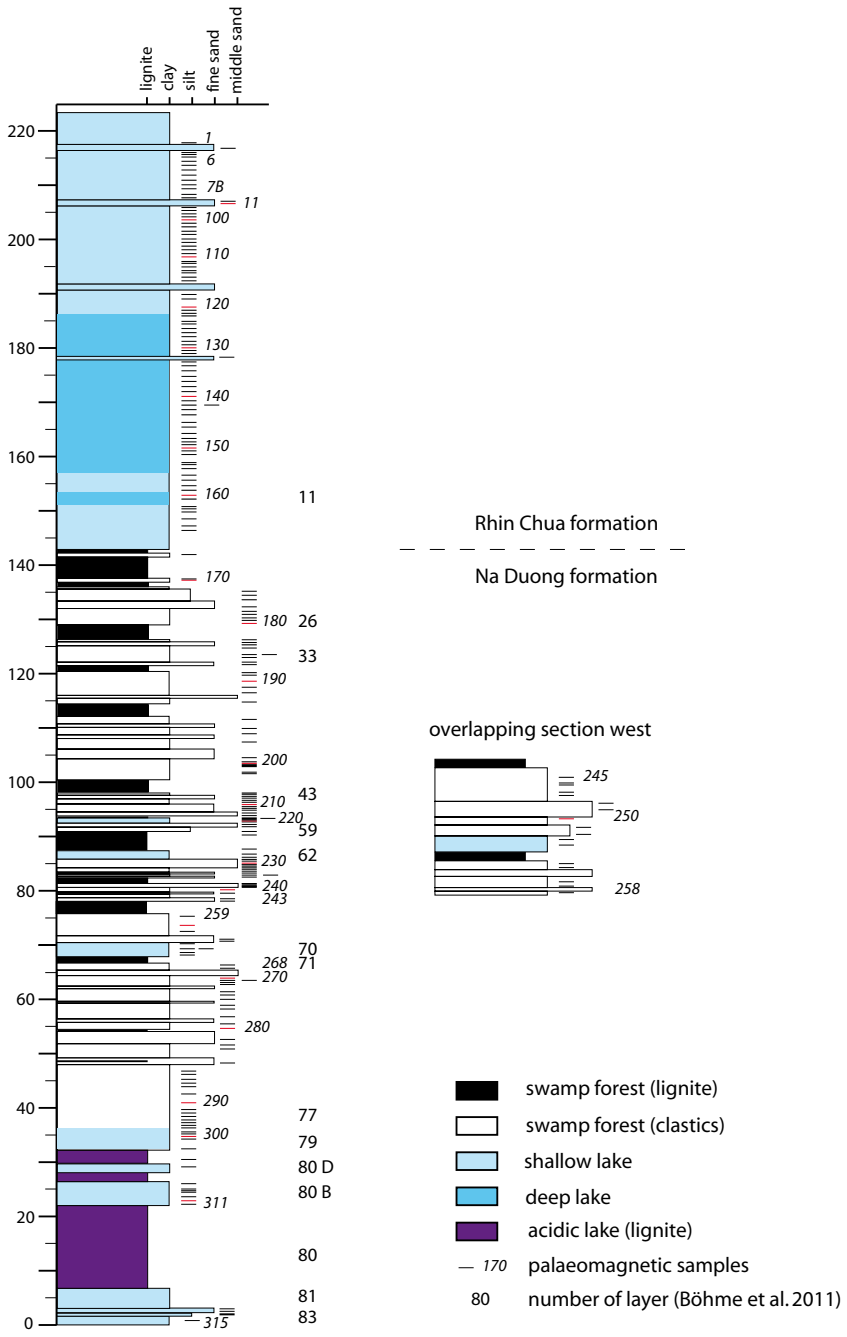

Figure 2: Sedimentological log of the Na Duong coal mine and palaeoenvironmental interpretation**.** The short parallel section was taken 2 km to the west of the main site. The stratigraphic positions paleomagnetic samples are indicated by their respective (italic) numbers (numbering of layers according to Böhme et al. 2011: fig. 3). Abbreviations: cl – claystone, silt – siltstone, fs – fine-grained sandtone, ms – medium-grained sandstone.

where the lithology was particularly disturbed, or in case of inaccessibility (steep walls), the sampling interval size was slightly adjusted. Furthermore, coal layers within the Na Duong formation were excluded from sampling. Depending on the lithology, cores were either drilled using a portable rockdrill (sandstones) or cut out and fixed in cylindrical plastic boxes (claystones). The samples were oriented with a magnetic compass.

Remanent magnetization was measured with a 2G Enterprises He-free u-channel SQUID magnetometer (model 760R) with a theoretical noise level of less than 10^{-7} A/m for a 10 cm³ sample. Alternating field demagnetization (AfD) was performed in steps of 2–20 mT, using an automatic sample degaussing device (model 2G 600) integrated in the magnetometer system. The maximum applied peak field was 100 mT.

2.3 Collection of micro-vertebrates

For collection of micro-vertebrates, in particular fish teeth, claystones were dissolved in diluted hydrogen peroxide and residues were wet-sieved, using a 300 µm mesh-size sieve.

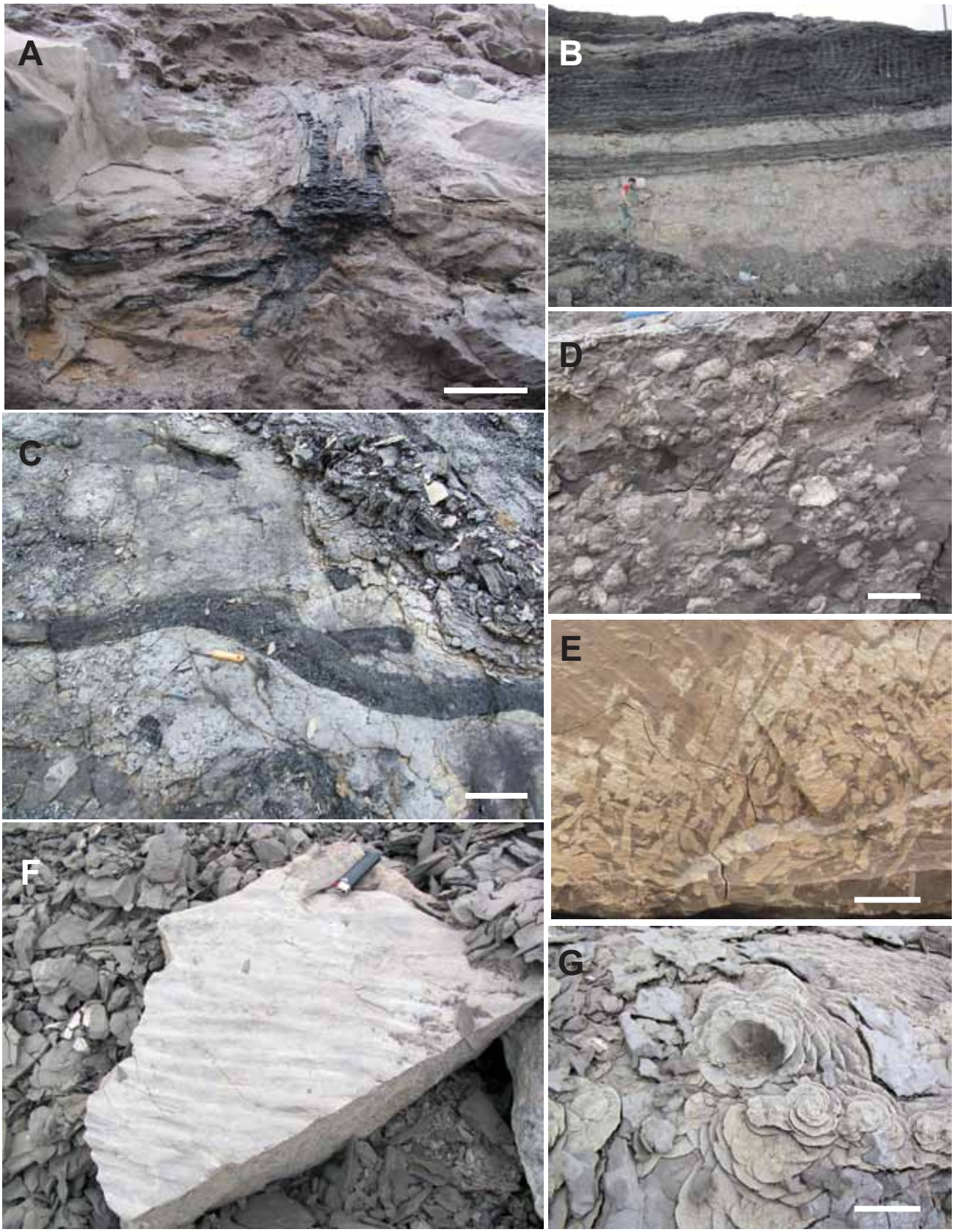

Figure 3: Images of sedimentary structures and fossils from the Na Duong coal mine; **(A)** in-situ tree-stump at 100 m (layer 43), Na Duong Fm. (scale 35 cm); **(B)** lignite seams and claystones, top of Na Duong Fm. (132–142 m, person as scale); **(C)** lignified tree trunk from the main vertebrate-bearing horizon (layer 80, scale 15 cm); **(D)** coquina of unionids and viviparids, lower part of Rhin Chua Fm. (~150 m); **(E)** traces of bioturbation in claystone at 156 m, Rhin Chua Fm. **(F)** fine-grained sandstone with ripple-marks, top of Rhin Chua Fm. (191 m); **(G)** cone-in-cone structures on the surface of a calcite concretion, Rhin Chua Fm. (178 m).

2.4 Anthracotheriid dental terminology

Anthracotheriid dental nomenclature follows Lihoreau & Ducrocq (2007). Measurements are given in millimeters. Upper cheek teeth are indicated by upper case letters (D, P, M), and lower cheek teeth by lower case letters (d, p, m), respectively.

2.5 Phylogenetic analysis of Bothriodontinae

Morphological data were compiled from the studied specimens and from the literature. We retained the 51 characters suggested in Lihoreau & Ducrocq (2007), but reduced the original ingroup taxa to 18 species by keeping a single representative of the Anthracotheriinae (*Anthracotherium magnum*) and a single representative of the Microbunodontinae (*Anthracokeryx ulnifer*). Likewise, we only kept the type species of each genus within the Bothriodontinae, with the exception of *Elomeryx* and *Brachyodus* (Appendix 2). The data matrix includes cranial and dental characters (Appendix 1) that are unordered and weighted equally. Characters not known for a taxon were coded as missing.

The matrix of characters was assembled in Mesquite 2.75 (Maddison & Maddison 2010). All multistate characters were treated as unordered. The morphology dataset was analyzed using collapsing rule 1 in TNT version 1.1 (Goloboff et al. 2000, 2008). Searching was performed with traditional search including 1000 RAS+TBR. The phylogenetic trees with morphological character state optimizations have been generated using Winclada v.1.00 (Nixon 1999–2002).

2.6 Rhinocerotid dental terminology

Rhinocerotid dental terminology follows Heissig (1969), Uhlig (1999), and Antoine (2002). Suprageneric systematics within Rhinocerotidae follows Antoine et al. (2010) and Becker et al. (2013). The dataset allowing for morphological comparison of the Na Duong rhino with other rhinocerotoids is derived from Antoine (2002), Antoine (2003), Antoine et al (2003a, 2010), and Becker et al. (2013). Upper and lower teeth are identified by upper case (I, C, P, M, and DP) and lower case letters (i, c, p, m, and d), respectively. Dimensions are given in mm.

2.7 Resin spectroscopy

To gain information about the chemical structure and botanical source of the fossil resins from the Na Duong mine, thin (<5 µm thickness), inclusion-free fragments of the resins were analyzed using micro-Fourier transform infrared (FTIR) spectroscopy. The samples were analyzed between 4000–650 cm^{-1} in transmittance mode using the analytical protocol described in Tappert et al. (2011).

3. Results

3.1 The Na Duong section

The sedimentary succession of the Na Duong coalmine was described by Böhme et al. (2011), referring to the outcrop situation documented in 2009. Due to progress in mining, additional strata have been exposed until 2012, which are described here in summary. Throughout the profile, the sediment layers generally dip gently to the north. Due to subordinate faulting and sliding of unconsolidated sediment, bedding is variable along the profile, ranging from almost horizontal layering to a dip of 29°. Dip direction varies between NW and NE.

Based on evidence from drill-cores, the Na Duong Formation is 240 m thick (Wysocka 2009), and the upper 140 m of the succession are exposed in the Na Duong opencast coalmine. The sediments are characterized by an alternation of lignite seams and brownish to greyish marly claystones, siltstones, and fine-grained sandstones, and occasional medium-grained sandstones (Figs 2, 3B). The lignite can be characterized as subbituminous coal to coaly shale (Wysocka 2009). The coaly shales of the main coal seam (layer 80 in Fig. 2) are laminated and particularly enriched in iron sulfide, mainly pyrite (Böhme et al. 2011: fig. 4C). In the lower part, the seam occasionally contains coalified tree trunks (Fig. 3C). Toward the top of the main seam, petrified driftwood occurs in high abundance (Böhme et al. 2011: fig. 4B), usually associated with yellowish, silty to sandy claystone interbeds of limited lateral extent (layers 80B, 80D), which preserve a rich fossil leaf flora. At the base of the main seam, within the transition zone from the underlying dark-brown claystone to the coaly shale, abundant vertebrate fossils are preserved.

Fresh, unaltered, fine-grained siliciclastic sediments of the Na Duong Formation contain a conspicuous amount of carbonate. Weathered sediments lack carbonate, but do not change in colour with regard to unaltered condition, in contrast to sediments of the overlying Rhin Chua Formation. In the upper part of the Na Duong Formation several horizons preserve laterally continuous fossil forests, comprised of in-situ tree stumps (between 100 and 101 m; layer 43, Fig. 3A and between 130 and 132 m; layer 26; three individual horizons in succession).

The contact between the Na Duong Formation and the up to 300 m thick Rhin Chua Formation is conformable (contrary to Wysocka 2009), and the northward progressing mining gradually exposes larger parts of the Rhin Chua Formation (80 m in 2012). The sediments of the Rhin Chua Formation consist predominantly of marly claystones. Thin beds of fine-grained sandstone with symmetric ripple marks occur in the upper part of the section (Fig. 3F). Weathering turns the brownish colour of the fresh claystones into reddish to purple colours, indicating the secondary formation of haematite. Weathered out-

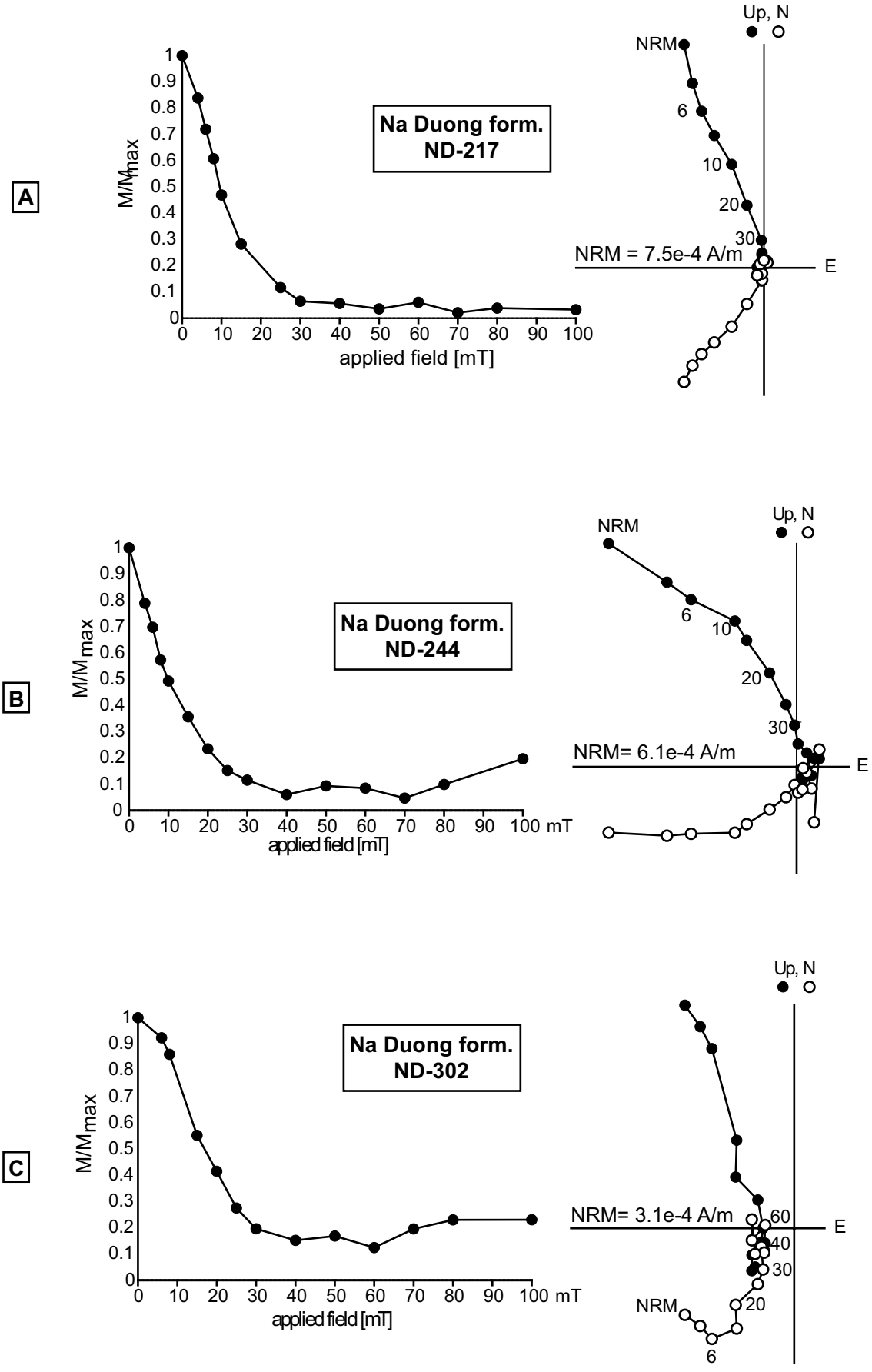

Figure 4: Zijderveld diagrams and intensity decay curves for representative samples from the Na Duong Formation. The applied field strength is given in millitesla (mT). Solid points represent the horizontal projection of the magnetization, whereas open points represent the vertical vector component. Abbreviations: NRM – natural remanent magnetization, A/m – ampere meter, ND – Na Duong sample number,

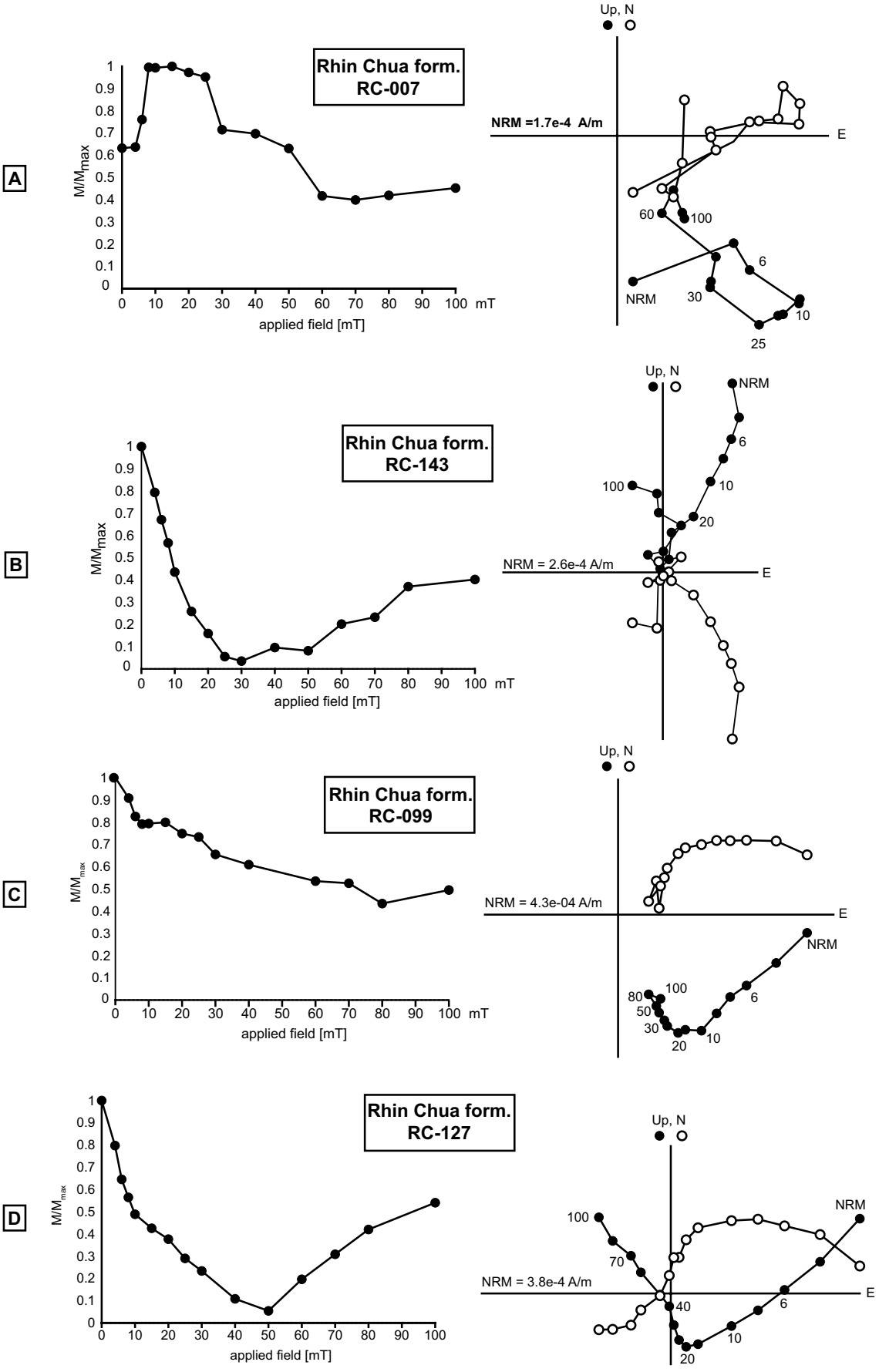

Figure 5: Zijderveld diagrams and intensity decay curves for representative samples from the Rhin Chua Formation. The applied field strength is given in millitesla (mT). Solid points represent the horizontal projection of the magnetization, whereas open points represent the vertical vector component. For abbreviations see Fig. 4.

crops show a cyclic occurrence of more solid horizons at intervals of ~ 0.5 m. Frequently, the claystones are bioturbated, in particular near the base and top of the succession (Fig. 3E). These bioturbated parts of the profile contain abundant fossil remains of benthic (mollusk shells) and nektonic fauna (cyprinid fish teeth). The upper 45 m of the section contain secondary calcite precipitations, either in the form of large stratiform concretions (1 m wide, 0.4 m high) or as precipitates along joints. The stratiform concretions exhibit cone-in-cone structures at their outside (Fig. 3G), which are of diagenetic origin (Usdowski 1963), but were recently misinterpreted as stromatolithes (Geptner et al. 2013). In the same part of the section (starting at 178 m) mollusks are preserved as moulds, indicating diagenetic dissolution of their shells.

3.2 Paleomagnetic analysis

The natural remanent magnetization (NRM) for samples from both the Na Duong and Rhin Chua formations is commonly in the range of 10^{-4} to 10^{-3} A/m. Intensity decay curves and Zijderveld plots reveal a stable demagnetization behavior for almost all samples from the Na Duong Formation (Fig. 4), whereas a few samples from the Rhin Chua Formation, particularly from the upper part of the sequence, show a tendency towards unstable behavior (Fig. 5A). In most samples from both units, a low-coercitive component (LC-C) and high-coercitive component (HC-C) could be separated by alternating field demagnetization using principal component analysis (Kirschvink 1980). The LC-C from the Na Duong Formation shows a very strong scattering and hence cannot be interpreted in a geologic context.

In samples from the Na Duong Formation, the magnetization has typically dropped below 20% of the initial value (NRM) at fields of around 30 mT indicating that magnetite is likely the main remanence carrier in these samples (Fig. 4). The demagnetization behavior of samples from the Rhin Chua Formation is more heterogeneous with several samples being almost completely demagnetized (<10% of NRM) at relatively moderate fields of 20–30 mT (Fig. 5B), whereas others reach this value only at much higher fields or do not fully demagnetize at all (Fig. 5C). In addition, many samples from the Rhin Chua Formation show an increase in magnetization at fields above 50–60 mT (Fig. 5D), which can be related to a laboratory induced gyromagnetic remanence (GRM) and therefore points to the presence of greigite (Hu et al. 1998). With regard to the existence of greigite, remanence directions derived from samples of the Rhin Chua Formation have to be considered with caution.

Furthermore, it was found that samples with high concentrations of greigite are unevenly distributed along the sequence and particularly occur in the Rhin Chua Formation in the intervals of sample numbers 140–155 and 123–129 (see Fig. 2). The intermediate interval from number 130 to 139 likewise contains a significant amount of greigite – albeit in lower concentration. In samples with numbers <123, greigite is generally significantly less abundant. With the exception of samples 160 and 161, which show an exceptionally high concentration in greigite, the same applies for the interval from number 155 to 170. The vast majority of samples with numbers >170, derived from the Na Duong Formation, virtually contain no greigite. For a few isolated samples, however, a small but distinct greigite fraction is indicated (sample numbers 315, 300, 254 and 221).

For all samples an individual tilt correction was applied based on the bedding attitudes determined in the field. For the Na Duong Formation, incremental unfolding gives an optimal degree of grouping for 30 % unfolding, indicating a post-tectonic remanence character (Fig. 6). The direction correction tilt test of Enkin (2003), however, is indeterminate; therefore no reliable assertions about the timing of remanence acquisition with regard to tectonics can be made. For the Rhin Chua Formation, no tilt test was performed, as the differences in the bedding directions within the Rhin Chua Formation are negligible compared to the strong scattering of the remanence directions.

The magnetostratigraphy and averaging of mean directions are discussed separately for the Na Duong and Rhin Chua formations. This is done, since (1) the magnetic mineralogy of both units differs, and, more importantly, since (2) the facies, and therefore the corresponding sediment accumulation rates may be different. Certainly, this has significant implications for the time scales involved.

With the exception of the uppermost sample of the profile, HC-C directions from the Na Duong Formation only indicate normal polarities (Fig. 7). Naturally, this outcome is unfortunate for a magnetostratigraphic investigation, as it makes a correlation with the geomagnetic polarity timescale (GPTS) very difficult. Dating based on the magnetic results is therefore impossible.

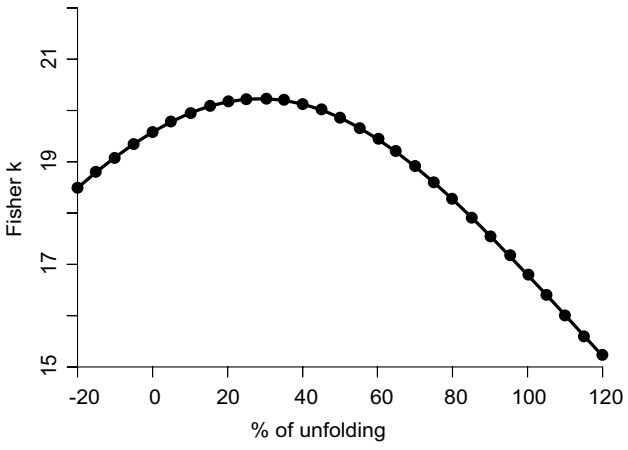

Figure 6: Results of stepwise unfolding of the HC-C from the Na Duong formation. The maximal degree of grouping is reached at 30% unfolding. The ration between k_{max}/k_{min} amounts to roughly 1.3.

Three possible explanations of the observed normal polarity throughout the Na Duong Formation can be brought forward: (1) The sedimentation rate was exceptionally high during deposition of the Na Duong Formation; (2) The time span of the Na Duong Formation coincides with a very long normal polarity interval; (3) The isolated remanence directions represent a secondary remagnetization. Of course, a combination of several of the aforementioned factors is also possible.

The first hypothesis is supported by field observations revealing vertically orientated fossil leaves and in-situ tree trunks in several horizons, which indicate rapid sediment deposition in these layers. The second hypothesis would for instance be supported by the rather long normal intervals C18n.1n (38.668–39.686 Ma) and C18n.2n (39.756–40.201 Ma) in the Bartonian, with only a short reverse interval in between (Gradstein et al. 2012). The resulting minimum values for the average sediment accumulation rates (SAR) of the 145 m thick Na Duong Formation would be 12.9 cm/kyr and 29.1 cm/kyr, respectively. If the very short intermediary reverse interval C18n.1r (39.686–39.756 Ma) was overprinted by remagnetization, the lowest possible SAR would be 8.5 cm/kyr. Although sediment accumulation rates of several tens of cm/kyr are reported for lacustrine environments (e.g., Zhang et al. 2012), it is yet questionable whether this is a realistic scenario for small scaled basins such as the one at Na Duong. In addition, the implied SAR would be much higher if, which is likely, the sampled profile would not exactly coincide with the start and end of one of the aforementioned long normal intervals.

In order to evaluate the likeliness of a secondary origin of the HC-C, the mean directions in both coordinate systems, in-situ (Dec=354.1°, Inc=28.2°, α-95=3.9°, k=11.9) and after bedding correction (Dec=355.1°, Inc=7.7°, α-95=4.0°, k=11.8) were compared with the present day magnetic field at the sampling site (Fig. 7A) and the expected direction from the apparent polar wander path (APWP) for the South China block and Eurasia (Fig. 7B). Samples with mean angular deviations (MAD) >15 were generally excluded as were further samples (N=12) with strongly outlying remanence directions. Within the 95% confidence limit, the in-situ HC-C matches with the present magnetic field at the sampling site (Dec=358.5°, Inc=31.6°), and it thus remains unclear whether or not the determined directions represent a paleoremanence. The analyses of bedding corrected data reveal very low inclination values, implying a far more southerly paleolatitude (3.9°N ± 2.0°) for the Na Duong Basin compared to today (21.7°N). This almost equatorial position, however, is not in-line with the pole position (Lat=85.2°N, Long=174.6°E, A_{95}=11.9°, K=46.0) of the South China block during the Middle and Late Eocene, which yields an expected direction of Dec=4.8°, Inc=40.9°, corresponding to a paleolatitude of 23.6 ± 9.7°N (Zhuang et al. 1988). However, since only few, and yet not even internally consistent paleomagnetic data from the South China block for the Cenozoic are available (Fuller et al. 1991), a comparison of our data with the APWP of Eurasia may be more reasonable. For an age of 40 Ma, the APWP of Eurasia (Lat=82.3°, Long=150.5°, A_{95}=2.8°) of Torsvik et al. (2008) gives a very similar expected direction (Dec=5.9°, Inc=45.7°), which corresponds to a pale-

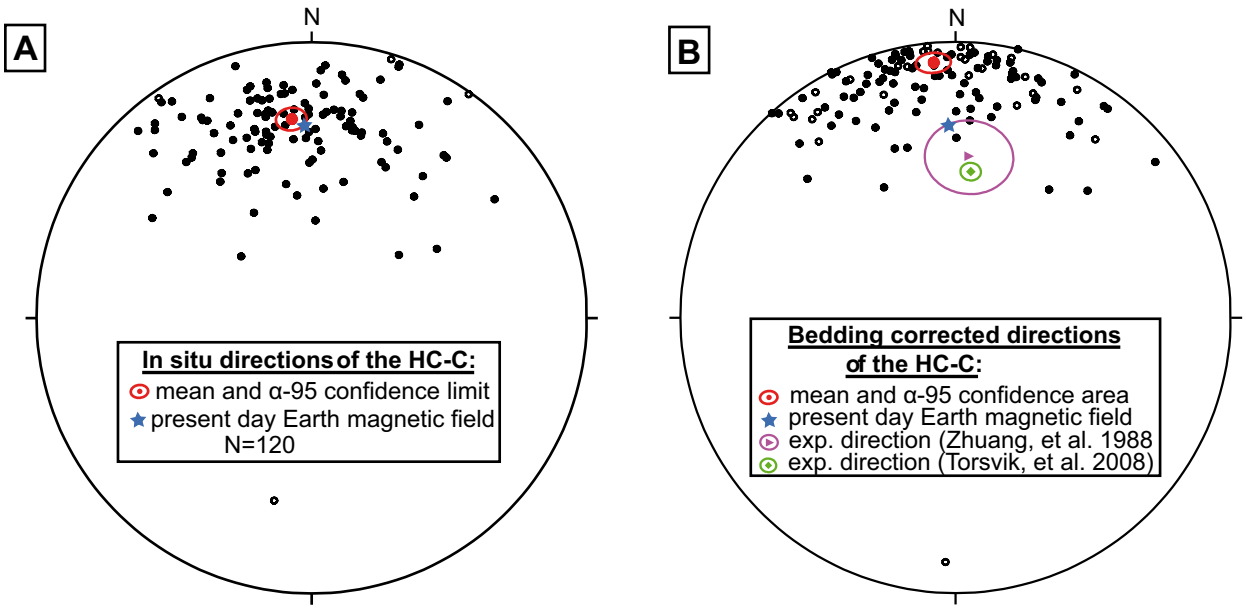

Figure 7: Stereo plots of single specimen directions of the HC-C from the Na Duong Formation. Equal area stereo plots of in-situ (left) and bedding corrected (right) single specimen directions of the HC-C from the Na Duong Formation. Solid dots: positive inclination; open dots: negative inclination. The overall means as well as the field directions of the present day Earth field and the expected directions for Middle to Late Eocene are also shown. Samples with mean angular deviations (MAD) >15 were generally excluded and are not illustrated.

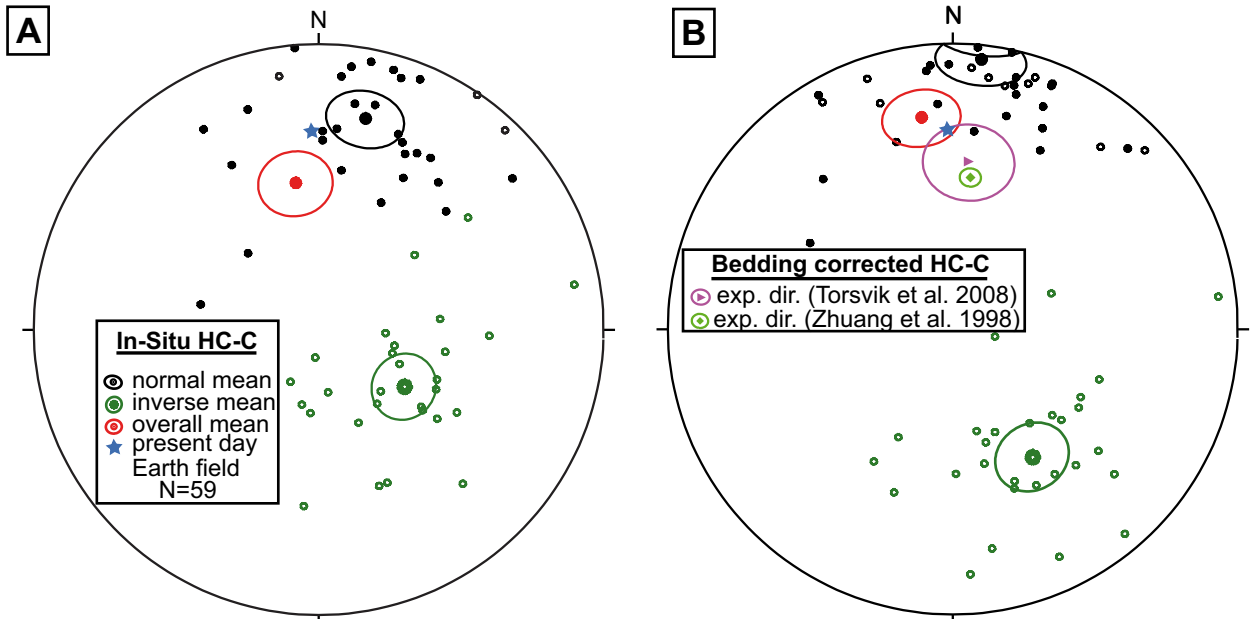

Figure 8: Stereo plots of single specimen directions of the HC-C from the Rhin Chua Formation. Equal area stereo plots of in-situ (left) and bedding corrected (right) single specimen directions of the HC-C from the Rhin Chua Formation. Solid dots: positive inclination; open dots: negative inclination. The overall means as well as the field directions of the present day Earth field and the expected directions for Middle to Late Eocene are also shown. Samples with mean angular deviations (MAD) >15 were generally excluded and are not illustrated.

olatitude of 27.2°N ± 2.3°. The difference between the observed bedding corrected paleolatitude and the expected one clearly is too high to be explained solely by inclination shallowing. It can therefore be concluded that the HC-C (at least for the majority of samples) is likely not of primary origin and postdates the tilting of the sediment layers.

The mean direction of the LC-C (Dec=10.5°, Inc=31.0°, α-95=8.8°, k=6.5) for the Rhin Chua Formation shows a by far better grouping than for the Na Duong Formation, closely matching the present day Earth magnetic field at the sampling site (Dec=358.5°, Inc=31.6°). A recent overprint of the LC-C is hence likely. The isolation of the HC-C is not always clear-cut due to the superimposing GRM. Probably, therefore, the mean in-situ (Dec=350.9°, Inc=46.9°, α-95=9.9°, k=4.5) and bedding corrected (Dec=351.5°, Inc=25.9°, α-95=9.5°, k=4.8) directions of the HC-C have a relatively large uncertainty (Fig. 8). The mean in-situ direction significantly differs from the present day field (Fig. 8A). Further, it could be revealed that samples from the uppermost 40 m of the profile yield predominantly negative inclinations, whereas samples from within the depth interval of 145–175 m mostly show positive inclinations. As illustrated in Figure 9, one normal and one reverse polarity interval can be confidently assigned to the lower and upper part, respectively. The sequence, however, is too short to be correlated with the GPTS. Although the occurrence of reverse polarities as well as the deviation of the HC-C from the present day field are indicative for a primary remanence character and the possibility for a recent overprint of the whole Rhin Chua Formation sequence can hence be ruled out, there are two indications for either a partial remagnetization or a falsification of remanence directions due to the GRM. (1) The reversal test according to McFadden & McElhinny (1990) is negative and (2) the bedding corrected mean value of the inclination strongly differs between samples with normal (5.1°) and reverse polarity (40.6°); samples with outlying directions from the main trend (small symbols in Fig. 9) were not considered, as they obviously do not carry a primary remanence.

The bedding corrected mean inclination of samples with reverse polarity further shows a strikingly good agreement with the expected inclinations for Middle to Late Eocene of 40.9° and 45.7°, respectively (Zhuang et al. 1988; Torsvik et al. 2008). The small difference between expected and observed inclinations is within the corresponding 95% confidence intervals and can easily be explained by inclination shallowing. The declination (328.1° ± 10.6°) on the other hand significantly differs from the expected value of 5.9° ± 4.0° (Torsvik et al. 2008), suggesting a counter-clockwise rotation of 36.7° ± 11.3°. Kawamura et al. (2013) have recently detected a gradual increase of counter-clockwise deflected declinations of up to 13.4° ± 4.7° towards the southwest of the South China Block (SCB) with respect to the stable part of the SCB. Samples with normal polarity yield inclination values, which are significantly shallower than expected from the APWP (Torsvik et al. 2008), but similar to the mean bedding corrected inclination of the Na Duong Formation. Like for the Na Duong Formation, the mean declination is indistinguishable from the present day field declination. Therefore, we presume that at least some, possibly even all, samples from the lower part of the Rhin Chua were remagnetized.

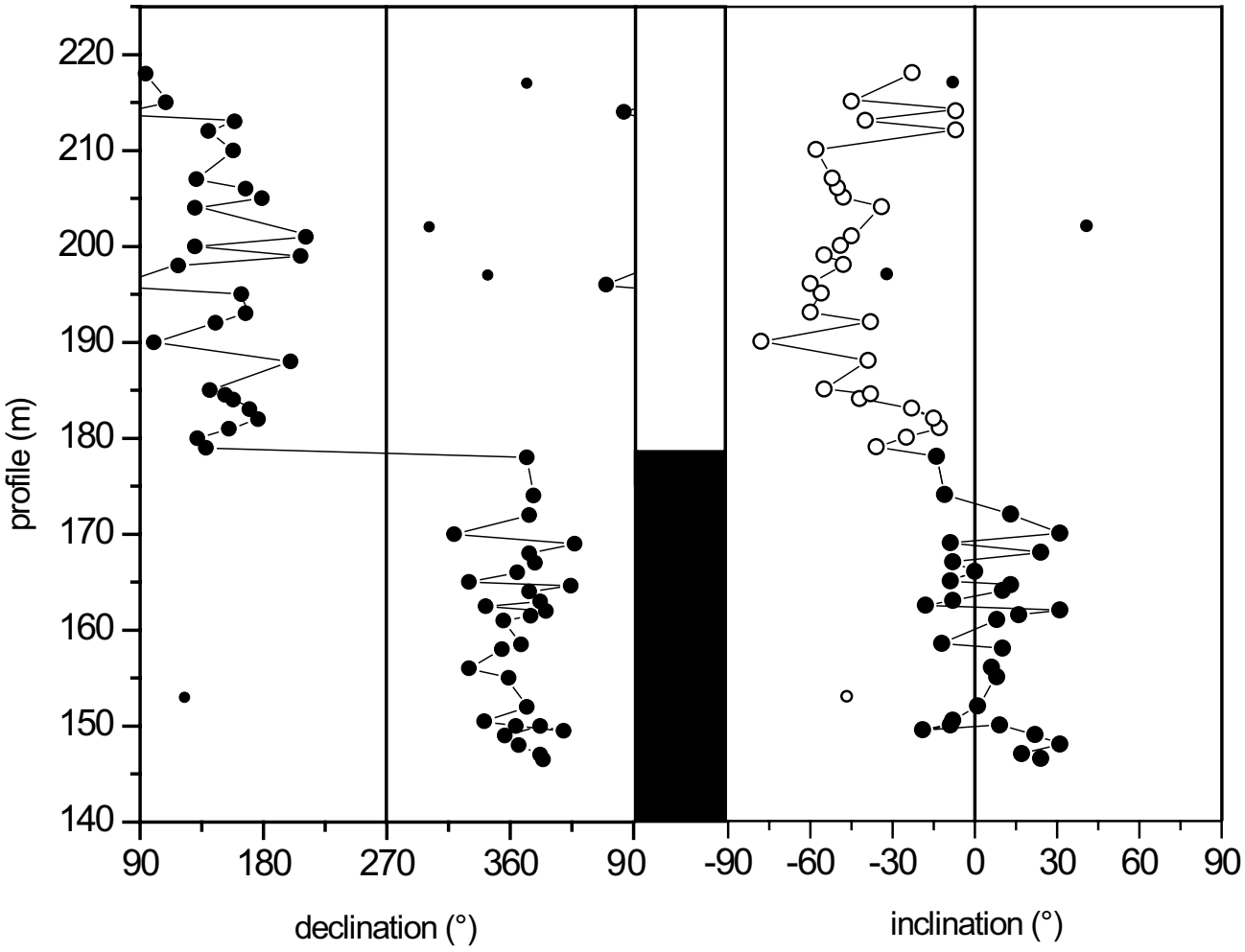

Figure 9: Magnetostratigraphic results of the bedding corrected HC-C from the Rhin Chua Formation. Declination vs. stratigraphic profile (left), inclination vs. stratigraphic profile (right) and interpreted polarity sequence (centre). Small symbols that are not connected by lines with the neighboring data represent single samples, which show outlying directions that do not concur with the main trend.

3.3 Systematic paleontology

3.3.1 Mammal fauna

Order Cetartiodactyla Montgelard, Douzery et Catzeflis, 1997
Family Anthracotheridae Leidy, 1869
Subfamily Bothriodontinae Scott, 1940

Genus *Bakalovia* Nikolov et Heissig, 1985

Type Species: *Elomeryx palaeoponticus* Nikolov, 1967 from the late Middle Eocene of Tscherno More, Burgas area, eastern Bulgaria, by original designation (Nikolov & Heissig 1985). Another species (originally also referred to *Elomeryx* by Nikolov (1967)), *Bakalovia astica* (Nikolov, 1967) was also reported from Tscherno More. The fossil material documenting these two species was collected from a single coal horizon at Tscherno More (Nikolov 1967). Both species are based exclusively on elements of lower dentition.

Bakalovia orientalis nov. sp.
(Figs 10–18)

Holotype: SAU 3: partially preserved skeleton (skull, both mandibles, some postcranials) of a female adult individual. SAU 3-21: extremely deformed skull preserving right P3-M3, and left P4-M3, and part of the muzzle (nasal and premaxilla) bearing alveoli of upper incisors, canines, and anterior premolars (Figs 10, 11); SAU 3-20a: right mandible preserving p4-m3 and alveoli of p1 to p3; SAU 3-20b: left mandible ramus preserving p4-m3 (and alveoli for double rooted p2-p3) (Figs 12, 13). Na Duong coalmine, Na Duong Formation (Loc Binh district, Lang Son Province, northern Vietnam). The temporary repository of the original material is the University of Tübingen (Germany).

Diagnosis: *Bakalovia orientalis* is of approximately the same size as *B. palaeopontica*, and slightly smaller (~20%) than *B. astica*. It differs from other species of *Bakalovia* in having relatively wider lower molars in transverse direction, more crescentic labial

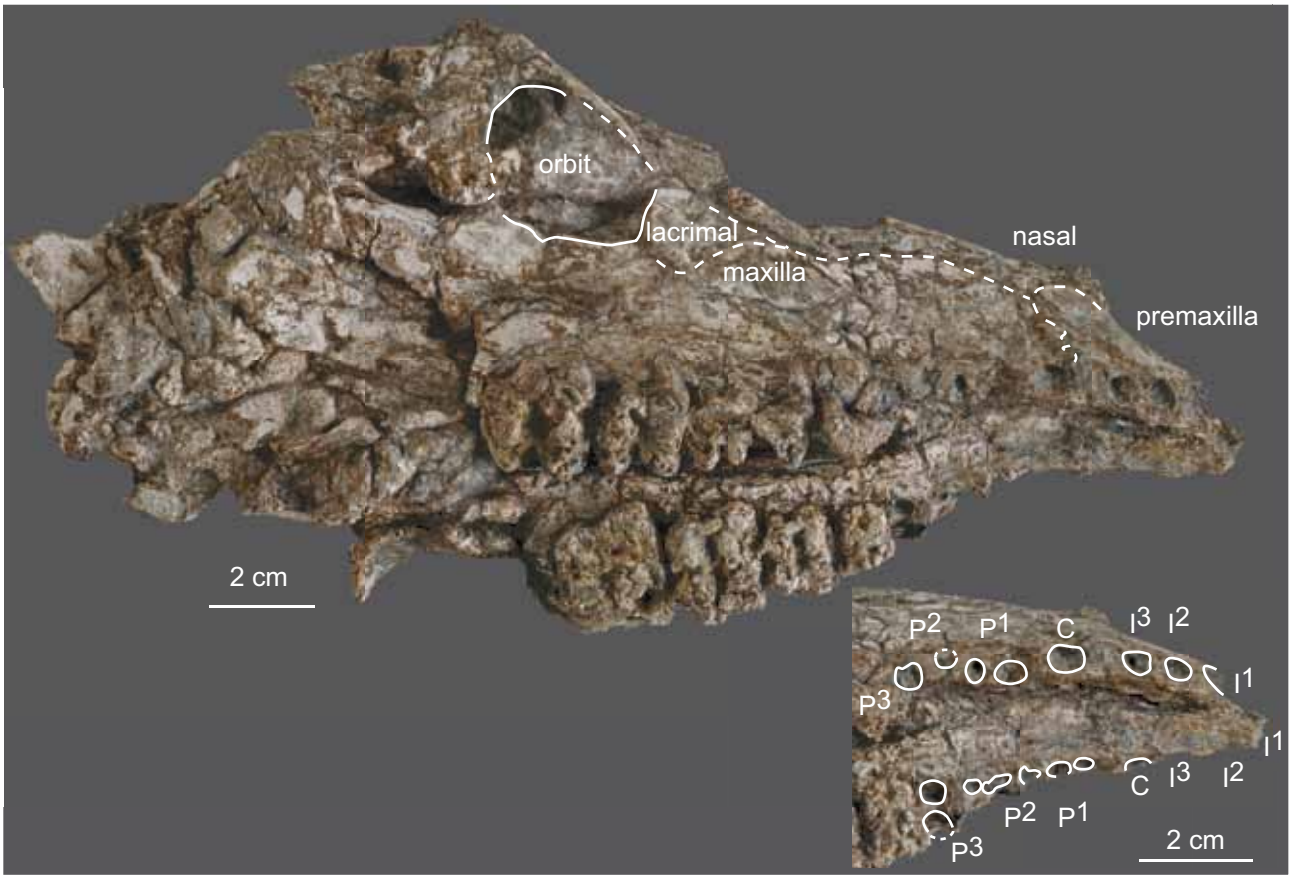

Figure 10: *Bakalovia orientalis* sp. nov. (Mammalia, Anthracotheriidae), partial cranium (holotype SAU 3-21), ventro-lateral view. For abbreviations see Material and Methods section.

cuspids, and a higher and more developed transversal hypocristid that forms a continous crest with the preentocristid. Furthermore, *Bakalovia orientalis* differs from *B. palaeopontica* in having a stronger lower canine (judging from the size of the alveoli), and a diastema between the canine and p1.

Derivatio nominis: Referring to the eastward enlarged distribution area of the genus *Bakalovia*, which was so far reported solely from the type locality, Tcherno More, in Bulgaria.

Type locality and horizon: Base of the main lignite seam of Na Duong coalmine (layer 80), late Middle to Late Eocene Na Duong Formation (Lang Son Province, northern Vietnam).

Stratigraphical range and geographic distribution: Only known from the type locality.

Referred material: All specimens listed below were recovered from Na Duong coalmine, in stratigraphic association with the holotype.

SAU 1: left mandible of an adult individual (Fig. 18C) preserving m2 (highly damaged) and m3 (especially the third lobe).

SAU 2: left mandible preserving damaged p4-m2, and right mandible preserving m1-2 of a juvenile individual.

SAU 4: right and left mandible, stongly weathered, lacking all teeth except left and right i1.

SAU 5: batch of specimens belonging to a single juvenile female individual, comprising a fragmentary maxilla preserving right P1-M3 (erupting) and left erupting I3 and canine, and left P2-M3 (erupting); and a damaged mandible preserving left p3-m2 and right p4-m2 (Figs 14–18).

SAU 6: right maxilla of a juvenile individual preserving D4-M2; this specimen is heavily weathered and features of the crowns are difficult to observe.

SAU 7: I3 and erupting canine (juvenile individual).

SAU 8: fragmentary maxilla of a juvenile individual with left and right P1, D2-M1 and a fragment of the mandible (Fig. 14B).

SAU 9: palate of a juvenile individual with D3-M2 (erupting).

Comparative Description: Since the cranium and upper dentition of *Bakalovia palaeopontica* and *B. astica* are not documented, comparison with other bothriodontines, in particular with *Elomeryx*, is most appropriate.

Cranium: Almost all fossil anthracotheres recovered from Na Duong coalmine are both dorsoventrally and laterally crushed, making the description of cranial bones difficult. Sutures between bones and positions of foramina are difficult to distinguish from the numerous cracks. SAU-3-21 is a crushed skull of

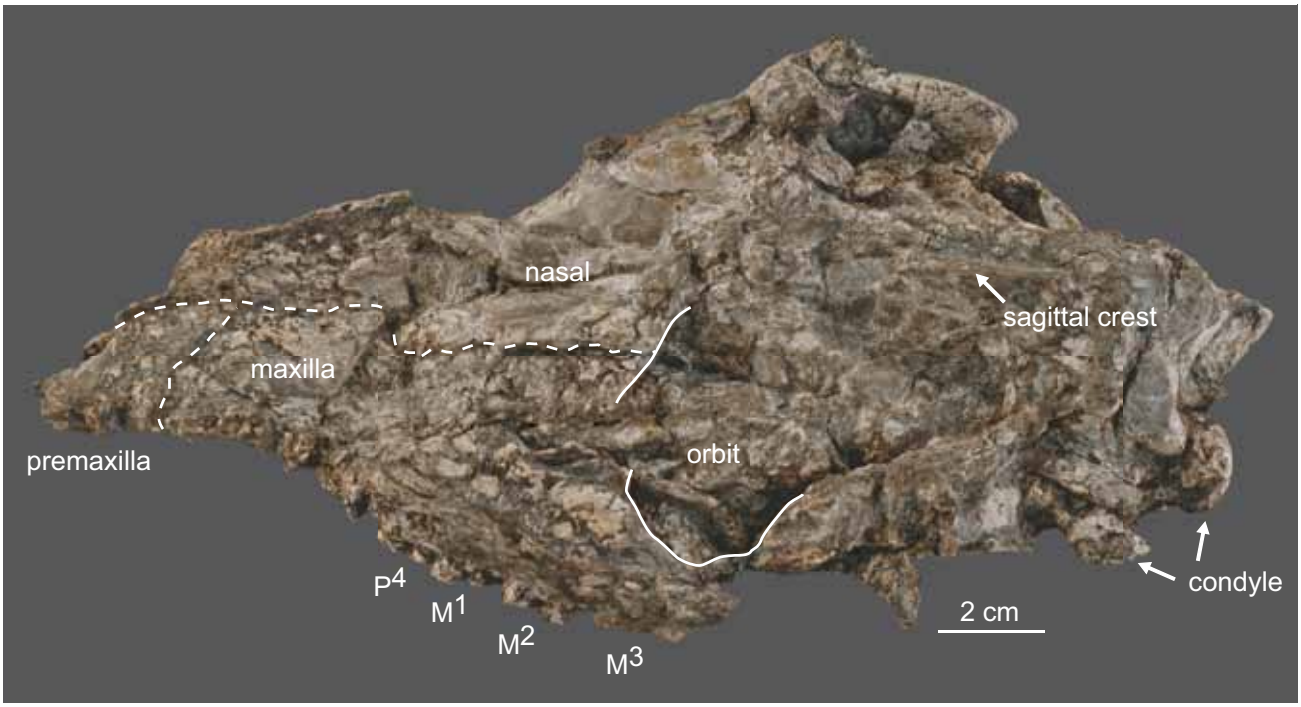

Figure 11: *Bakalovia orientalis* sp. nov. (Mammalia, Anthracotheriidae), partial cranium (holotype SAU 3-21), dorso-lateral view. For abbreviations see Material and Methods section.

an adult individual; in dorsal view, it is of sub-triangular outline, with a rather sharp-pointed snout. The widest part of the skull is situated just behind the orbits, which seem to be open backwardly and communicate with the temporal fenestra. No foramen is visible on the maxilla. In ventral view, the suture between the premaxilla and maxilla is barely visible behind I3, and it extends backwardly. The teeth preserved on the maxilla display swelling and alteration of enamel caused by chemical degradation during neoformation of gypsum, which hampers observation of important details. However, alveoli of lacking teeth are generally visible and the dental formula as well as the presence or absence of diastema can be inferred. The three-rooted P3 is preserved on the right maxilla as are the alveoli of P2 and P1 (both two-rooted); they may have been separated by a very short diastema. A very short diastema (about 0.5 cm) also occurs between the anterior alveoli of P1 and the alveoli of the canines; this character is clearly plesiomorphic with respect to the much larger diastema reported for *E. crispus* from Moissac III (Lihoreau et al. 2009). The small canine alveoli suggest that the individual was a female, because the closely related *Elomeryx* is known to display sexual dimorphism with regard to upper canines (Geais 1934; Hellmund 1991). There is also a short diastema (about 0.8 cm) between the canine and I3. Alveoli of incisors are also separated by very short diastemata, and they are almost aligned with the premolar row.

Mandible: The right lower jaw (SAU-3-20) of the same adult individual is shallow, the posterior part of the mandible is lacking and the teeth (p4-m3) are fairly damaged (cracks and swelling due to growth of both pyrite and gypsum crystals), preventing from any detailed description. There is a short diastema (about 0.7 cm) between p1 and the lower canine; the anterior part of the mandible is partially broken, and it is impossible to observe whether or not there is a diastema in front of the canine (Fig. 13). There is no evidence of constriction at the level of the canine. The ventral border of the mandible is concave below p1-2, and becomes slightly convex below the molars (Fig. 12). There is at least one anterior mental foramen below the anterior root of p2 and possibly a second, smaller, posterior foramen located just below the anterior root of the p3. The symphysis is broad, U-shaped in cross section, and extends backward towards below the mid-length of p2 (Figs 12, 13). There seems to be no diastema between the lower premolars, which are all two-rooted (with the exception of p1, for which the number of roots is uncertain).

Figure 12: *Bakalovia orientalis* sp. nov. (Mammalia, Anthracotheriidae), right mandible (holotype SAU 3-20), medial view. The symphysis is highlighted by a white line, and first three pre-molars are reconstructed according to the position of their roots.

Figure 13: *Bakalovia orientalis* sp. nov. (Mammalia, Anthracotheriidae), lower jaw (holotype, SAU 3-20). Montage of right and left lower jaws in occlusal view.

Dentition: The cheek teeth are brachydont and bunoselenodont, and the enamel is wrinkled in SAU-5 (the only specimen in which the dental enamel is not altered, Figs 14, 18). Upper deciduous dentition is best preserved in SAU 8: the D3 has a triangular occlusal outline and bears three distinct lobes; the distal lobe is transversely extended, with two distinct weakly crested cups; the central lobe bears three cusps of which the middle one is the largest; the mesial lobe shows a single cusp. The D4 is built on the same model as the M1: five main cusps with disposition of crests roughly similar to that of definitive molars, except for the parastyle, which is much more developed and salient labially than it is on permanent molars. The upper premolars are best observable on SAU 5. This specimen also preserves I3 and the external rib of the canine, which seems to be relatively small, suggesting that SAU 5 belongs to a female individual. The premolars are arranged in a continuous row as in all species of *Elomeryx* except *E. borbonicus* where there is a short diastema between P1 and P2 (Geais 1934). This character is difficult to ascertain in the material from Na Duong, although there seems to be a short diastema (about 0.5 cm) between P2 and P1 on SAU-5; however, the maxilla is severely damaged, and this short diastema may well result from post-mortem breakage and slight shifting. The first three premolars show the same simple occlusal pattern, with a main tranversely compressed triangular cusp, from which two crests reach the mesial and distal margins of each tooth.

The size (length and width) of premolars increases from P1 to P3. The P2 is a larger version of P1, with a stronger lingual cingular shelf; both teeth have two roots and are mesiodistally elongated, with the apex of the cusp situated between both roots. The P3 has a relatively enlarged distolingual basin and is three-rooted. The P4 has a thick lingual cingulum, which extends from the mesiolabial to the distolabial corners of the tooth; it displays the common, bicuspidate occlusal pattern of anthracotheriids, with both cusps being crescentic, with a mesial and a distal crest. The distal crest of the lingual cusp does not reach the distal border of the tooth, as in all *Elomeryx* species (Lihoreau et al. 2009). Upper premolars and molars tend to be obliquely oriented in relation to the longitudinal axis of the tooth row. The upper molars also increase in size from M1 to M3. They are typically pentacuspidate with a well-developed and pyramidal paraconule as in all primitive bothriodontines. The protocone is just slightly larger than the paraconule (a plesiomorphic condition compared to derived bothriodontines in which the protocone is enlarged; Ducrocq & Lihoreau 2006) and displays a single mesial crest (preprotocrista) and two distal crests (postprotocristae). The preprotocrista is mesiolabially oriented and is clearly distinct from the preparacristule on the unworn M2 preserved in SAU 5 (Fig. 14). The short and transverse postprotocrista extends towards (although not connecting to) the postparacristule, which reaches the transverse valley. The second postprotocrista extends towards the

centre of the tooth where it connects the premetaconule crista and a distinct spur raising from the base of the metacone. This triple junction is also observable on moderately worn molars. The metaconules of M1-M3 display four crests on the unworn M2 preserved in SAU 5 (Fig. 14): the mesiolingual crest connects down to the lingual cingulum as in *Elomeryx* (Hellmund 1991); the mesiolabial crest of the metaconule reaches the more distal crest of the protocone and consequently prevents the establishment of a transverse valley (Figs 15, 16), which is a diagnostic feature of all *Elomeryx,* except *E. borbonicus* (Ducrocq & Lihoreau 2006; Lihoreau et al. 2009). Two additional and twinned crests extend distolabially on unworn teeth (Fig. 16); this configuration of a postmetaconule crista and another (more mesial) crest or rib is observable on *E. crispus* from Dvérce, Czech Republic (Fejfar & Kaiser 2005). The parastyle is labially salient, and proportionally augments in size from M1 to M3. The characteristic loop-like mesostyle is also well-developed, whereas the metastyle is poorly developed. There is a weak labial rib on the paracone; it is also present but quite attenuated on the metacone.

The morphology of the lower dentition is partially observable on SAU-5 (Fig. 18). The lower molars show highly crescentic labial cuspids, but are overall the same size as the lingual cuspids; the hypoconulid of m3 (SAU 1) appears to be bicuspid, like that of *E. crispus* from Dvérce, Czech Republic (Hellmund 1991). However, in *Bakalovia orientalis* the separation of these cusps in not as obvious as in *E. crispus*; the hypoconulid forms a transversely compressed loop that is relatively narrow and labially shifted, as in other species referred to *Bakalovia* (Nikolov 1967). The trigonid of the lower molars lacks a paraconid, and in SAU 5 the preprotocristid and premetacristid are fused only at the base, whereas the postprotocristid reaches the metaconid. The prehypocristid (cristid obliquid) is strong and straight, extending downward to the distal trigonid wall, but without reaching the lingual border of the tooth. On m1-2 (SAU 2 and 5), the entoconid and the hypoconid are connected by two transversal crests. The mesial one (hypolophid) is high and straight, whereas the distal one is curved, lower, and forms the distal wall of the molar. Three cristids (those two cristids plus the cristid obliquid) are issued from the hypoconid, a dental feature shared with *Bothriogenys fraasi* from the late Eocene of Egypt (Ducrocq 1997). There are prominent mesial and distal cingulids, and a cingular shelf restricted to the base of the labially opened valley between the protoconid and the hypoconid.

Systematic discussion: The identification of several remains of anthracotheres from Asia remains dubious (e.g, Chow 1957; Chow 1958; Xu 1961; Xu 1977), and awaits both taxonomic revision and additional fossil material. The material from Na Duong displays a combination of dental characters including a looplike mesostyle, the development of transversal cristids, and a preprotocrista distinct from the preparacristule, which is typical of the bothriodontine anthracotheriids (Lihoreau & Ducrocq 2007). The specimens from Na Duong can be distinguished from the genus *Elomeryx* by the presence of three cristids on the molar hypoconid (plesiomorphic) and the lack of diastema (even short ones) behind p1 (Nikolov &

Figure 14: *Bakalovia orientalis* sp. nov. (Mammalia, Anthracotheriidae), upper jaw teeth; **(A)** SAU-5-1, skull with both maxillary bones, displaying right P1-M3 (erupting), left erupting I3, canine, and P2-M3 (erupting), in occlusal view; **(B)** SAU-8, detail of right maxilla with D2-D4 in occlusal view.

Figure 15: *Bakalovia orientalis* sp. nov. (Mammalia, Anthracotheriidae), fragmentary skull in occlusal view. Line-drawing of specimen in Fig. 14A (SAU-5-1).

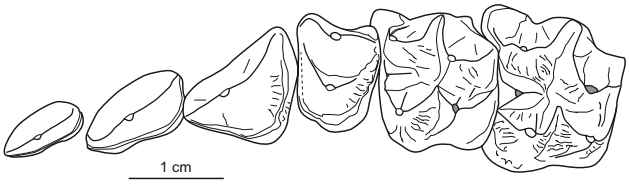

Figure 16: *Bakalovia orientalis* sp. nov. (Mammalia, Anthracotheriidae), idealized tooth row (P1 to M2) of the maxilla. Line-drawing of idealized orthogonal toothrow, reconstructed from SAU-5-1.

Heissig 1985; Hellmund 1991). Though larger in size than SAU-5, SAU-3 has similar proportions and dental morphology, and we therefore consider that only one species is so far represented in the Na Duong lignites. The limited number of specimens (nine individuals in different states of preservation) does not allow for a confident estimate of size variability of the Na Duong anthracotheres, but an overlap of *B. orientalis* nov. sp. and *B. palaeopontica* with regard to molar dimensions is obvious (Nikolov 1967; *B. asticus* is significantly larger). Nevertheless, there are sufficient morphological differences between these two forms to warrant a specific differentiation of *B. orientalis* nov. sp.

Although there are some dissimilarities, the well-preserved lower molars of *B. orientalis* nov. sp. clearly resemble those of *B. palaeopontica* from Tcherno More, suggesting a close relationship with this eastern European form. Both species share several characteristics, such as the absence of significant diastema in the lower dental row, the incipient (in *Bakalovia* species from Bulgaria) to well expressed (in *B. orientalis* nov. sp.) transversal cristid joining the entoconid and hypoconid, and the shape of the symphysis in sagittal section.

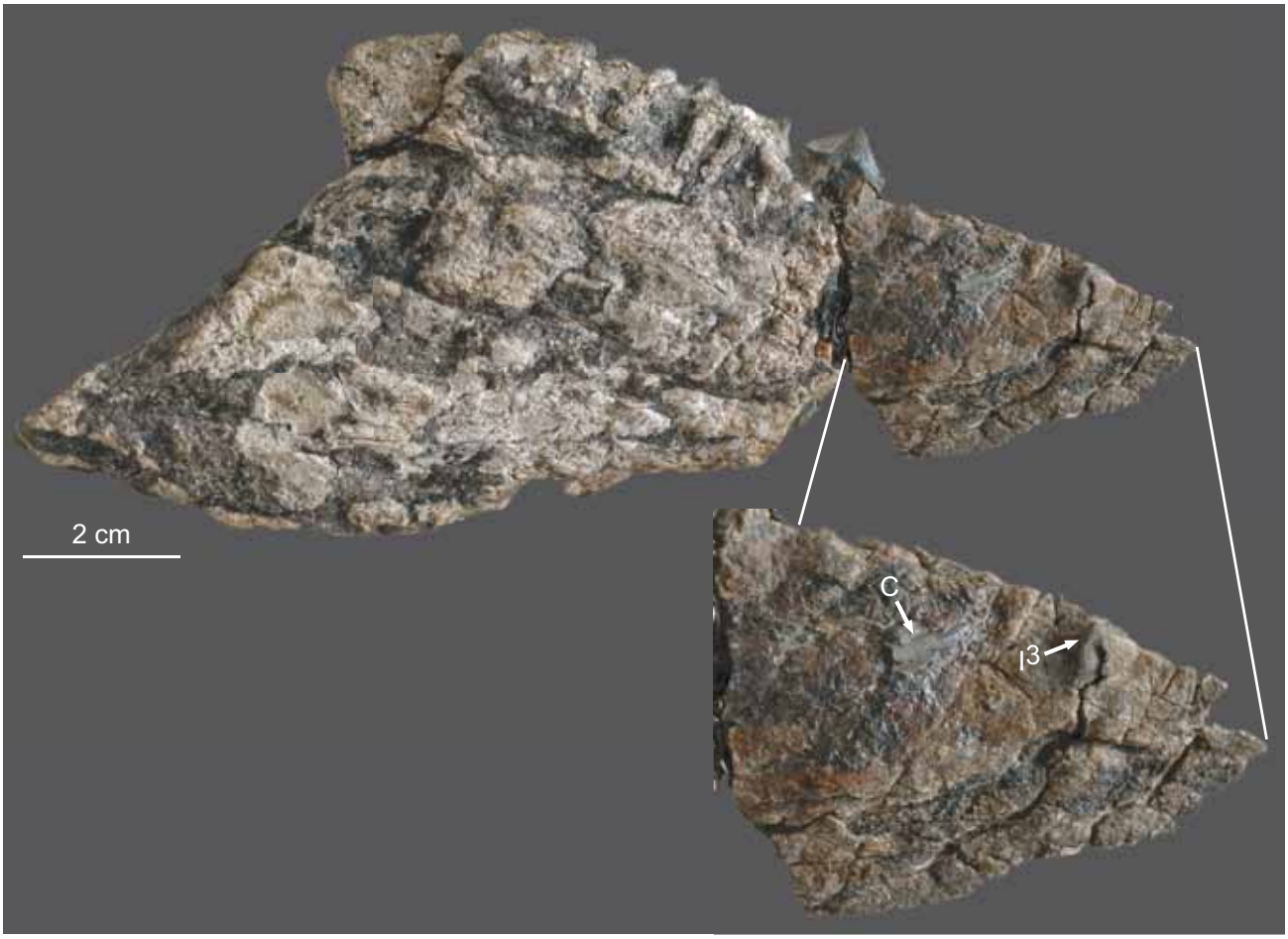

Figure 17: *Bakalovia orientalis* sp. nov. (Mammalia, Anthracotheriidae). SAU-5-1, in dorsal view, showing a fragmentary upper canine and an upper I3.

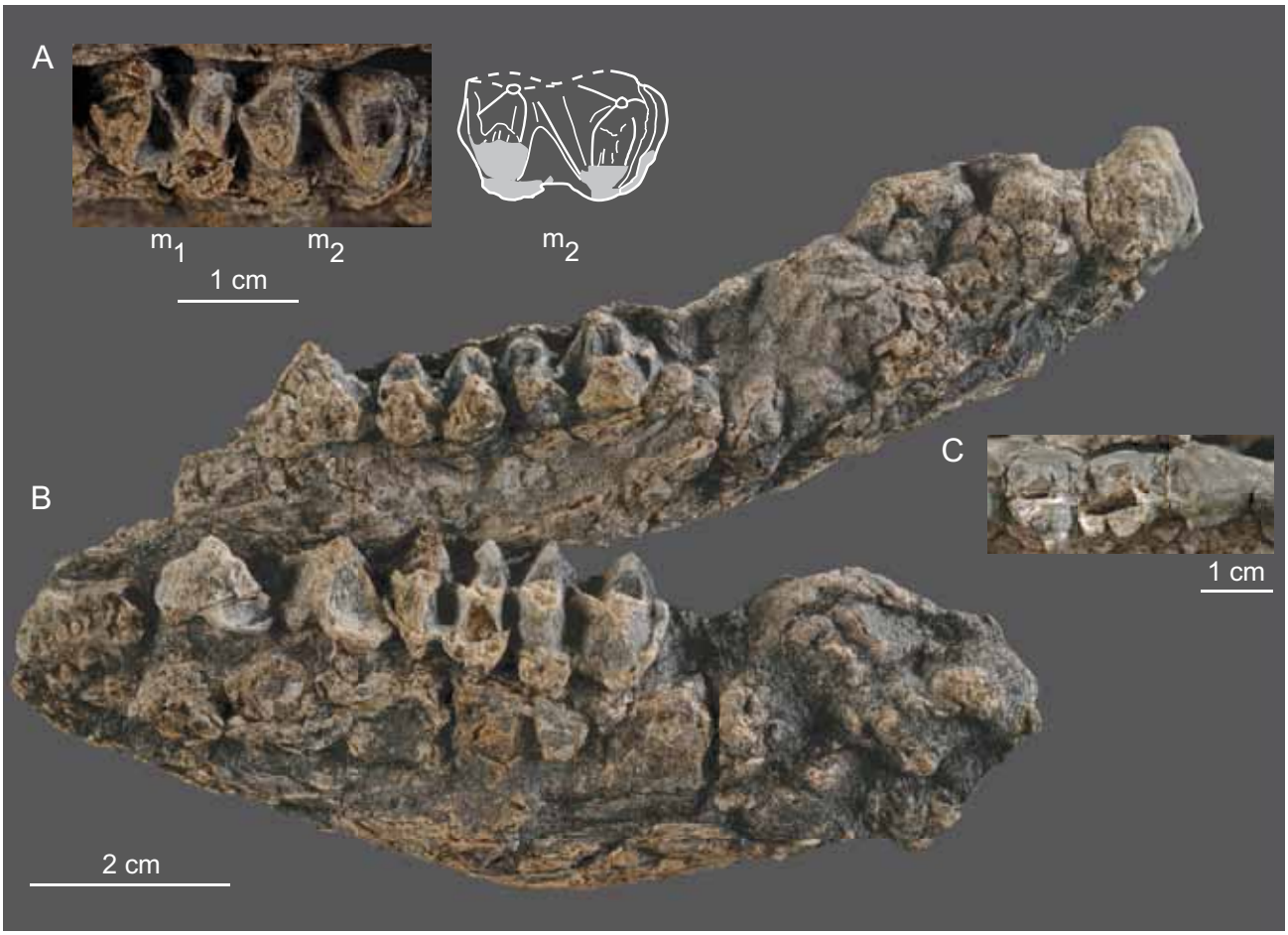

Figure 18: *Bakalovia orientalis* sp. nov. (Mammalia, Anthracotheriidae), lower molars; **(A)** SAU-5-2, focus on the left m1-2 in occlusal view; **(B)** SAU-5-2, left and right hemi-mandible preserving left p3-m2 and right p4-m2 in sub-occlusal view; **(C)** SAU-1, damaged left m3 in occlusal view.

The overall shape of the mandible of *B. orientalis* nov. sp. (Fig. 14) is also similar to that of the holotypes of *B. palaeopontica* and *B. asticus* from Tscherno More, only differing in the presence of a short diastema between the canine and p1, the accentuated crescentic labial cuspid, and the overall less bunodont dental pattern. The upper molars of *B. orientalis* nov. sp. (Figs 14–16) closely resemble those of *Elomeryx crispus* (Hellmund 1991) in having a mesio-lingual spur on the metacone and two postprotocristae. The lack of information regarding the morphology of the upper dentition of *Bakalovia* species from Tscherno More prevents any additional comparison. The present evidence, however, suggests that *Elomeryx* (at least *E. crispus*) and *Bakalovia* are closely related (see phylogenetic analysis below).

Phylogenetic analysis: In order to test the phylogenetic relationships of *Bakalovia orientalis* nov. sp. within the bothriodontine anthracotheriids, we have scored the fossil material currently available from Na Duong in the character-taxon matrix of Lihoreau & Ducrocq (2007) recently updated by Rincón et al. (2013). The taxa included in the analysis are 18 out of the 28 species of Lihoreau & Ducrocq (2007) (a large selection of Eurasian and North American anthracotheriids) plus *Bakalovia palaeopontica* (Nikolov & Heissig 1985). Two species originally referred to *Elomeryx* by Nikolov (1967) are now referred to *Bakalovia*, i.e. *B. palaeopontica* (Nikolov, 1967, type species) and *B. astica* (Nikolov, 1967) from Tscherno More (Nikolov & Heissig 1985). Both species are based exclusively on elements of lower dentition but we have scored *Bakalovia* on the base of all the material referred to this genus, and figured in the literature [i.e. one isolated m2 and one isolated m3 for *B. astica* (Nikolov & Heissig 1985; Hellmund 1991), and left mandible bearing i2-3, c?, alveoli of p1, and p2-m3, figured in Nikolov (1967)]. *Siamotherium krabiense*, usually considered as the most primitive anthracotheriid (e.g., Tsubamoto et al. 2011), was set as the outgroup taxon (for technical details see Material and Methods section).

The analysis resulted in four equally most parsimonious trees (MPTs) with tree lengths of 98 steps, a consistency index (CI) of 0.66, and a retention index (RI) of 0.77 (Fig. 19). Despite the large amount of missing data for the upper dentition of *Bakalovia palaeopontica*, the resolution of the strict consensus tree is quite good (Fig. 19). Our results clearly

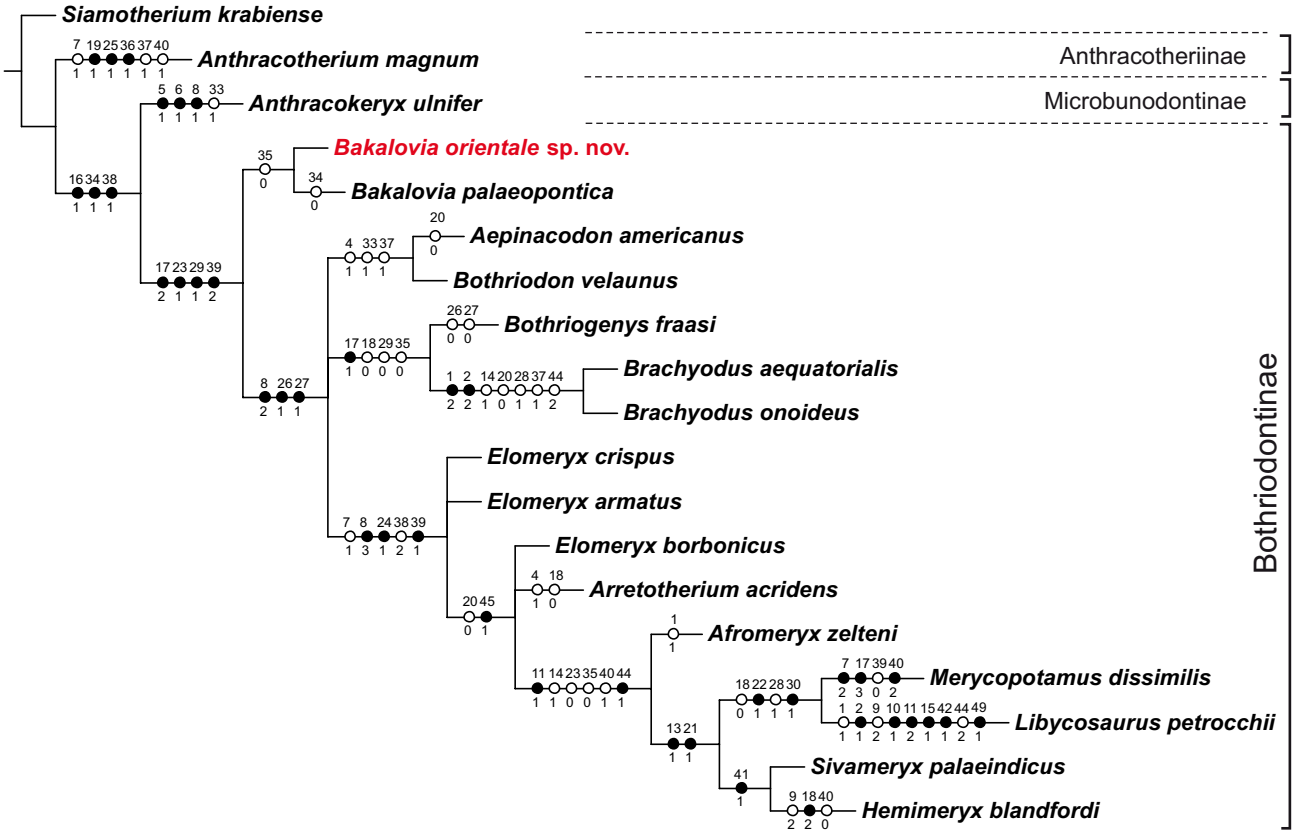

Figure 19: Phylogenetic relationships of bothriodontines (Mammalia, Anthracotheriidae). Strict consensus tree of hypothesized phylogenetic relationships of bothriodontine anthracotheriids including *Bakalovia orientalis* sp. nov. from the Na Duong coal mine, northern Vietnam. This tree is the consensus of four most parsimonious trees generated by TNT version 1.1 (Goloboff et al. 2008) applying an equally weighted traditional search (TL=98, CI=0.66, RI=0.77). All characters are non-additive. Data matrix includes 51 dental and cranial characters of Lihoreau & Ducrocq (2007) emended by Rincon et al. (2013). Characters definition is listed in the appendix 1. Synapomorphies are indicated on the tree by black dots (strict synapomorphy) or circles (homoplasic synapomorphy). Upper and lower numbers indicate character and state numbers, respectively.

identify *Bakalovia orientalis* sp. nov. as a sister taxon of the type species of *Bakalovia* (*B. palaeopontica*). Although still poorly defined, this genus is primarily supported by the synapomorphic features of the Bothriodontinae (17[2], 23[1], 29[1], 39[2]; see appendix 1 and 2). Consequently, it is identified as a stem bothriodontine by the analysis, as recently suggested by Kostopoulos et al. (2012), and lacks non-homoplastic autapomorphic features. The *Bakalovia* clade is currently solely supported by the lack of diastema between p1 and p2 (35[0]). Further fossil evidence is necessary to increase the morphological data set, and substantiate these preliminary results.

A second important result of the cladistic analysis is the paraphyly of the genus *Elomeryx*, a point that has been raised by several studies (Hellmund 1991; Ducrocq & Lihoreau 2006; Lihoreau & Ducrocq 2007; Hooker 2010). *Elomeryx* is a widely distributed genus of Eocene-Oligocene bothriodontines including several species and subspecies which are in need of systematic revision. Our results also suggest that there is a great deal of homoplasy in the phylogenetic tree; few non-homoplastic characters seem reliable to define the different species of *Elomeryx* or to differentiate European and North American forms such as *Bothriodon velaunus* and *Aepinacodon americanus*. Therefore, this analysis confirms the difficulty to discriminate widely distributed species of the '*Elomeryx* complex'. *Bakalovia orientalis*, sp. nov. is the easternmost representative of the genus and noticeably extends the geographic distribution of the genus *Bakalovia*. Furthermore, the inferred late Middle to Late Eocene age (see below) for the Na Duong fossil assemblage identifies *B. orientalis* as one of the earliest members of bothriodontine anthracotheriids in Southeast Asia. The generic assignment of Late Eocene bothriodontine dental remains from eastern Asia is highly controversial, documenting an urgent need of systematic revision of this material, which is often used to establish long-distance biochronological correlations. *Elomeryx* and potentially also *Bothriodon*/*Aepinacodon* have been reported from several late Eocene localities of southern China and Mongolia (Ducrocq & Lihoreau 2006; Tsubamoto & Tsogtbaatar 2008). Although the relationship of *Bakalovia* with other Eurasian and American bothriodontines is still poorly resolved, results from cladistic analysis suggest that its geographic distribution was much wider than previously known, and involved trans-Eurasian dispersal during the Middle or Late Eocene.

Order Perissodactyla Owen, 1848
Family Rhinocerotidae Owen, 1845
Subfamily Rhinocerotinae Owen, 1845

Genus *Epiaceratherium* Abel, 1910

Type Species: *Epiaceratherium bolcense* Abel, 1910 from the ?late Eocene of Monteviale (Italy). Other species referred to the genus: *Epiaceratherium magnum* Uhlig, 1999 from the earliest Oligocene (MP21–MP22) of Germany, Czech Republic, Switzerland, and France. *Epiaceratherium* aff. *magnum* is reported from the Early Oligocene (MP23) of Germany, Switzerland, and France (Uhlig 1999; Becker 2009). *Epiaceratherium* cf. *magnum* is mentioned from the Early Oligocene (MP23) of Southwestern Pakistan (Antoine et al. 2003a).

Emended diagnosis: Stem rhinocerotine lacking i3 and a lower canine, with wide postfossette on P2-P4, a usually constricted protoloph on M1-M2, a straight posterior half of the metaloph on M1-M2, and a posterior valley usually closed on p2.

Epiaceratherium naduongense nov. sp.
(Fig. 20)

Holotype: SAU 10, complete skull including lower jaw with a complete upper and lower dentition, Na Duong coal mine, Na Duong Formation (Lang Son Province, northern Vietnam). The temporary repository of the holotype is the University of Tübingen (Germany).

Differencial diagnosis: *Epiaceratherium naduongense* differs from *E. bolcense* in being slightly larger (~10%) and in having a partly closed auditory pseudomeatus, a lingual wall on P3-P4, usually no labial and lingual cingula on upper molars, a generally constricted protocone on M1-M2, a long metaloph with respect to the protoloph on M1, a trigonid forming an acute dihedron on lower cheek teeth, and a generally closed posterior valley on p2. *E. naduongense* differs from *E. magnum* in the absence of a labial cingulum on the upper molars, a protocone constriction on P3-P4, and a crista on the upper molars, and in the presence of a developed metastyle on M3. It differs from *E*. cf. *magnum* in having a DP1 with an undulated ectoloph, a M3 with a low anterolingual groove on the hypocone, a simple crochet, and a lingual cingular spur.

Derivatio nominis: From Na Duong, the name of the type locality and formation.

Type locality and horizon: Base of the main lignite seam (layer 80) of Na Nuong coal mine, late Middle to Late Eocene (Lang Son Province, northern Vietnam).

Stratigraphical range and geographic distribution: Only known from the type locality (Na Duong coal mine, Na Duong Formation, Late Eocene).

Comparative description: *Cranium:* The cranium SAU 10 is slightly crushed dorsoventrally (Fig. 20A, B). The premaxillae and the anterior tip of the maxillae were broken and disarticulated after deposition, but the complete anterior tooth set (left and right I1-3 + C) could be recovered nearby the cranium (Fig. 20D). Dimensions of the cranium (dorso-caudal length c. 500 mm), mandible (dorso-caudal length c. 400 mm; maximum height = 180 mm), and upper and lower tooth row lengths are comparable to those of the smallest individuals of the living Sumatran rhino, *Dicerorhinus sumatrensis* (Guérin 1980).

The cranium is elongated rostro-caudally (bizygomatic width c. 230), as in most Paleogene rhinocerotids. The nasals and frontals lack any rugosity or boss tied to the presence of horns. There is no lateral apophysis on the nasals, unlike in *Teletaceras radinskyi* and *Ronzotherium filholi*, but like in most advanced Rhinocerotidae, including *Epiaceratherium bolcense* and *Penetrigonias dakotense*. The nasal notch is short (above the P2-P3 transition), contrary to that seen in *T. radinskyi*. The anterior tip of the processus zygomaticus maxillary is located high, like in *Trigonias osborni*, *E. bolcense*, *P. dakotense*, and *R filholi*, while it is low in *Uintaceras radinskyi* and *T. radinskyi*. The zygomatic arch is higher than in *U. radinskyi* and *R. filholi*. The external auditory pseudomeatus is partly closed, as in *Molassitherium albigense* (= "*Acerotherium albigense* Roman, 1912"; see Becker et al. 2013) and *T. osborni*, but unlike in *E. bolcense*. The posterior margin of the hamulus pterygoideus is subvertical, as it is only observed in *E. bolcense* and *Diceratherium armatum* among Paleogene rhinocerotoids. The processus posttympanicus is little-developed, like in *M. albigense*, *U. radinskyi*, *T. osborni*, and *E. bolcense*. There is a median horizontal ridge on the occipital condyle, a feature which is only observed in *E. bolcense* within Paleogene rhinocerotoids.

Mandible: The mandible preserves both sides and ascending rami. The left and right sides are slightly twisted and closely apposed due to depositional processes (Fig. 20C). The symphysis is upraised, contrary to what occurs in *T. osborni* (nearly horizontal) and in *R. filholi* (very upraised). There is no "hippo-like" rostral widening of the symphysis contrary to what is observed in *Aprotodon*. The posterior margin of the symphysis and the foramen mentale are located below the middle of p2, instead of being in front of p2, like in *U. radinskyi*, *T. radinskyi*, and *R. filholi*. The base of the corpus mandibulae is straight, unlike in *P. dakotense*. The ramus is vertically oriented in lateral view (pointing up- and forward in *U. radinskyi*).

Dentition: The dental formula includes I1-I3, C, DP1-P4, M1-M3; i1-i2, p1-p4, and m1-m3. All the upper incisors and canines are unicuspidate (Fig.

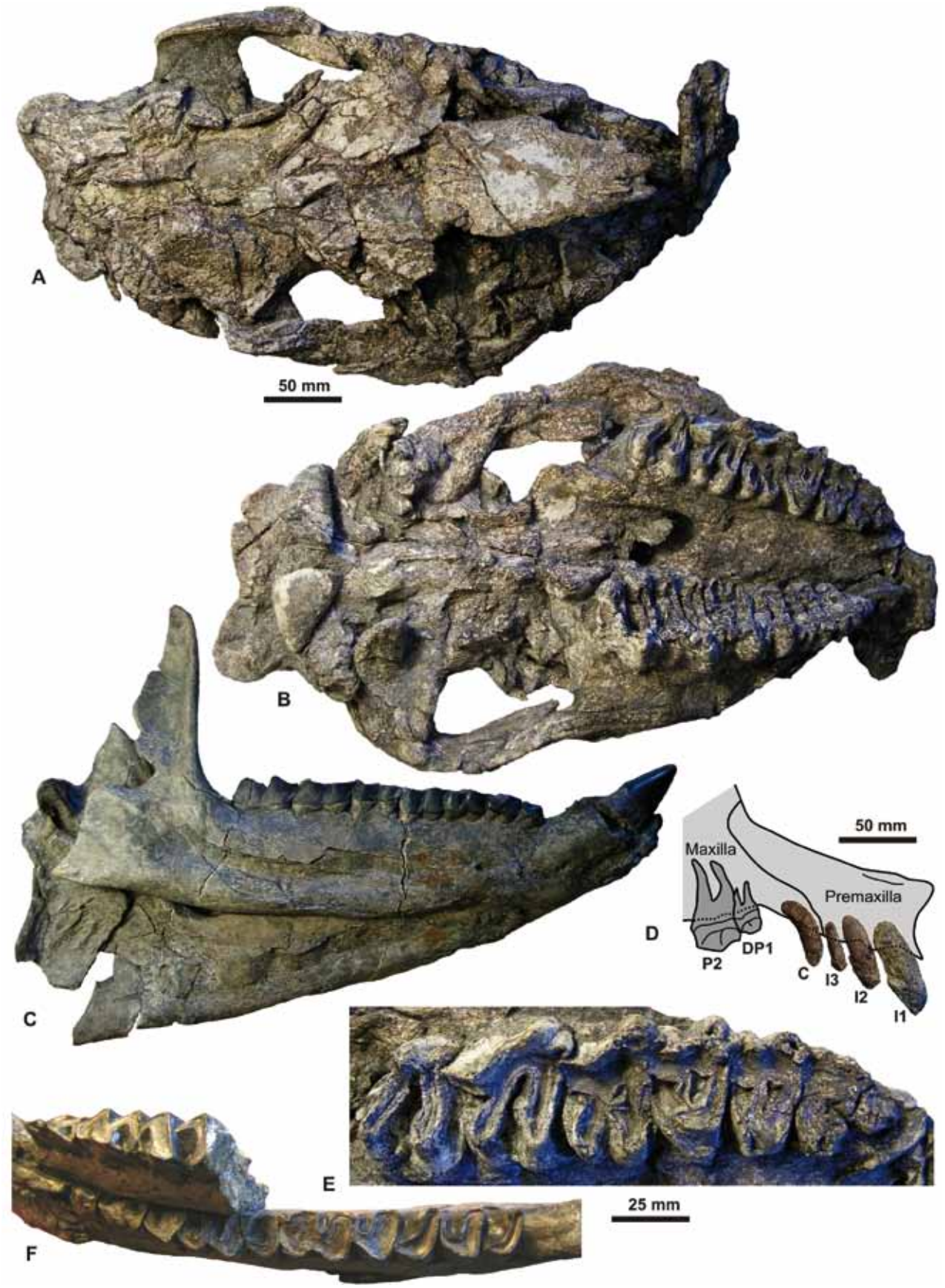

Figure 20: *Epiaceratherium naduongense* sp. nov. (Mammalia, Rhinocerotidae) from Na Duong (layer 80), holotype (SAU-10); **(A)** Cranium, in dorsal view; **(B)** Cranium, in palatine view; **(C)** Mandible, in right lateral view; **(D)** Anterior upper dentition (I1-3 + C), in lingual view. Tentative reconstruction of the premaxilla-maxilla region based on that of the early rhinocerotid *Trigonias* (modified from Radinsky, 1966); **(E)** Upper dentition, right tooth row (DP1-M3), in occlusal view; **(F)** Lower dentition, with left p1-m3 and right p1-p4, in occlusal view. Scale bars: 50 mm (A–D) and 25 mm (E–F).

20D). I1 is much larger than I2, I3, and C, which is a characteristic feature of early diverging Rhinocerotidae among Perissodactyla (Prothero et al. 1989; the latter tooth has a curved root, which makes it distinct from all incisors). These anterior teeth are perfectly similar to those illustrated by Dal Piaz (1930) for *E. bolcense*, both in morphological and metrical perspectives. The i1 is small, with a reduced crown, and closely apposed to large and sabre-like i2s, unlike in hyracodontids and *U. radinskyi* (incisiform). There are neither i3 nor c, contrary to what is recorded in *U. radinskyi* and *T. radinskyi* (Fig. 20C).

The upper and lower premolar rows are longer with respect to the molar rows than in *U. radinskyi*, *T. radinskyi*, *T. osborni*, and *P. dakotense*. The enamel is both wrinkled and arborescent, a very distinctive feature among Paleogene rhinocerotids, thus far observed only in *E. bolcense* and *E*. aff. *magnum* from Pakistan (Antoine et al. 2003a).

Upper premolars display neither labial cingula (like in *T. radinskyi* and *P. dakotense*), nor crochets (unlike in *T. radinskyi* and *P. dakotense*), or cristae (unlike in *M. albigense* and *R. filholi*). They display a strong and continuous lingual cingulum (a generalized feature among early rhinocerotids). P2-4 have a lingual wall with close protocone and hypocone, as in *T. radinskyi*, *E. bolcense*, and *E. magnum* (Fig. 20E). The protoloph of P2 is complete, contrary to what occurs in *T. radinskyi*, *T. osborni*, and *R. filholi* (always interrupted).

Among upper molars, only M1s have a faint labial cingulum (otherwise absent), whereas it is always present in M1-3s of *M. albigense* and *T. osborni*. The lingual cingulum is usually absent on upper molars, as in *T. radinskyi* and *E. bolcense* (always present in other Paleogene rhinocerotids). At the current stage of wear, there is no crochet on M1-2, while a small crochet is restricted to the apical part of the crown on M3 (no crochet at all in *G. simplex*). There is no crista on M1-M3. A shallow anterior constriction of the protocone is observed on M1-2, like in *E. magnum*, *M. albigense*, and some specimens of *E. bolcense*, but contrary to other Paleogene rhinocerotids. This constriction is absent on M3, whereas it occurs in *E. magnum* and *M. albigense*. The paracone fold is very strong, with a parastyle widely displaced antero-lingually (weak/not displaced in *T. osborni*, *P. dakotense*, and *G. simplex*). There is an antero-lingual groove on the hypocone of M2, as in *M. albigense*, *E. magnum*, and *E. bolcense*. M3 is quadrangular in occlusal view (ancestral condition for rhinocerotids). Moreover, on M3, the ectoloph and metaloph are not fused into an ectometaloph but distinct, with a developed metastyle. This plesiomorphic trait is retained in early hyracodontids as well as in most Eocene rhinocerotids and *E. bolcense*, whereas *M. albigense*, *E. magnum*, *E*. cf. *magnum* from Pakistan (Antoine et al. 2003a), cf. *Teletaceras* from Pondaung (Holroyd et al. 2006), *G. simplex*, *G. youjiangensis* and all other post-Eocene rhinocerotids have M3s with a fused ectometaloph. A deep groove on the postero-labial side of the ectometaloph of the M3 (IVPP V 5005-4) of *G. simplex* is likely to prove an incomplete fusion of the metaloph and ectoloph in the latter species.

Lower cheek teeth do not display lingual cingulids, a feature only documented in *U. radinskyi* and *E. bolcense* thus far among Paleogene rhinocerotids (Fig. 20F). The labial surface of the ectolophid of all lower premolars is corrugated by deep and irregular vertical grooves as observed only in *E. bolcense* within the Rhinocerotidae. The p1 is biradiculate, whereas it is uniradiculate in *M. albigense* and *T. radinskyi*. The p2 has a forked paralophid, a feature so far only documented in *E. bolcense* among rhinocerotids (Fig. 20C). At a more advanced stage of wear, the posterior valley of p2 would be closed by a thin and sharp lingual ridge, as it occurs in *U. radinskyi*, *E. magnum*, *E. bolcense*, and *R. filholi*. The metaconid of lower cheek teeth is not constricted, unlike in *T. radinskyi*, *T. osborni*, *E. magnum*, and *E. bolcense*.

Systematic discussion: The Na Duong rhino has been compared to all Eocene and Oligocene rhinocerotid genera from North America (*Uintaceras*, *Teletaceras*, *Trigonias*, *Penetrigonias*, *Subhyracodon*, *Amphicaenopus*, and *Diceratherium*) and Eurasia (*Teletaceras*, *Guixia*, *Ronzotherium*, *Epiaceratherium*, *Molassitherium*, *Mesaceratherium*, *Aprotodon*, and *Diaceratherium*), as well as to other taxa typifying each suprageneric group recognized within Rhinocerotidae (Teilhard de Chardin 1926; Heissig 1969; Tanner & Martin 1976; You 1977; Brunet 1979; Michel 1983; Hanson 1989; Dashzeveg 1991; Holbrook & Lucas 1997; Qiu & Xie 1997; Uhlig 1999; Antoine 2002; Antoine et al. 2003a; Antoine et al. 2003b; Prothero 2005; Holroyd et al. 2006; Lihoreau et al. 2009; Antoine et al. 2010; Antoine et al. 2011; Becker et al. 2013).

With a focus on the earliest rhinocerotid remains documented from Southeast Asia, comparison to *Guixia simplex* You, 1977 shows that dental remains of SAU 10 are 20 to 25% larger than the ones from the Bose Basin (Guangxi Province, Southern China), with a much stronger paracone fold but no developed crochet on upper molars, a long metastyle on M3 (ectometaloph fused, with a remnant groove, in *G. simplex*), a protocone with a rounded lingual side on M3 (sharp, almost pinched in occlusal view), and a m2 that is not wider than the m3 (contrary to *G. simplex*). The m2-m3 of *G*. cf. *simplex* from the earliest Oligocene of Krabi, Thailand (Antoine et al. 2003b) are 30% smaller than the ones in the specimen from Na Duong, with a shorter hypolophid and more U-shaped posterior valleys in lingual view, while the posterior cingulum is narrow and spur-like on m3. In addition, the lower teeth are more globulous, more brachydont, and comparatively wider in *G. simplex* from China and *G*. cf. *simplex* from Thailand than in the specimen from Na Duong.

The other species referred to *Guixia*, *G. youjian-*

giensis You, 1977, is much larger than the Na Duong rhino (and a fortiori than *G. simplex*); its upper teeth have a smoother paracone fold and a shallower parastylar groove; the metaloph is straight and continuous on the upper premolars; M1-M2 have a crochet, but neither a protocone constriction nor an antecrochet; M3 has a fused ectometaloph and no metastyle.

The specimens referred to cf. *Teletaceras* sp., from the Pondaung formation (Myanmar; Holroyd et al. 2006), are characterized by a ~40% smaller size, the lack of protocone or hypocone constriction on M2-M3, the possession of a fused ectometaloph (but a remnant postero-lingual groove) on M3, and a constricted entoconid on m1/2.

The Na Duong cranium can be confidently referred to the genus *Epiaceratherium* Abel, 1910 known from Europe (*E. bolcense* Abel, 1910 and *E. magnum* Uhlig, 1999; Abel 1910; Dal Piaz 1930; Uhlig 1999; Becker 2009; Becker et al. 2013) and South Asia (*E.* cf*. magnum*; Antoine et al. 2003a). This assignment is supported by the absence of a lower canine, the presence of a wide postfossette on P2-P4, the usual presence of a constricted protoloph on M1-M2, a straight posterior half of the metaloph on M1-M2, and the usual closure of the posterior valley on p2. As in Eocene rhinocerotids, it has a complete set of upper anterior teeth (3I+C), but it is more derived than the former in having lost both i3 and c. The rhinocerotid from Na Duong has its closest affinities to *Epiaceratherium bolcense* Abel, 1910 (Vicenza; Dal Piaz 1930, Uhlig 1999) in sharing similar cranial and mandibular morphology, and being of similar dimensions. Both taxa share the same dental formula (3I+C+4P+3M / 2i+4p+3m), morphologically and metrically identical anterior teeth, a wrinkled and corrugated enamel, a complete but sinuous and constricted metaloph on P3-P4, a similarly developed metastyle on M3 (incomplete fusion of the ectoloph and metaloph), a low and shallow antero-lingual groove on the hypocone of M3, a forked paralophid on p2, but no labial cingulum on the lower molars, and a similar posterior cingulum on m3 (thin, horizontal, and widely developed transversely). On the other hand, the Na Duong rhino differs from *E. bolcense* in being slightly larger (~10%) and in having a partly closed auditory pseudomeatus, a lingual wall on P3-P4 (only present in some specimens referred to *E. bolcense*), usually no labial or lingual cingula on the upper molars, a protocone that is always constricted on M1-M2 (usually constricted in *E. bolcense*), a long metaloph with respect to the protoloph on M1, a trigonid forming an acute dihedron on lower cheek teeth, and a principally closed posterior valley on p2 (usually closed in *E. bolcense*). It differs from *E. magnum* (Uhlig 1999; Böhme 2001; Uhlig & Böhme 2001; Becker 2009) in the absence of a labial cingulum on the upper molars, a protocone constriction on P3-P4, and a crista on the upper molars, and in the presence of a developed metastyle on M3. Size and general features (enamel thickness; bilophodont DP1; M3 with a smooth antecrochet) closely match the dental remains referred to as *E*. cf. *magnum* from Paali-C2 (Early Oligocene, Pakistan; Antoine et al. 2003b). Yet, several differences are observed, such as a DP1 with an undulated ectoloph (convex in specimens from Paali-C2) or an M3 with a low anterolingual groove on the hypocone (absent), a simple crochet (multiple), and a lingual cingular spur (absent). As a result, the Na Duong rhino is referred to a new species, *Epiaceratherium naduongense*, which is considered a sister taxon to *E. bolcense.*

3.3.2 Herpetofauna

During the excavation campaigns of 2009 to 2012 at Na Duong opencast coal mine more than 150 reptile specimens were found at the base of the main coal seam (base of layer 80). The fossil remains belong to approximately 50 specimens of crocodiles and 100 specimens of turtles. Although not studied to detail yet, the turtle assemblage is known to be considerably diverse (five to six species), comprising aquatic (Trionychidae, soft-shell turtles) as well as semi-aquatic (Geoemydidae, pond turtles) taxa (Böhme et al. 2011). The faunal composition differs significantly from the turtle fauna of the Middle Eocene Youganwo Formation in the Maoming Basin (Guangdong, South China, Junda et al. 1994), which

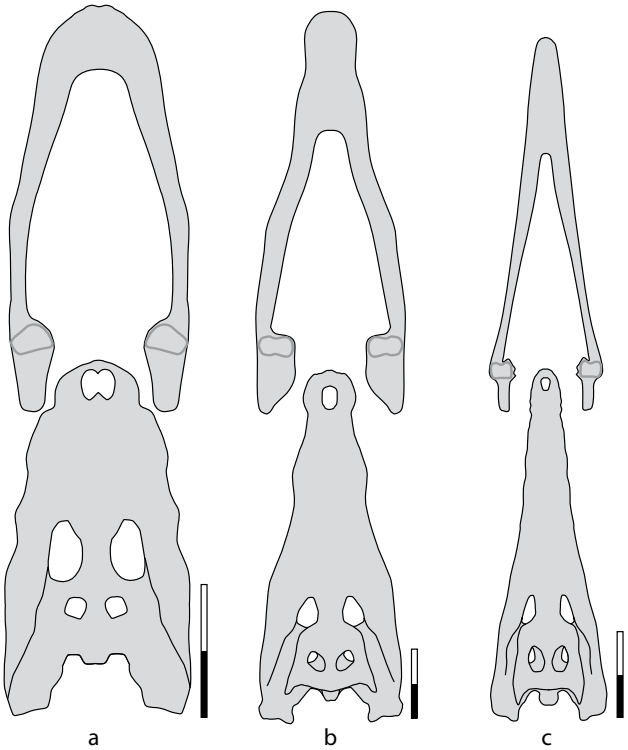

Figure 21: Skull morphotypes of crocodiles. Schematic drawing of the skull outline of the three different crocodylian morphotypes from Na Duong based on several different individuals: a) brevirostrine type, b) longirostrine crocodyline type, c) longirostrine gavialoid type (scale bar: 10 cm).

yields only a few geoemydids and trionychids (Claude et al. 2012), but is dominated by carettochelid turtles (Tong et al. 2010).

Crocodylian remains have been found as articulated or partly articulated skeletons, isolated skulls, and occasionally isolated bones. They can be assigned to three different morphotypes (Fig. 21). (1) The dominant taxon, a brevirostrine, *Alligator*-shaped species, attains a body length of up to 2 m and comprises approximately two-thirds of all specimens. (2) A longirostrine, *Crocodylus*-shaped taxon attains a body length of up to 6 m and comprises approximately one-third of all specimens. Additionally, a single (3) longirostrine, *Gavialis*-shaped specimen with a median skull length of 0.5 m was found.

The three morphotypes clearly refer to different ecologic adaptations, and occupy different trophic levels within the food web, which can also be inferred from the dentition. The longirostrine *Gavialis*-type species is characterized by more or less homodont, acute, elongated, and bicarinate teeth (only slightly more curved in the anterior part of the jaw) and can be interpreted as a fish-hunter, similar to living and fossil gavialoid and tomistomine crocodylians (e.g., Brochu 2001; Brochu 2006). The brevirostrine *Alligator*-type and the longirostrine *Crocodylus*-type taxa both show bivariate heterodont dentition (Fig. 22), with elongated, bicarinate and linguolabially flattened premaxillary and anterior maxillary and dentary teeth. The fifth premaxillary and fifth maxillary teeth are enlarged, and the posterior maxillary and dentary teeth are relatively wider and shorter, and are circular in cross-section at their base. The widened and more robust back teeth clearly show adaptation to hard-shelled or shielded diet. A similar heterodont dentition has been observed in the Eocene genera *Allognathosuchus* and *Wannangasuchus* from North America (Lower Bridger Beds, Wyoming; Mook 1921; Abel 1928; Simpson 1930; Brochu 2001; Brochu 2004). Extreme heterodonty with a globular, crushing posterior dentition was recently described in the Caimaninae *Globidentosuchus brachyrostris* from the Miocene of Venezuela (Scheyer et al. 2013). The observation of heterodont dentition in two taxa with entirely differently shaped snouts co-occurring with a single elongate-slender snouted species is unexpected. Usually sympatric crocodilian taxa show strong annidation and lack similar food adaptation (Brochu 2001).

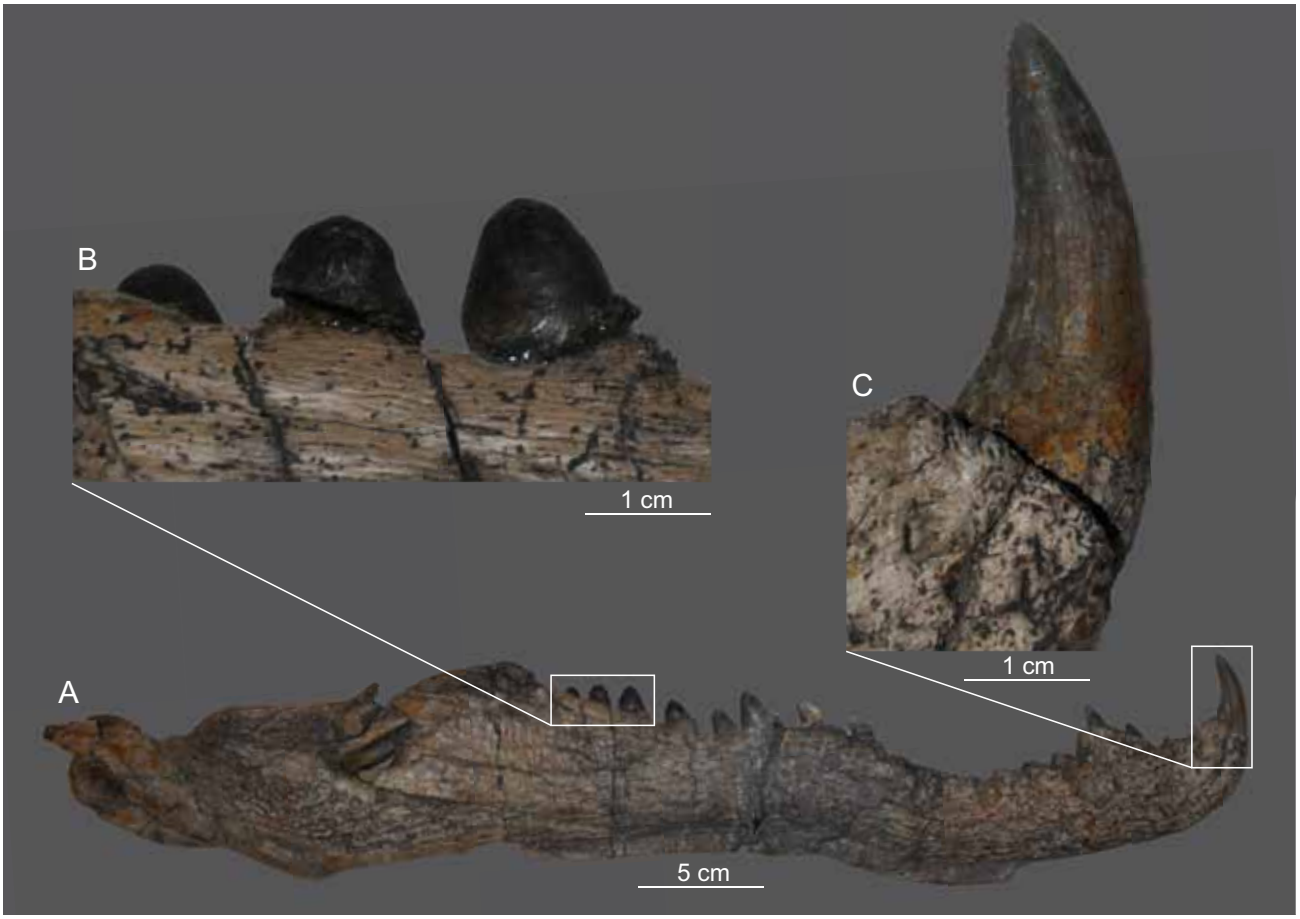

Figure 22: Right lower jaw of the crocodylinae specimen K 22 from layer 80 showing heterodontous dentition; **(A)** overview; **(B)** rounded, posterior dentary teeth; **(C)** acute, anterior cheek-tooth.

Dietary interpretation for heterodontous species ranges from specialized cheloniphagous (Abel 1928) to generally durophagous (Simpson 1930; Brochu 2001; Brochu 2004). A specialization to dominantly cheloniphagous diet seems likely for both the brevirostrine *Alligator*-type and the longirostrine *Crocodylus*-type crocodiles, since bite marks are frequently observed on turtle shell plates, and certain accumulations of turtle remains may represent regurgitates (Böhme et al. 2011: fig. 14). Bite marks on limb bones of large mammals (Böhme et al. 2011: fig. 7C, D) and isolated crocodile skulls with obvious marks of predepositional fragmentation (Fig. 23) may indicate predation on mammals and other crocodiles, in particular by large individuals of the longirostrine *Crocodylus*-type crocodile.

3.3.3 Ichthyofauna

Fish remains are very abundant at Na Duong, but only represented by disarticulated bones and isolated pharyngeal teeth. Fossils belonging to two fish families have been recorded. Remains of Amiidae (bowfins) occur frequently in the basal part of the main coal seam (layer 80), while Cyprinidae (carps and minnows) are abundant in all lacustrine sediments, especially those of the Rhin Chua Formation.

Amiids (Amiinae) are represented by numerous isolated vertebra and cranial bones (Fig. 24A, B); for determination at genus or species level, however, articulated specimens would be required. Based on the largest vertebra found, a maximum body length of approximately 50 cm is calculated. The first Cenozoic amiins from East Asia have recently been described from four formations of Early and Middle Eocene age from central and northern China (Chang et al. 2010). Interestingly, the Na Duong Formation (layer 80) is so far the first stratum in East and Southeast Asia where Amiidae and Cyprinidae are documented as sympatric groups. Na Duong also represents the global southernmost record of crown-group bowfins (Amiinae), which usually live in mid-latitudinal regions of the northern hemisphere.

Among the cyprinids, eight taxa belonging to at least five subfamilies are identified: Barbinae gen. indet. sp. 1, Barbinae gen. indet. sp. 2, Barbinae gen. indet. sp. 3, Cultrinae gen. et sp. indet., Xenocyprininae gen. et sp. indet., ? Acheilognathidae gen. et sp. indet., *Planktophaga minuta* gen. et sp. nov. ('East

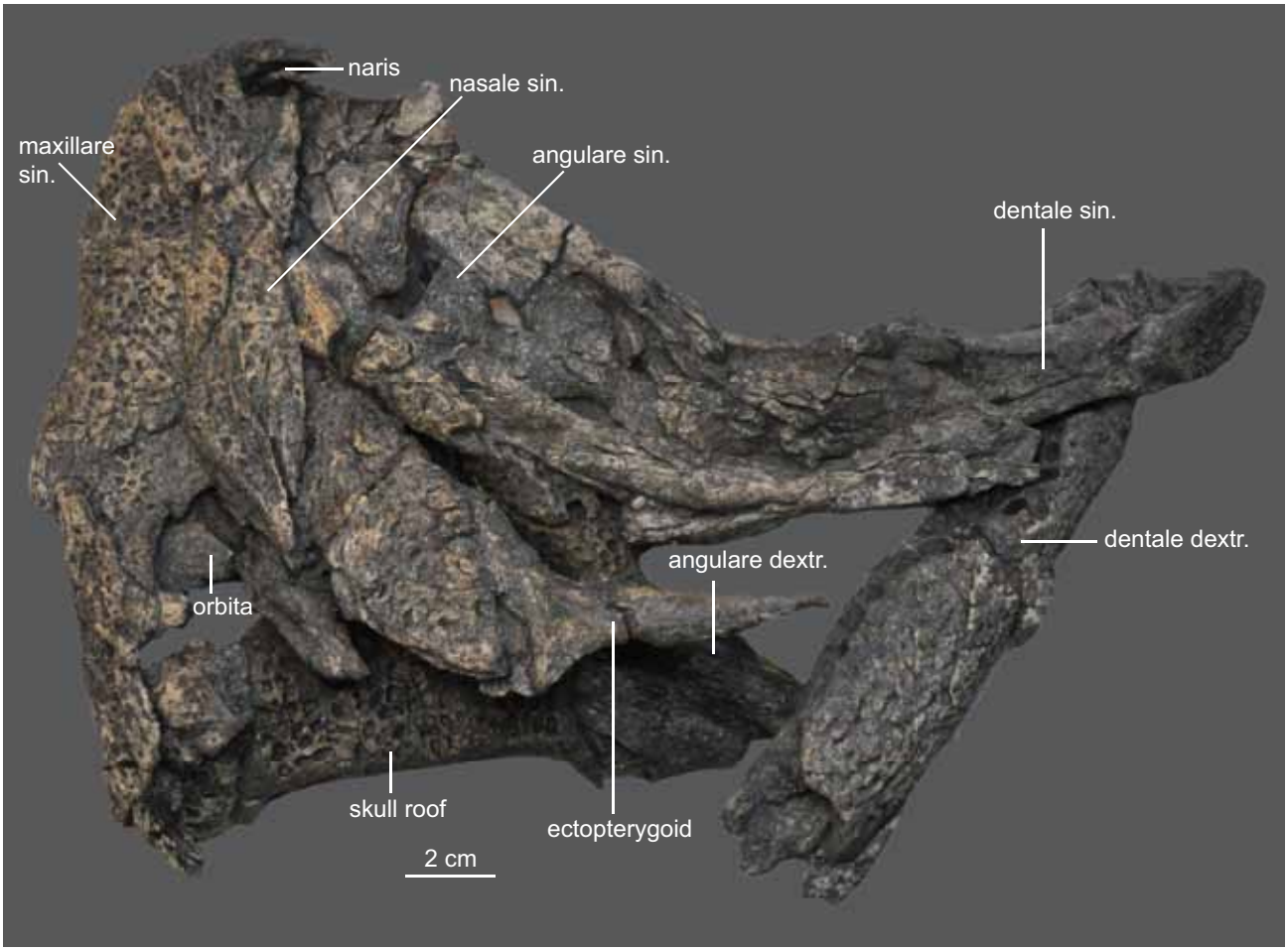

Figure 23: Taphonomic features of a crocodile skull. Skull of a brevirostrine crocodile (specimen K 25) from Na Duong Formation (layer 80). The skull is strongly fragmented along suturelines and several transversal cracks (e.g., posterior end of right dentary).

Asian Group of Leuciscinae' sensu He et al. 2008), and Cyprinidae subfam., gen. et sp. indet. Except for Barbinae gen. indet. sp. 1, all carps are restricted to the Rhin Chua Formation.

Barbinae gen. indet. sp. 1 is typical for the Na Duong Formation and co-occurs with Amiinae gen. et sp. indet. in layer 80. The pharyngeal dentition of this medium-sized carp is developed in three rows; the posterior pharyngeal teeth are characterized by a narrow grinding surface (Fig. 24E) and the anterior tooth A1 is not significantly (globularly) expanded. In contrast, barbins from the Rhin Chua Formation, indentified as Barbinae gen. indet. sp. 2 and Barbinae gen. indet. sp. 3, have expanded, globular A1 teeth, which are terminally hooked (Barbinae gen. indet. sp. 2, Fig. 24J) or flattened (Barbinae gen. indet. sp. 3, Fig. 24C). Posterior pharyngeal teeth of barbins also show two morphotypes: a spoon-like one (Fig. 24F, G) resembling the European Barbus sensu stricto, and a spatula-like one (Fig. 24H, I) resembling the western Eurasian Luciobarbus. However, the attribution of these isolated teeth to either of the two taxa (Barbinae gen. indet. sp. 2 or sp. 3) is impossible.

The pharyngeal teeth of Cultrinae gen. et sp. indet. closely resemble those of extant members of this group (e.g. *Culter, Toxabramis*) in the presence of a narrow grinding surface and a small curved terminal hook (Fig. 24K), which is absent in the pharyngeal teeth of Xenocyprininae gen. et sp. indet. (Fig. 24L). The latter closely resemble the pharyngeal teeth of extant *Acanthobrama*. Tiny, hooked pharyngeal teeth without a grinding surface (Fig. 24D) closely resemble morphotypes described from the Miocene of Japan as Acheilognathinae indet. by Yasuno (1984). Because of limited availability of recent material for comparison, these teeth are tentatively referred to this subfamily. Pharyngeal teeth with a strong and relatively straight terminal hook (Cyprinidae subfam., gen. et sp. indet, Fig. 24M) occur today in several cyprinid subfamilies (e.g. Labeoninae, Cultrinae, and Leuciscinae) and are therefore difficult to determine below family level.

Finally, one cyprinid pharyngeal tooth type from Na Duong is morphologically well distinct from all documented living and fossil cyprinids, and thus assigned to a new genus and species below.

Class Actinopterygii Cope, 1887
Order Cypriniformes Bleeker, 1859
Family Cyprinidae Bonaparte, 1832
'East Asian Group of Leuciscinae' He et al., 2008

Genus *Planktophaga* gen. nov.

Etymology: Greek for "plankton eater".

Type species: *Planktophaga minuta* sp. nov.

Diagnosis: Same as for type species.

Planktophaga minuta sp. nov.
Fig. 24O–Q

Holotype: isolated pharyngeal tooth (Fig. 24P), GPIT/OS/817

Type locality: Na Duong coal mine, northern Vietnam

Type horizon and stratigraphy: Rhin Chua Formation, layer 11 (Böhme et al. 2011), corresponding to ~155 m in Figure 2, late Middle to Late Eocene.

Etymology: Latin for "very small".

Referred material: three additional isolated pharyngeal teeth from the same horizon; GPIT/OS/816 (Fig. 24O), GPIT/OS/818 (Fig. 24Q).

Diagnosis: Pharyngeal teeth small (up to 3 mm high), resembling teeth of extant *Hypophthalmichthys* with regard to general morphology, but differing from the latter in the shape and position of the grinding surface, which is (1) transversally convex and longitudinally concave (flat in *Hypophthalmichthys*), (2) has a proximal emargination and irregular-oval general outline (regular-oval in *Hypophthalmichthys*), and (3) is longitudinally inclined (bent), forming an angle of 120–130˚ with the tooth neck (~170˚ in *Hypophthalmichthys*).

Remarks: Cyprinids are the most diverse living freshwater fish family of the world (Nelson 1994), and their systematic arrangement is still highly controversial and unsettled (He et al. 2008). It is well established that the morphology of pharyngeal teeth may differ significantly between the more than 200 living genera, and thus often provides key characters for their systematic arrangement, at least at genus level (Haeckel 1843). The peculiar pharyngeal tooth morphology of *Planktophaga minuta* gen. et sp. nov. has only a single living analog in the genus *Hypophthalmichthys* (*H. molitrix, H. nobilis,* and *H. harmandi*; silver and bighead carps), which comprises large, filter-feeding, planktivore carps native to East Asia (Kolar et al. 2005). The close morphologic similarity between *Hypophthalmichthys* (Fig. 24N) and the new taxon suggests a similar feeding strategy for the Eocene fish, and most probably a basal phylogenetic position with regard to *Hypophthalmichthys*. The earliest fossil representatives of *Hypophthalmichthys* are documented from the late Early Miocene of eastern China (Xiacaowan, Li et al. 1985), and thus from sediments that are approximately 20 million years younger than those of the Rhin Chua Formation.

Discussion: A high cyprinid diversity is also recorded from the Paleogene (?Eocene) Cao Bang Basin in northern Vietnam (Böhme et al. 2011). Similar to the fauna from the Rhin Chua Formation at Na Duong, the assemblage from Cao Bang is dominat-

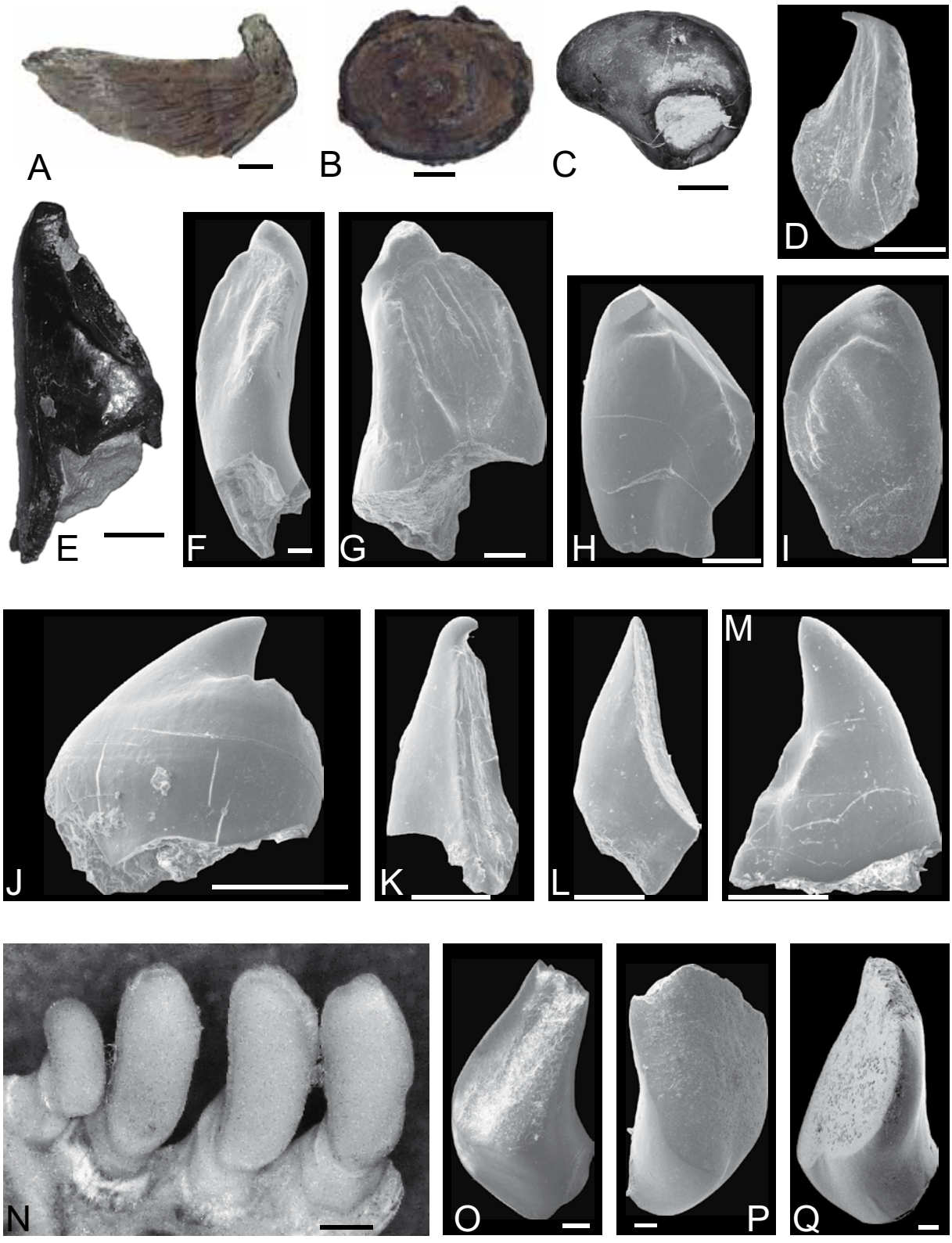

Figure 24: Freshwater fishes from the Na Duong section; **(A)** Amiinae indet., right suboperculum (Na Duong Fm., layer 80; GPIT/OS/803); **(B)** Amiinae indet., trunk vertebra (Na Duong Fm., layer 80; GPIT/OS/804); **(C)** Barbinae sp. 3, flat globular A1 pharyngeal tooth (Rhin Chua Fm., layer 6; GPIT/OS/805); **(D)** ?Acheilognathinae indet., pharyngeal tooth (Rhin Chua Fm., layer 8/9; GPIT/OS/806); **(E)** Barbinae sp. 1, posterior pharyngeal tooth from the main tooth-row (Na Duong Fm., layer 70; GPIT/OS/807); **(F, G)** Barbinae sp. 2 or 3, spoon-shaped posterior pharyngeal teeth (Rhin Chua Fm., layer 8/9; GPIT/OS/808, 809); **(H, I)** Barbinae sp. 2 or 3, spatula-shaped posterior pharyngeal teeth (Rhin Chua Fm., G from layer 8/9, GPIT/OS/810; H from layer 18, GPIT/OS/811); **(J)** Barbinae sp. 2, hooked globular A1 pharygeal tooth (Rhin Chua Fm., layer 8/9; GPIT/OS/812); **(K)** Cultrinae indet., pharyngeal tooth (Rhin Chua Fm., layer 18; GPIT/OS/813); **(L)** Xenocyprininae indet., pharyngeal tooth (Rhin Chua Fm., layer 8/9; GPIT/OS/814); **(M)** Cyprinidae indet., anterior pharyngeal tooth cusp (Rhin Chua Fm., layer 18; GPIT/OS/815); **(N)** *Hypophtalmichthys molitrix*, pharyngeal tooth row, Recent; **(O–Q)** *Planktophaga minuta* nov. gen. et sp., pharyngeal teeth, (Rhin Chua Fm., layer 11), P holotype (GPIT/OS/817), O, Q paratypes (GPIT/OS/816, 818). Scale bars: 2.5 mm (A, B, N), 1 mm (C, E), and 0.25 mm (D, F–M, O–Q).

ed by barbins, xenocyprinins and cultrins. A cyprinid closely related to cultrins and xenocyprinins has also been described from the ?Early Oligocene of the adjacent Ningming Basin (Guangxi, South China; 50 km to the north of Na Duong; Chen et al. 2005). As a result, typical late Paleogene (>30 Ma) freshwater fish faunas from the Vietnamese-Chinese borderlands may be characterized by the co-occurrence of xenocyprinin, cultrin, barbin, and possibly acheilognathin cyprinids. This composition is significantly different from the present-day Southeast Asian ichthyofauna of the Mekong drainage system (Rainboth 1991), which lacks acheilognathins, xenocyprinins, and cultrins other than hemicultrines (Dai & Yang 2003). The fossil cyprinid ichthyofauna from Na Duong has its closest biogeographic affinities to the fishes from the present-day Pearl River and Yangtse River drainage systems [see Bănărescu & Coad (1991) and Rainboth (1991) for a biogeographic summary of living Asian cyprinids].

Interestingly, several morphologic and molecular phylogenies (e.g. Cavender & Coburn 1992; Liu & Chen 2003; Chen et al. 2005) identify the cultrins and xenocyprinins as a monophyletic group, which forms a well supported clade together with the 'southern leuciscines' (including *Hypophthalmichthys*), referred to as the 'East Asian Group' (He et al. 2008). It has been proposed that the limited evolution observed in certain sectors of the nuclear genes of this clade may relate to rather conservative evolution (He et al. 2008). Our results are in line with this hypothesis, since they demonstrate that cultrins, xenocyprinins, and a genus closely allied to *Hypophtalmichthys* occurred in East Asia at least 34 million years ago.

3.3.4 Malacofauna

The Na Duong and Rhin Chua formations both yield rich mollusk assemblages (Böhme et al. 2011). A systematic account of the Unionidae from Na Duong was recently published by Schneider et al. (2013). In the Na Duong Formation, shells are restricted to marly intervals intercalating with the coal seams. Judging from the rich and diversified vertebrate fauna preserved at the base of the main coal seam at Na Duong coal mine, which indicates a prolific environment, it may be assumed that mollusks also were abundant in the coal swamps. Most likely, the lake water has been rather soft and enriched in humic acid during these intervals and the shells have been dissolved immediately after the animals passed away (see discussion in Schneider et al. 2013).

Most characteristic of the Na Duong mollusk assemblage are specimens of the small unionine bivalve ?*Nodularia cunhatia* (Fig. 25B). Moreover, the anodontiform bivalve *Cristaria mothanica* occurs in large numbers (Fig. 25A). Both species are usually found with contiguous valves, indicating autochthonous deposition. Frequently, these two species are joined by large, smooth-shelled viviparid gastropods (Böhme et al. 2011). Furthermore, an indeterminable species of anodontine mussels and a cerithioid gastropod (?*Brotia* sp., Fig. 25C) occur accessorily.

The Rhin Chua Formation also yields *Cristaria mothanica*. Additionally, a few specimens that are tentatively assigned to the posteriorly tapering unionine genus *Cuneopsis* have been recorded (Schneider et al. 2013). New excavations in spring 2012 have unearthed several individuals of an additional, still undescribed, large, alatiform unionid, which closely resembles the recent genus *Hyriopsis* with regard to exterior shell shape. Furthermore, highly abundant Viviparidae occur and may form coquinas reaching several decimeters in thickness, often accompanied by strongly ornamented cerithioid gastropods (?*Tarebia* sp., Fig. 25D).

3.3.4.1 *Unionid affinities*

The bivalve fauna of the Na Duong and Rhin Chua formations comprises genera that persist until today, mostly within rivers and lakes in China and northern Vietnam. This also holds true for the fossil bivalve fauna of the presumably contemporaneous Cao Bang Basin (CB) situated approximately 100 km to the north-northwest of Na Duong (Schneider et al. 2013). Consequently, the genera *Cristaria*, *Cuneopsis* and *Lamprotula* (CB only), and, pending on correct tentative assignment, also *Nodularia*, *Hyriopsis* and *Lanceolaria* (CB only) have their origins in the Eocene or earlier. To date, none of the unionid genera from Na Duong has been reported from contemporary sedimentary basins in adjacent China, Thailand or Laos. Moreover, the records from Vietnam clearly provide first occurrence dates for all genera except *Cristaria*, which has several dubious early records from other regions (see Schneider et al. 2013 for details).

Caused by the collision of the Asian and Indian plates and the resulting uplift of the Himalaya, all major rivers of continental Southeast Asia originate from a comparably small area on the South Tibet Plateau (Clift et al. 2008). Due to the complex tectonic history of Southeast Asia, drainage patterns have repeatedly shifted during the Cenozoic (see Köhler et al. 2012 and Schneider et al. 2013 for brief summaries). In particular, the Red River has undergone dramatic changes in several steps. Presumably, the expansive catchment area of the Eocene to Lower Miocene Paleo-Red River incorporated major parts of the upper reaches of the modern Yangtze and Pearl rivers. During the Miocene, the Paleo-Red River lost its Yangtze portion, but the Pearl River headwaters prevailed within the system until the rivers shaped to the present constellation during the Pliocene (see Clift et al. 2008 and Hoang et al. 2009 for details). This scenario is largely reflected in the fossil and extant distribution patterns of freshwater mussels. With exception of the generalist *Cristaria*, the

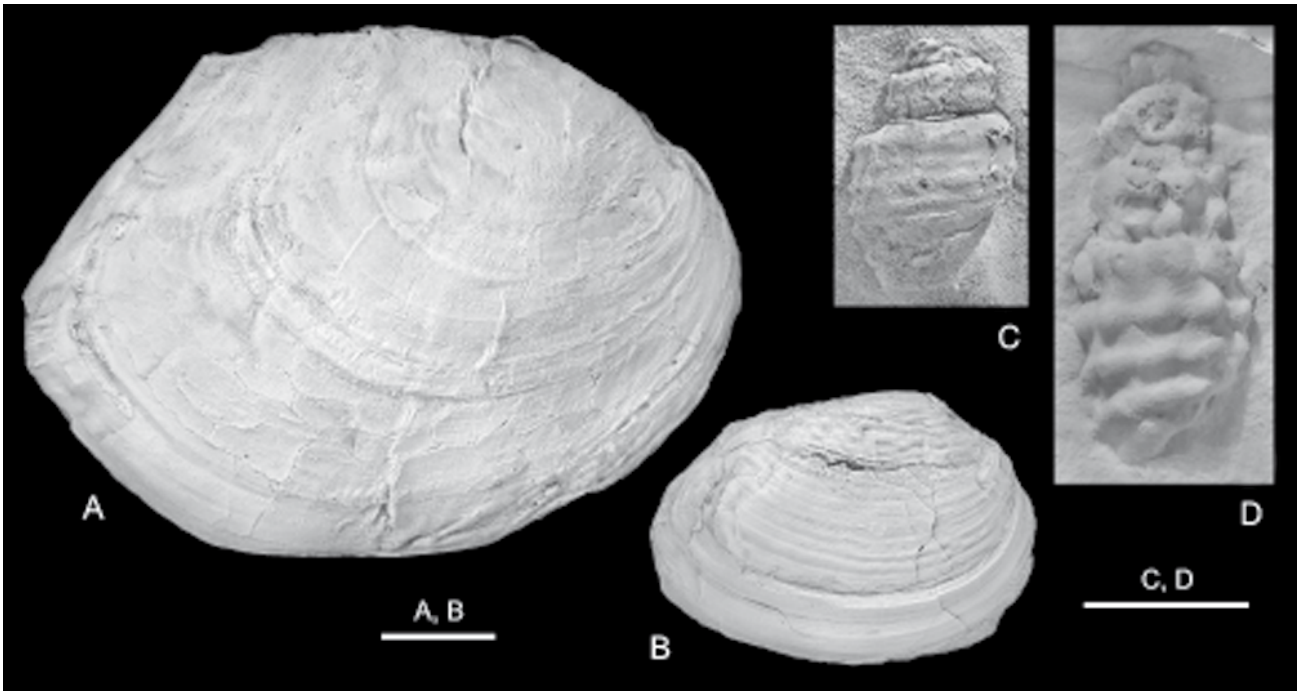

Figure 24: Mollusks from the Na Duong coal mine; **(A)** *Cristaria mothanica* Schneider, 2013, holotype, articulated specimen with fully preserved shell, right valve view (Na Duong Fm.; GPIT/BI/5567); **(B)** ?*Nodularia cunhatia* Schneider, 2013, paratype, short articulated specimen ornamented with rugae, right valve view (Na Duong Fm.; GPIT/BI/5560); **(C)** ?*Brotia* sp., fragmentary specimen with remnants of shell (Na Duong Fm.; GPIT/GA/5053); **(D)** ?*Tarebia* sp., latex cast (Rhin Chua Fm.; GPIT/GA/5052).

unionid genera listed above basically share a common distribution across the Red River, Pearl River, and Yangtze catchment areas, but are absent from more southerly rivers, e.g., the Mekong, Chao Phraya, and Salween (Schneider et al. 2013). Most of the respective extant unionid species, however, occur in only one of the Yangtze, Pearl, and Red River drainage systems, probably reflecting the gradual decoupling of the rivers during the Neogene.

Potential affinities of fossil European unionid faunas with recent genera from East and Southeast Asia have repeatedly been discussed. The taxa that were proposed to occur disjoint in Europe and East Asia, e.g. *Hyriopsis*, *Cristaria*, *Cuneopsis*, and the 'Lamprotulinae' of Modell (1964), were usually considered relics of a once continuously distributed fauna that had been split by the Indian-Asian collision (e.g., Schütt 1993). However, parallelization of Mesozoic and Recent forms as attempted by Modell (1964) is today regarded as misleading (Watters 2001; Schneider et al. 2013). Anyway, in Europe all fossil unionids of potential Asian affinities occur in Oligocene to Pliocene strata and fossil evidence for the proposed common fauna in pre-collision times is lacking. For extant mussel genera, close affinities have at least in part been ruled out by molecular phylogenetics (e.g., Graf & Cummings 2007; Whelan et al. 2011).

Ecological aspects strongly argue against an invasion of freshwater bivalves from Asia subsequent to the *Grande Coupure*. Freshwater bivalves do not easily enter new water bodies. Apparently, even neighboring rivers in Asia have stocks of different species and genera, indicating that dispersal across catchment boundaries is an exception (Köhler et al. 2012; Schneider et al. 2013). In our case, the unionids would have needed to cover a distance of more than 8000 km, crossing several major mountain ranges devoid of suitable environment for unionid settlement on their way. Moreover, solid fossil or extant evidence for such migration, which should be available from river basins in between East Asia and Europe, is lacking. To sum up, the scenarios outlined by Wenz (1942), Modell (1964), Schütt & Besenecker (1973), Schütt (1993) and others cannot be confirmed by solid data, and obviously result from misinterpretation of the striking convergence of unionid taxa produced during distinct faunal radiations.

3.3.4.2 *Gastropod affinities*

A solid interpretation of the gastropod fauna of the Na Duong and Rhin Chua formations is hampered by the limited preservation of the specimens, lacking well-preserved early ontogenetic shell portions. On one hand, adult shell morphology of Cerithioidea may vary strongly within families, genera, and species; on the other hand, it is highly convergent in different families, including the Pachychilidae and Thiaridae (e.g., Glaubrecht et al. 2009; Köhler et al. 2009; Strong et al. 2011). Thus, assignment of the gastropods from Na Duong is very much tentative and arbitrary, and simply based on overall resemblance of typical recent species.

As has been proposed for other widespread gastropod lineages (e.g., Davis 1979), the Pachychilidae and Thiaridae are assumed to be of Gondwanan origin, occurring today in South and Central America, Africa, Southeast Asia, and Australia (e.g., Köhler & Glaubrecht 2007; Strong et al. 2008; Köhler & Dames 2009). It would thus seem reasonable to assume that, similar to the Pomatiopsidae (Davis 1979; Neubauer et al. 2012), early Cenozoic representatives of these families entered Southeast Asia subsequent to the Indian-Asian collision, used the Paleo-Red River as a distribution vector, and consequently appear in Paleogene sediments of the respective catchment area at Na Duong. Molecular data, however, indicate the opposite way of propagation for Pachychilidae, i.e. pachychilids from an Asian stock entered the Indian Subcontinent (Köhler & Glaubrecht 2007). Present day Asian Pachychilidae are spread over eastern India, continental Southeast Asia, southern China and Indonesia (Köhler & Dames 2009; Köhler et al. 2010). Interestingly, molecular data confirm a distinct subclade that is confined to Vietnam and southern China, i.e. mainly to the Red River, Pearl River and southern Yangtze catchment areas (*Sulcospira* C subclade of Köhler & Dames 2009), thus suggesting a distribution pattern that is basically similar to the one seen in the Unionidae. The closely related Semisulcospiridae, which often display morphologies rather similar to those seen in the two aforementioned families also occur with an extant species in Vietnam (Strong & Köhler 2009), and may have fossil forerunners in the area.

Today, Pachychilidae, Thiaridae, and Semisulcospiridae do not occur with autochthonous species in Europe. However, both the Pachychilidae and Thiaridae were present in Europe significantly before the *Grande Coupure*. The Pachychilidae exhibit a fairly continuous fossil record from the Early to Middle Eocene (Lutetian; *Gantmelanatria*; Hungary, Italy) up to the Late Miocene (Tortonian; *Tinnyea*; Central and Southern Europe; Kowalke 2001, 2004). The European fossil species obviously lack the typical brood pouch of modern East Asian representatives and thus clearly represent a distinct evolutionary lineage (Kowalke 2004). The Thiaridae appeared parallel to the Pachychilidae in the Middle Eocene (Lutetian; *Melanotarebia*, *Bayania*; Hungary; Bandel & Kowalke 1997; Kowalke 2001).

For smooth-shelled Viviparidae like those occurring at Na Duong it is impossible to seriously propose any paleo-biogeographic patterns or potential origins. Viviparids occur on all continents except Antarctica and South America (where they are recorded as fossils; Wenz 1938–1944), indicating Pangean instead of Gondwanan origin, and their phylogeny is less well understood than in the families discussed above (Strong et al. 2008). Several scholars, e.g., Neumayr (1883) and Odhner (1930) have proposed close relationships between strongly ornamented East Asian and European fossil Viviparidae. However, these phenomena were already revealed as convergences and the misinterpretations rejected by Annandale (1919, 1924), who studied fossil and extant Viviparidae from Southeast Asia, in particular with regard to the evolution of shell sculptures (see also Ying et al. 2013 for a brief overview). In summary, there is no evidence for migrations of freshwater gastropods between Asia and Europe during the Late Eocene to Oligocene.

3.3.5 *Vegetation reconstruction from macroflora and chemofossils*

During fieldwork in the years 2009 to 2012 numerous plant macrofossils have been discovered, although plant-bearing horizons were not systematically sampled so far. The main coal seam at Na Duong (layer 80 of Fig. 2) contains abundant unidentified calcified tree trunks with stem diameters of up to more than one meter, and up to one meter long stems of large arborescent Osmundaceae (royal ferns) (Böhme et al. 2011: fig. 5A).

Fossils of aquatic plants are particularly abundant in unlaminated dark-brown lacustrine claystones. Especially layers 81 and 83, directly below the main seam containing the fossil vertebrates, yielded numerous seeds, which are tentatively assigned to *Nelumbo* (lotus, Fig. 26C). Rhizome tubers and plant bases with attached rootlets, which probably also belong to *Nelumbo* (Fig. 26D, E) are common in layer 70 (misidentified as remains of the lycopsid *Isoëtes* in Böhme et al. 2011). Leaves and rhizoms of the genus *Nelumbo* have recently also been described from the Eocene flora of the Changchang Basin, Hainan Island (southern China, He et al. 2010).

Of particular interest for paleobotany are laterally restricted interbeds in the upper part of the main coal seam (layers 80B and 80D), which, based on their geometry, may be interpreted as distal deltaic bottom-set beds. These horizons yielded abundant angiosperm leaves and fragments of ferns (Figs 26A, 27). Surprisingly, the majority of the leaves has non-entire (toothed) margins (Fig. 26G–K), a character commonly associated with plants from rather temperate climates (Wolfe 1979; Wilf 1997; Greenwood 2005; Traiser et al. 2005), but not expected to dominate a leaf flora from sediments deposited under subtropical to tropical conditions, as assumed for the Na Duong Formation (Böhme et al. 2011). However, the dominance of leaves with toothed margins may be explained by the fluvial origin of the respective sediment layers. Vegetation on wet soil, e.g. on river banks, usually has a higher proportion of taxa growing leaves with toothed margins than vegetation from more mesic habitats (Burnham et al. 2001). A single leaf with a deeply emarginate apex and legume-like venation pattern resembles the legume genus *Bauhunia* (Fig. 26B), a pantropical genus of about 300 species. This

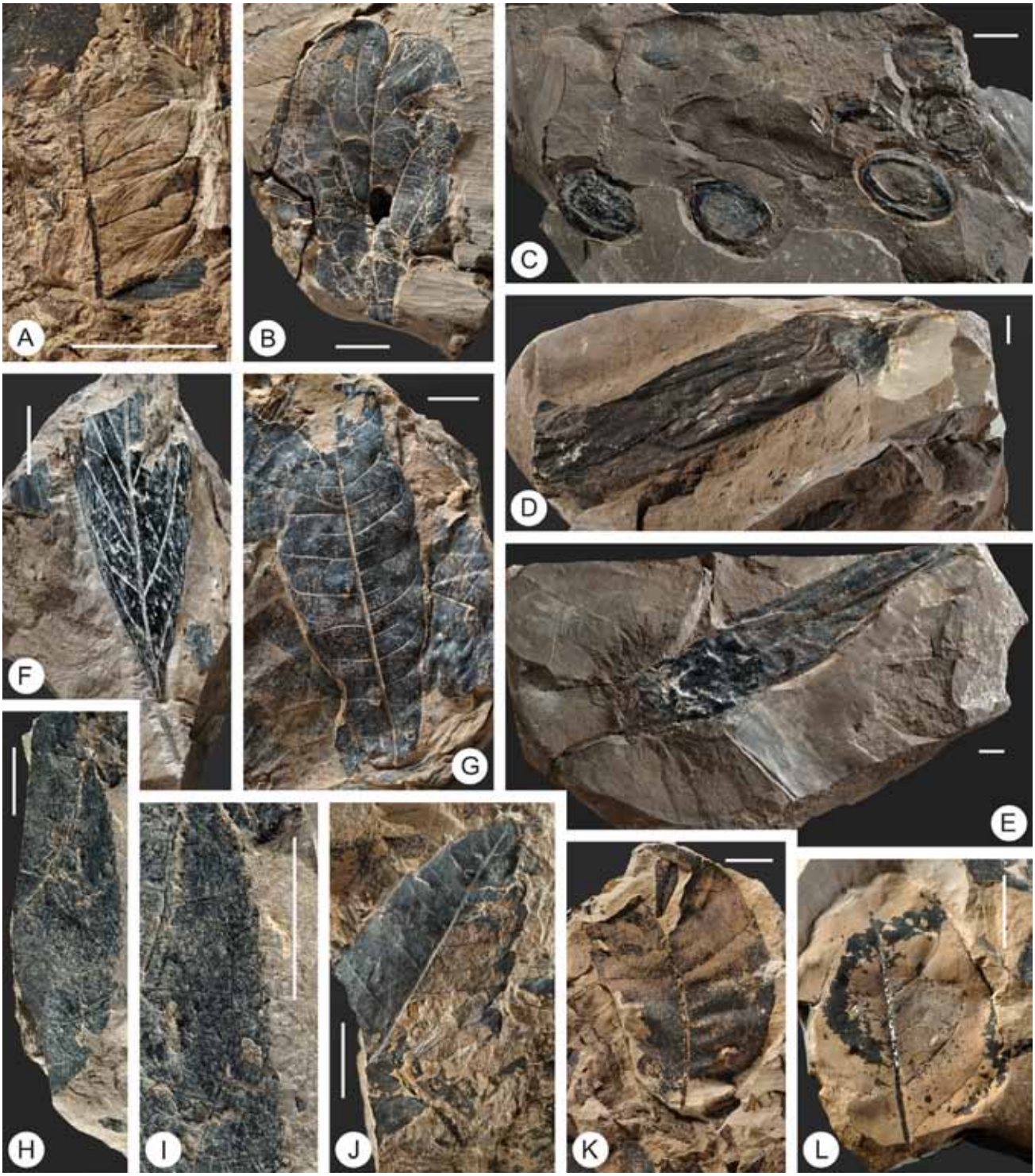

Figure 26: Selected plant remains from the Na Duong Formation (all scale bars = 1 cm); **(A)** Fragment of a fern with open, dichotomous venation, morphologically resembling *Pronephrium stiriacum* (Unger) Knobloch & Z. Kvaček from the European Tertiary (layer 80B, GPIT/PL/619); **(B)** Leaf of *Bauhinia* sp. (layer 80B, GPIT/PL/611); **(C)** Seeds of *Nelumbo* sp. (layer 81, GPIT/PL/609); **(D)** Rhizome of *Nelumbo* sp. (layer 70, GPIT/PL/610); **(E)** Bulbous base of a plant of *Nelumbo* sp. with attached rootlets (layer 70, GPIT/PL/617) (misidentified by Böhme et al., 2011 as *Isoëtes* sp.); **(F)** Unidentified entire margined leaf (layer 80B, GPIT/PL/612); **(G)** Unidentified non-entire margined (toothed) leaf morphologically resembling the extinct Fagaceae *Eotrigonobalanus furcinervis* (Rossmaessler) Walther & Z. Kvaček from the European Paleogene (layer 80B, GPIT/PL/619); **(H)** Unidentified non-entire margined (toothed) leaf with closely spaced teeth (layer 80B, GPIT/PL/613); **(I)** Detail of H showing small teeth on leaf margin; **(J)** Unidentified non-entire margined (toothed) leaf with relatively coarse teeth (layer 80B, GPIT/PL/618); **(K)** Unidentified non-entire margined (toothed) leaf with widely spaced, small teeth (layer 80B, GPIT/PL/620); **(L)** Unidentified entire margined leaf (layer 80B, GPIT/PL/616).

genus includes numerous lianas (Wunderlin et al. 1987), which generally have a higher proportion of toothed-leaf taxa than zonal vegetation (Burnham et al. 2001). *Bauhunia* is also known from the Late Eocene–Oligocene of Guangxi in southern China (Chen & Zhang 2005).

Figure 27: Overview of leaves on surface of rock sample from layer 80B (GPIT/PL/621).

Superficially, the leaf flora from Na Duong resembles the Lower Oligocene floral complex of Haselbach in central Germany (Mai & Walther 1978). However, due to highly homologous leaf forms in systematically unrelated taxa solid determination of fossil leaves based only on general shape and venation is impossible. Accordingly, previous determinations of macroflora from Na Duong by Dzanh (1996) are doubtful since they are only based on general morphology. Cuticules, which would provide reliable information on systematic affinities, have not been analyzed to date. Gross morphologic similarity of taxonomically unrelated floras, however, may still preserve an ecological signal. The leaves from layers 80B and 80D are thus interpreted as riparian elements adapted to high water tables.

Zonal vegetation during the formation of the Na Duong Formation is indicated by relative abundance of fossil resin. Allochthonous, honey-coloured up to 2 cm large pieces occur in greyish-brownish, non-lacustrine clay- to silt-stones, often directly above coal layers (e.g. layers 26, 59, 70, 79), where sediments are rich in organic detritus (up to the size of small tree trunks). Resin also occurs within coal seams (layer 71, 80), usually forming elongate agglomerations in lignified wood, probably filling former resin canals. To infer on the botanical affinities of the resin, one sample from the sediments of layer 59 and a second sample from the lignified wood of layer 71 were spectroscopically analyzed.

The two resin samples were found to be spectroscopically identical (Fig. 28). Comparison with the spectrum of a modern Asiatic dipterocarp resin from *Shorea rubriflora* (Dipterocarpaceae) shows close similarities, particularly in the spectral region of 1500–1350 cm^{-1}. This region is most distinctive for the identification of different types of resin and their botanical source (Tappert et al. 2011). The absorption peak triplet located between 1400–1350 cm^{-1}, in combination with a single broad peak at 1460–1455 cm^{-1} is characteristic for dipterocarp resins (Fig. 29). Chemically, dipterocarp resins primarily consist of polymerized sesquiterpenoids (mainly cadinene) and triterpenoids (Anderson et al. 1992). Although the Na Duong resins show the characteristic spectral features of dipterocarp resins, slight differences to the spectrum of the modern *Shorea* resin exist, particularly in the spectral range of 1350–650 cm^{-1} (Fig. 29). These differences are probably due to a lower degree of polymerization of the modern *Shorea* resin compared to the fossil resins. This notion is supported by the presence of a high hydroxyl (OH) peak in the *Shorea* resin spectrum (located between 3700–3100 cm^{-1}) and its absence in the Na Duong resins. However, it cannot be excluded that Na Duong resins were produced by a member of the Dipterocarpaceae, which produced compositionally slightly different resins compared to modern *Shorea*.

These result clearly suggest botanic affinities of the allochthonous and autochthonous resins to the Dipterocarpaceae, which obviously played an important role in the zonal vegetation of the Na Duong Formation. Dipterocarps (sensu lato) are a pantropic, mostly evergreen angiosperm family, which is highly diverse in Southeast Asia (Maury-Lechon & Curtet 1998). Today, their up-to-more-than-70-meters-tall trees (Yamakura et al. 1986) comprise the most conspicuous elements of the upper canopy in both everwet rainforests and seasonal forests in Southeast Asia.

The earliest dipterocarps (resin, pollen) have been documented from the Early Eocene (53 Ma) of India, which suggests that these trees may have started colonizing Southeast Asia subsequent to the Indian-Asian collision (~50 Ma; 'out-of-India' dispersal; Rust et al. 2010; Dutta et al. 2011). Fossil macrobotanic remains of dipterocarps (*Shorea maomingensis)* have recently been described from the Late Eocene Huangniuling Formation (Maoming Basin, Guangdong, South China; Feng et al. 2013). Together with our results these data suggest that Dipterocarpaceae may have been an important element of the Late Eocene zonal vegetation of East and Southeast Asia.

4. Synthesis

4.1 Mammalian biochronology and stratigraphy of Na Duong

4.1.1 Stratigraphic background

Na Duong is the first locality in Eurasia where species closely related to *Epiaceratherium bolcense* and *Bakalovia palaeopontica* occur together. With regard to European mammal biochronology (Schmidt-Kittler et al. 1987), this association – at genus level, given that both taxa are new species – would indicate placement in the interval of MP18 to MP21 (FADs of European Anthracotheriidae and Rhinocerotidae), extending from the Late Eocene to the basal Oligocene. However, the stratigraphic evaluation is complicated by the still poorly understood continen-

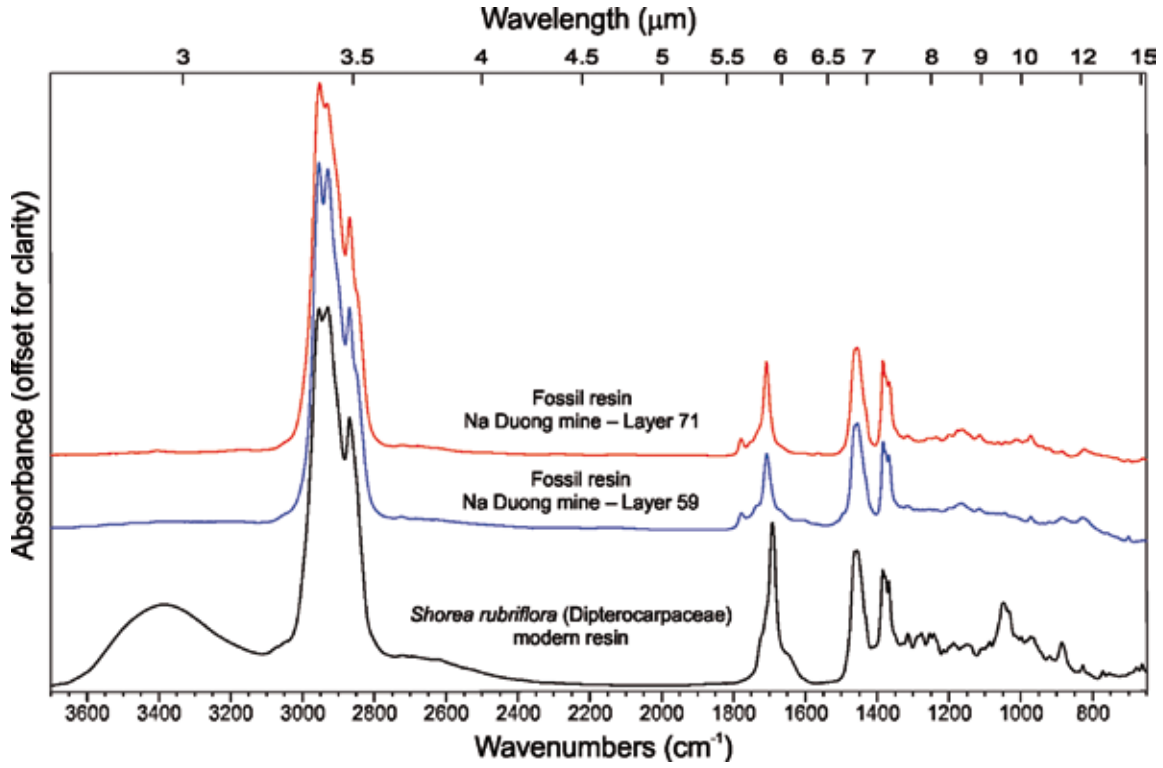

Figure 28: FTIR overview spectra of fossil resins from the Na Duong coal mine. The spectrum of a modern dipterocarp resin, in this case from *Shorea rubriflora,* is shown for comparison. The broad peak between 3700–3100 cm^{-1} in the spectrum of *Shorea rubriflora* is due to a higher abundance of free OH-groups in the *Shorea* resin compared to the fossil resins, and indicates a lower degree of polymerisation.

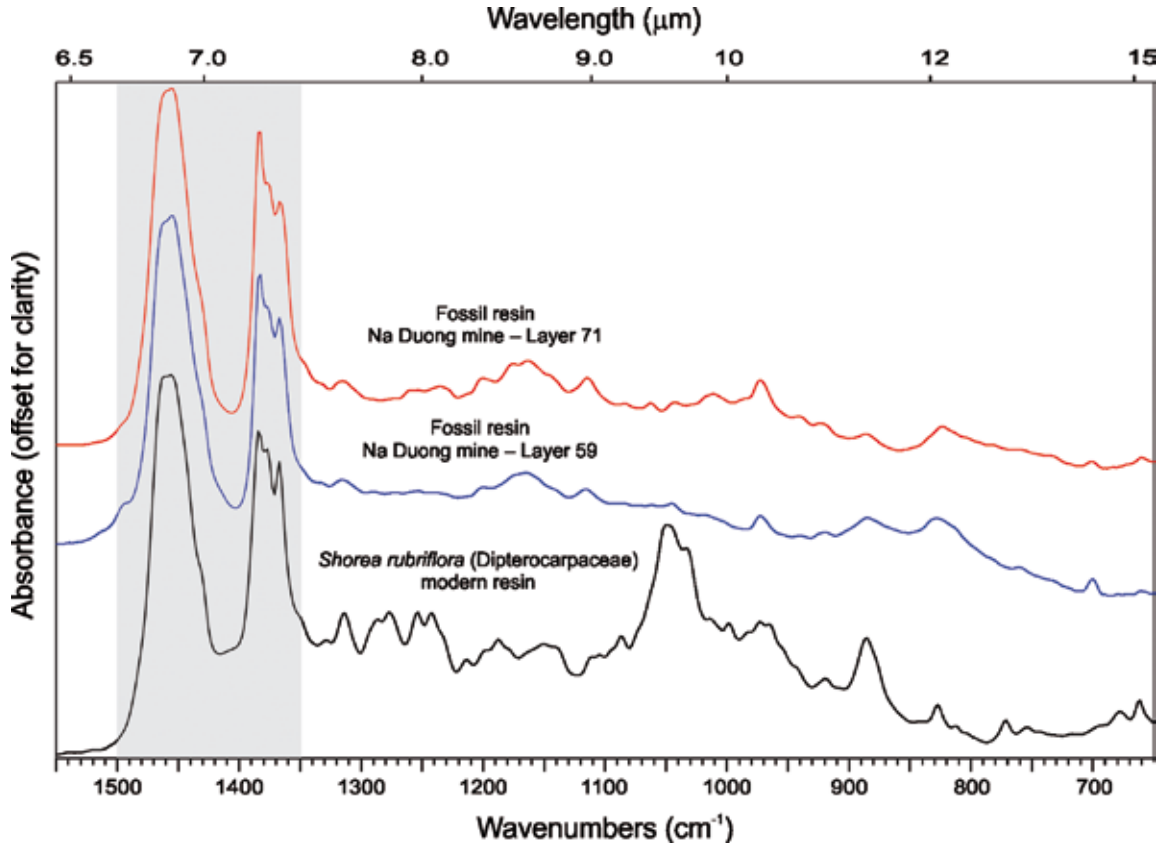

Figure 29: FTIR close-up spectra (fingerprinting region) of fossil resins from the Na Duong coal mine. Close-up of the FTIR spectra of fossil resins from the Na Duong mine and a modern resin from *Shorea rubriflora* in the spectral region between 1550–650 cm^{-1}. The grey box marks the spectral region that is most characteristic for different types of resin.

tal Paleogene Eurasian mammalian biogeography (Heissig 1979). Because reliable chronostratigraphic tiepoints are rare (Russell & Zhai 1987), a continental scale mammalian biostratigraphy can currently not be established. This is especially true for the Eocene of Southeast Asia (Burma, Yunnan, Guangxi, Vietnam, and Thailand), where only two fossil mammal faunas are dated independently from mammal biochronology.

One of these is the Pondaung Formation (Burma), which is overlain by marine Priabonian limestones (Cotter 1938). The lower member of the Pondaung Formation interfingers with marine Bartonian sediments (Bender 1983). Moreover, zircons from volcanic ashes within the upper member, situated just above the bone-bearing strata have been dated by fission-track method to 37.2 ± 1.3 Ma (Tsubamoto et al. 2002; Maung et al. 2004), therefore indicating a latest Bartonian to early Priabonian age for the mammalian assemblage from Pondaung. The second independently dated Paleogene mammal assemblage from Southeast Asia comes from the Krabi Basin (Thailand), where paleomagnetic analysis (Benammi et al. 2001) documents inverse polarization of the 100 m-long section, which has been correlated to chron C13r (latest Eocene) or alternatively to chron C12r (Early Oligocene).

In addition to Southeast Asia, the late Paleogene terrestrial sediments from Tethyan islands and micro-continents (e.g. Tisza, Dinaria, Balcano-Rhodopia, Anatolia; see Fig. 30), which yielded mammalian faunas of Asiatic affinities (Heissig 1979), provide two chronostratigraphically tied mammal localities, i.e. the browncoal mine of Tscherno More in Bulgaria (type locality and single occurrence of *Bakalovia palaeopontica*), and the Valea Nadasului Formation (Rădaia locality) in Transylvania (Romania). In Tscherno More, palustrine and lacustrine mammal-bearing sediments of the Ravnec Formation contain Bartonian palynomorphs (Cherniavska 1970) and are transgressively overlain by marine Priabonian marls that yielded planktonic foraminifers indicating zone P15 (Juranov 1992). The mammal assemblage of Tscherno More (Nikolov & Heissig 1985) is thus essentially contemporary with the Pondaung fossils (late Bartonian). The continental Valea Nadasului formation follow above the marine Vistea Limestone and the Ciuleni Formation, which contain lower Priabonian nummulites and nannoplankton referred to zones SBZ 19 and NP 18, respectively (Rusu et al. 2004). The Valea Nadasului formation is overlain by gypsum deposits and the marine Cluj Limestone formation, containing nannofossils of zone NP19/20 (Mészáros & Moisescu 1991), indicative for the middle and late Priabonian (Vandenberghe et al. 2012). As a result, the mammals from Rădaia are Priabonian in age.

In contrast, the ages of the Paleogene mammal assemblages from Southern China (Yunnan, Guangxi) can only be interpreted from mammalian biochronologic evidence (Russell & Zhai 1987; Wang et al. 2007). In the following paragraphs, we discuss the biochronologic implications of the Na Duong mammals with regard to the current stratigraphic framework.

4.1.2 Biochronologic comparison of *Epiaceratherium naduongense* nov. sp.

Referral of SAU-10 to *Epiaceratherium* confirms the wide geographical range of this primarily European rhinocerotid genus, as proposed by Antoine et al. (2003a) based on fragmentary remains from Pakistan. Yet, the specimen described here does not belong to the same species as the latter (referred to as *E*. cf. *magnum*), which is closely related to *E. magnum* from Germany, Switzerland, and France (Early Oligocene; Uhlig 1999; Antoine et al. 2003a; Becker 2009). The skull from Na Duong shows the strongest affinities with *E. bolcense*, a species thus far only documented from its type locality Monteviale (Vicenza, northern Italy; Dal Piaz 1930).

As a matter of fact, Rhinocerotidae have a well-documented Late Eocene record in both North America and Eastern/Southern Asia (Antoine et al. 2003a; Prothero 2005), but their first appearance date (FAD) in Europe is traditionally considered as coinciding with the *Grande Coupure*, correlated with the Eocene-Oligocene transition (Stehlin 1909; Brunet 1979; Schmidt-Kittler et al. 1987; BiochroM'97 1997; Ménouret & Guérin 2009; Becker et al. 2013). Whilst earliest Early Oligocene localities from Europe repeatedly yield *Ronzotherium filholi* and/or *Epiaceratherium magnum* (Uhlig 1999; Becker 2009), there is no record of *E. bolcense* but in the Tethyan paleo-island of Monteviale. The lignites of Monteviale formed on a volcanic island in the southern, offshore part of the Alpine insular belt (Mietto 2006). Based on the occurrence of this true rhino and irrespective of co-occurring endemic mammals with few, obscure, or no close relatives (*Archaeopteropus transiens, Epapheliscus italicus*, cf. *Dyspterna woodi, Anthracochoerus stehlini*, ?*A. fabianii*, *Propaleochoerus paronae*, *Anthracotherium monsvialense*, cf. *Bothriodon*; Dal Piaz 1930; Van Valen 1966; Kotzakis 1986), Monteviale is biochronologically referred to the earliest Oligocene reference level MP21 (Uhlig 1999; Antoine et al. 2003b; Becker 2009; Ménouret & Guérin 2009). However, both the faunal singularity of Monteviale and the phylogenetic affinities of its mammals could point to an older age, i.e. latest Eocene. According to Hellmund (1992), the small suoid *Propalaeochoerus paronae* prefigures the Oligocene "Old-World tayassuids" of Western and Central Europe, which are first documented with *P. gergovianus* in the MP21 level of Detan (Fejfar 1987; Hellmund 1992). Furthermore, in a phylogenetic analysis of Eocene-Oligocene Rhinocerotidae from Europe, Becker et al. (2013) demonstrate that *E. bolcense*

diverged earlier than *E. magnum*, *Epiaceratherium* being thus paraphyletic. As the FAD of *E. magnum* is recorded in several localities dating back to the earliest Oligocene MP21 reference level (Uhlig 1999; Antoine et al. 2003a; Becker 2009; Becker et al. 2013), *E. bolcense* necessarily diverged prior to the *Grande Coupure* and is likely to have occurred as early as in the late Eocene. *E. naduongense* nov. sp. shows the closest affinities with *E. bolcense*, which likely has diverged at the same time as the latter. In other words, based on rhinocerotid data, the Late Eocene is the favored stratigraphic interval for the Na Duong fossil mammal horizon, even though an earliest Oligocene age cannot be discarded.

4.1.3 Biochronologic comparison of *Bakalovia orientalis* nov. sp.

The family Anthracotheriidae has long been considered to be very useful from a biochronological and paleobiogeographical point of view (for example Ducrocq 1997). Within the Anthracotheriidae, the subfamily Bothriodontinae ('selenodont anthracothers') is widespread in the late Paleogene of North America, Eurasia and Africa (Ducrocq 1997). The earliest bothriodontines are recorded from the late Middle Eocene (late Bartonian) of Eurasia, together with the genera *Ulausodon*, *Elomeryx* and *Bakalovia*. *Ulausodon* Hu, 1963 is an incompletely known genus (Lihoreau & Ducrocq 2007) reported so far only from the late Middle Eocene Shara Murun Formation in Inner Mongolia (China, Fig. 30). The widespread and well-known genus *Elomeryx* has its first occurrence in the upper Middle Eocene Naduo Formation (Naduan Chinese Land Mammal Age; Wang et al. 2007) of the Bose and Yongle basins (Guangxi, Fig. 30; Ducrocq & Lihoreau 2006) and subsequently occurs in Europe during the middle part of the Late Eocene (MP18, La Débruge; De Bonis 1964; Hellmund 1991). The Naduan *Elomeryx* material from Guangxi has been described by Xu (1977) as *Bothriodon chyelingensis* (Naduo Formation) and *Bothriodon tiengtongensis* (Gongkang Formation); both taxa were later referred to *Elomeryx* cf. *crispus* by Ducrocq & Lihoreau (2006).

Several late Middle Eocene, and late Eocene localities of southern China have yielded (often scarce) remains of bothriodontine anthracotheriids that are reported under various generic names including *Bothriodon* and *Brachyodus* (Chow 1957; Chow 1958; Xu 1961). Some of these Eastern Asian occurrences of bothriodontines certainly predate the first occurrence of the subfamily in Western Europe (MP18), at least the *Bothriodon* sp. reported from the Lumeiyi Formation, Yunnan, China (Chow 1958). In southeastern Europe, bothriodontines appear slightly earlier than in Western Europe, documented by the genus *Bakalovia,* so far only known from two species from the late Bartonian of Tscherno More, Bulgaria (Balcano-Rhodopian island, Fig. 30, Nikolov & Heissig 1985). The close phylogenetic relationships between *B. orientalis* from Na Duong and the type species of the genus *B. palaeopontica* from Tscherno More suggest a similar chronostratigraphic position for the two localities, i.e. around the Middle to Late Eocene transition.

4.1.4 Statigraphic and biochronologic integration

Paleomagnetic investigations have shown that the sediments of the Na Duong Formation and probably also from the lower part of the Rhin Chua Formation were remagnetized after tilting. Only the uppermost 40 m of the Rhin Chua formation, with reverse polarity and good agreement with expected Eocene inclination, show the original magnetization. These data prohibit any magnetostratigraphic interpretation of the Na Duong section. The stratigraphic evaluation thus only relies on biochronology.

All mollusk species recorded from the Na Duong and Rhin Chua formations can be more or less confidently assigned to genera or families that still persist today. From this enormous time range, it can easily be inferred that freshwater bivalves and gastropods usually are no reliable stratigraphic markers at genus or family level. Since all mollusk species occurring at Na Duong have been first described from this locality, or are not sufficiently well preserved to be properly determined, their shells are generally inapplicable for biochronology.

The chronologically most significant fishes from the Na Duong Formation are the Amiinae (bowfins). Amiinae are characteristic freshwater fishes of the Eocene in Central and Eastern Asia, e.g., from China (Chang et al. 2010), Mongolia, and Kazakhstan (Sytchevskaya 1986). No Asian bowfins are recorded with certainty from Oligocene strata. Whether the fragmentary remains from the Lower Oligocene Buran Formation from the Zaissan Basin in Kazakhstan (Sytchevskaya 1986) really belong to the Amiinae is ambiguous.

In contrast to mollusks and fishes, mammals do provide explicit biochronologic evidence. Based on the evolutionary states of the rhinocerotid *Epiaceratherium naduongense* nov. sp. and the anthracotheriid *Bakalovia orientalis* nov. sp. the vertebrate bearing horizon at Na Duong is most likely latest Middle-early Late Eocene in age and may be correlated to the Naduan Chinese Land Mammal Age (LMA). The Naduan LMA was introduced by Tong (1989) for Eocene mammal assemblages from southern China, which are characterized by (1) high diversity and abundance of artiodactyls, especially anthracotheres and basal ruminants and (2) the absence of taxa typical of the Ulangochuan Asian Land Mammal Age (ALMA), e.g. the perissodactyls *Embolotherium* and *Cadurcodon*, and the artiodactyls *Entelodon*, *Miomeryx*, and *Lophiomeryx*. Tong (1989)

interpreted the Naduan LMA as chronologically intermediate between the Sharamurunian ALMA and the Ulangochuan ALMA (both defined on the Mongolian Plateau). This relative position corresponds to the Bartonian-Priabonian boundary interval (see Hooker 2012 for correlation of ALMAs; Vandenberghe et al. 2012), or to the late Bartonian (Wang et al. 2007). However, Paleogene biochronology of Southeast Asia is not well enough constrained to allow for solid correlation with Central Asian ALMAs, or Chinese LMAs. The Na Duong Formation at its stratotype is thus correlated with the late Bartonian-late Priabonian interval, corresponding to 39–34 Ma in absolute ages. This is in agreement with previous palynological investigation of the Na Duong and Rhin Chua formations (Trung et al. 2000; Dy et al. 1996), which revealed typical Paleogene pollen and sporomorph assemblages (Böhme et al. 2011).

4.2 The Na Duong ecosystems

4.2.1 Na Duong Formation

The Na Duong Formation can generally be considered as deposits of a swamp ecosystem with both aquatic and non-aquatic environments. Aquatic environments are documented by three lithologic facies corresponding to three environments: dark-brown claystones (shallow pond), coaly shales (anoxic lake), and fine- to medium-grained sandstones (brooks and rivulets).

Shallow pond sediments occur directly below and above the main coal seam (layers 77, 81, 83), as well as in the middle part of the formation (layers 70, 62, 43). Their sediments contain a distinct greigite fraction (see discussion below). The shallow pond ecosystem consisted of *Nelumbo*-meadows (layer 70, 81, 83) inhabited by viviparids, unionids (?*Nodularia cunhatia*, *Cristaria mothanica*), and medium-sized barbine fish (Barbinae gen. indet. sp. 1). Rare disarticulated turtle fragments and isolated crocodile teeth provide evidence of vertebrate life in the pond.

The main lignite seam (coaly shale, layer 80) is interpreted as an anoxic lake deposit, and characterized by abundant pyrite concretions and driftwood (see Böhme et al. 2011 fig. 4). Small-scale deltaic sediment bodies (layers 80B, D) indicate sediment input by rivers during the late stage of the lake. The rivers transported plant remains (leaves) from azonal (probably riparian) vegetation (e.g. ferns and *Bauhunia*) into the lake, and carried up to three meters long driftwood logs during flooding events. All driftwood logs are mechanically abraded and lack root balls and branches, indicating extensive fluvial transport, and were lithified after compaction. The transitional stage from the shallow pond (layer 81) to the anoxic lake (layer 80) formed the main vertebrate bearing horizon. Aquatic life during this time was characterized by common amiin (bowfins) and rare cyprinid fishes (Barbinae gen. indet. sp. 1), trionychid and geoemydid turtles (up to five species), and three crocodile species. Mollusks, which may have been a food source for fishes and turtles, are lacking, probably due to early diagenetic dissolution of their shells in waters enriched in humic acid (Schneider et al. 2013). Recent bowfins like the facultative air breathing *Amia calva* are known to tolerate comparative environmental conditions and even hypoxia (Randall et al. 1981). Fishes were the food source for the rare *Gavialis*-type crocodile, whereas the *Alligator*-type and the up to 6 meter long *Crocodylus*-type crocodiles, depending on their individual size, may have preyed on turtles, mammals, or even congeners.

Non-aquatic environments of the Na Duong Formation ecosystem are represented by thin lignites and pedogenically influenced greyish clay- to sandstones, and are attributed to swamp forests. Palaeomagnetic analysis indicates the presence of magnetite (Fe_3O_4) in these sediments, implying organic or inorganic mineral formation under reducing soil conditions, which is typical for waterlogged soils (Maher & Taylor 1988; Torrent et al. 2006). Macrofossil evidence only occurs in the form of in-situ tree stump horizons and allochthonous tree trunks in lignite seams, which may contain fossil resin (e.g., in layer 71) attributed to the Dipterocarpaceae based on spectroscopy. In-situ tree stump horizons can be employed to infer on the structure of the swamp forest. Based on the fibrous root system, stump diameters (7 to 50 centimeters), and medium distance between individual trees (3 to 5 m) a tree density of more than 600 trees per hectare has been reconstructed, which is well in the range of tree densities (with similar tree diameter) in undisturbed recent peat swamp forests in Sumatra and Kalimantan (Anderson et al. 1992; Gunawan et al. 2012; most of these extant forests are characterized by distinct dipterocarp species). Maximum canopy height of the Na Duong swamp forest is estimated to 35 meters (Niklas 1995), which also compares well to present-day Indonesian peat swamp forests (Englhart et al. 2013), and Southeast Asian swamp forests in general (Yamada 1997). Since macroscopic charcoal, as an indicator of local fires within a forest or peat-bog (Scott 2000, 2010) has so far not been detected, the forests of the Na Duong Formation, at least those in the direct vicinity of the area of deposition, have not been disturbed by palaeo-wildfires. Periodic disturbance by riverine flooding is indicated by intercalations of medium-grained sandstones (Fig. 2). In summary, the zonal vegetation of the Na Duong ecosystem may be interpreted as a lowland swamp forest, probably characterized by Dipterocarpaceae (layer 71), and similar in structure to recent Indonesian swamp and peat forests.

4.2.1.1 Paleoecology of Na Duong mammals

Fossils of anthracotheres, in particular of bothrio-

dontines, are commonly found in lignitic deposits, and their latinized Greek name 'coal beast' refers to their preferred environment. It has been hypothesized that they had a hippo-like life style; however, postcranial anatomy of anthracotheres contradicts this idea (Pickford 2008). A semiaquatic life style, similar to modern water buffalos and other aquaphilous artiodactyles, seems more likely (Pickford 2008). Having this life style, *Bakalovia orientalis* nov. sp. is vulnerable to crocodile predation, which would be supported by the fact that six of the eight specimens of *B. orientalis* are not mature, indicating high juvenile mortality.

Contrary to *Bakalovia*, *Epiaceratherium naduongense* nov. sp. lived entirely terrestrial. According to its brachydont dentition and plesiomorphic tapir-like dental formula, this early diverging rhinocerotid can be interpreted as an obligate browser. Other representatives of *Epiaceratherium* have long and slender bones and a tapir-like tetradactyl manus (e.g., Dal Piaz 1930; Uhlig 1999); such postcranial features identify *Epiaceratherium* as a potential forest dweller.

4.2.2 Rhin Chua Formation

Numerous samples of marly claystones from the lower part of the Rhin Chua Formation, especially between 151–153 and 163–185 m, contained the iron sulfide greigite (Fe_3S_4) in significant proportions. Greigite is formed under anoxic conditions, either autigenic (early diagenetic) or by anaerobic, sulphate reducing magnetotactic bacteria (Vasiliev et al. 2008). Fossils of benthic organisms are absent from these parts of the section. Autochthonous gastropods (Cerithioidea, Viviparidae) and bivalves (Unionidae in live-position) are found in the lower 7 m of the Rhin Chua Formation (143–150 m) and from 185 m onwards. Nektonic organisms, represented by seven taxa of cyprinid fishes, can be found throughout the Rhin Chua claystones. Botanic remains have not been documented from the Rhin Chua Formation.

As a result, the Rhin Chua Formation preserves sediments that have been deposited in a lake ecosystem, with variable oxic conditions in the bottom water, probably related to fluctuating water-depth. In a first stage (143–150 m), a shallow lake with well-oxygenated bottom water established, and was inhabited by unionids (*Cristaria mothanica*, ?*Cuneopsis* sp.), viviparids, and omnivorous barbels (Barbinae sp. 2, 3), zooplanktophagous cultrins, and phytoplanktophagous xenocyprinins. In the second stage of the lake evolution (151–153 m and 163–185 m) water depth increased and bottom waters became depleted in oxygen. Accordingly, body fossils of benthic organisms are lacking and bioturbation can only be observed in sediments of an intercalated, potential shallowing interval (e.g. at 156 m, Fig. 3E). Isolated pharyngeal teeth of cyprinids are common in most layers, indicating autochthonous presence of these fishes (Böhme 2010). They comprise a new genus and species of small, filter-feeding planktivores (*Planktophaga minuta*) and a small omnivorous barbel.

During the last stage of the lake evolution (185–223 m), the water level dropped and bottom waters became well-oxygenated again. The clayey sedimentation in the upper part of the profile is cyclically interrupted by thin sandstone beds showing symmetric ripple-marks on their top, indicating very shallow, lake-shore environments. The mollusc community of the first phase becomes re-established; viviparids and cerithioids occur in abundance, and unionids are now represented by three species including an alatiform *Hyriopsis*-like form. Cerithioids may also be found in monospecific assemblages, or form, together with viviparids, coquina-like mass accumulations in sandstone beds. The fish fauna is similar to that from the first stage; however, cultrins are lacking and become replaced by a large-sized malacophagous barbin.

4.3 Na Duong fossils and Eurasian biogeography during the Middle to Late Eocene

The fossil mammals from Na Duong in northern Vietnam show unexpected similarities to European faunas located about 9.000 km to the west. The occurrence of *Bakalovia orientalis* nov. sp. and of *Epiaceratherium naduongense* nov. sp. at Na Duong might therefore be a key to understanding the faunal exchanges between Europe and Asia at the end of the Eocene.

In western Eurasia, species of the genus *Bakalovia* (*B. palaeopontica, B. asticus*) did not reach the European archipel and are only known from late Bartonian sediments of the Tethyan micro-continent Balcano-Rhodopia (Fig. 30), indicating a biogeographic connection between Southeast Asia and the Tethyan islands during the Middle to Late Eocene. Like *Bakalovia orientalis*, the close affinities of *Epiaceratherium naduongense* to *E. bolcense* support biogeographic connections with a Tethyan island, the volcanic island of Monteviale (northern Italy, Mietto 2006), situated between the Tisza micro-continent and the Alpine island (Fig. 30).

We acknowledge that Rhinocerotidae from the Late Eocene–earliest Oligocene interval are far from being well known, in particular from Asia (e.g., Antoine et al. 2003a). Although scarce and poorly constrained in both taxonomic and biostratigraphic perspectives, the corresponding rhinocerotid record testifies the co-occurrence of several distinct lineages in Asia at this time. Importantly, the rhino from Na Duong does not resemble the Eocene and lower Oligocene rhinocerotids described from China (*Guixia simplex* and *G. youjiangensis*; *Protaceratherium* sp.; Teilhard de Chardin 1926; You 1977), Mongolia (*Ronzotherium brevirostre*; Dashzeveg 1991), Thai-

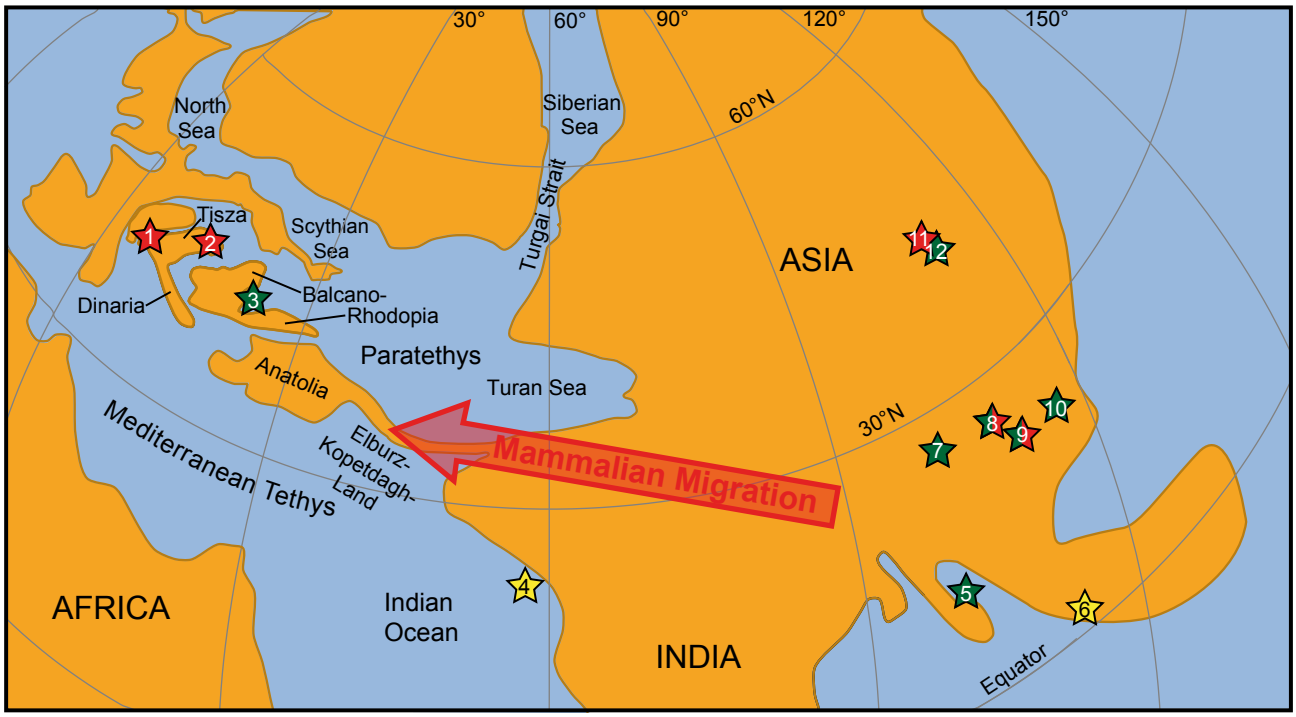

Figure 30: Palaeogeographic map for the Late Eocene (Priabonian) of Eurasia. The hypothetic transcontinental migration route of certain Middle to Late Eocene mammalian taxa is indicated by a red arrow. Numbers refer to important mammal localities discussed in the text: 1 – Monteviale (Italy), 2 – Radaia (Romania), 3 – Tscherno More (Bulgaria), 4 – Paali (Pakistan), 5 – Poundaung (Myanmar), 6 – Krabi (Thailand), 7 – Lumeiyi (Yunnan, China), 8 – Bose (Naduo and Gongkang formations; Guangxi, China), 9 – Na Duong (Vietnam), 10 – Maoming (Youganwo Formation; Guangdong, China), 11 – Ergilin Dzo (Mongolia), 12 – Shara Murun (Nei Mongol, China). Colours of the asterisks indicate stratigraphy: green – late Bartonian, red – Priabonian, yellow – Rupelian. Map modified from Popov et al. (2004) and Bosboom et al. (2011).

land (*G.* cf. *simplex*; Antoine et al. 2003a), or Myanmar (cf. *Teletaceras* sp.; Holroyd et al. 2006). It basically resembles *Epiaceratherium* cf. *magnum* from the Early Oligocene of Pakistan (Antoine et al. 2003a), but its closest affinities are unambiguously with *E. bolcense* from Monteviale, northern Italy (as illustrated by Dal Piaz 1930).

These results provide solid evidence that *Bakalovia* and *Epiaceratherium* dispersed from southern Asia towards Europe, along a Tethyan route, well before the Eocene–Oligocene transition. Furthermore, according to Mihlbachler (2008) (see also Nikolov & Heissig 1985), the late Bartonian Poundaung (Myanmar) brontothere *Sivatitanops birmanicum* (Pilgrim & Cotter, 1916) is synonymous to the late Bartonian "*Menodus*" *rumelicus* Toula, 1892 from Kameno (= Kajali) and Tscherno More (both Bulgaria; Balcano-Rhodopian micro-continent), and a possible junior synonym of *Brachydiastematherium transsylvanicum* Böckh & Matyasovski, 1876 from the Priabonian of Rădaia (= Andrásháza, Romania; Tisza micro-continent, see Fig. 30). The latter locality also yielded the hyracodontid rhinocerotoid *Prohyracodon orientalis* Koch, 1897, which is very similar to *P. meridionale* Chow and Xu, 1961 from the late Middle Eocene (Sharamurunian, Chinese LMA, Tong 1989) Lumeiyi formation in Yunnan (Heissig 1989). Therefore, most Eocene mammals from the Tethyan micro-continents (*Sivatitanops, Prohyracodon, Epiaceratherium,* and *Bakalovia*) have Southeast Asian affinities and point to immigration from the East (Fig. 30).

The mammal pattern reinforces the hypothesis that Southeast Asia was an important source of Eocene immigrants, which eventually replaced most of the European Eocene endemic faunas, with a culmination at the 'Grande Coupure' (Heissig 1979; Baciu & Hartenberger 2001). The available mammalian data further testify to the absence of significant paleogeographical-paleoenvironmental barriers between remote areas in the southern Eurasian mid-latitudes (20°–40°N) during the late Middle and Late Eocene. On the other hand, especially the new rhino species does not support any close affinity with much closer Southeast Asian basins, such as Bose, Pondaung, or Krabi.

However, the palaeogeography of the Late Eocene Tethyan landbridge or island chain is extremely difficult to reconstruct because of its extensive orogenic overprint (Popov et al. 2004). This is especially true for the Elburz-Kopetdagh-Land (sensu Popov et al. 2004), which may be very important for the East-West migrations, because of its possible filter effect on terrestrial organisms. The Elburz-Kopetdagh-Land was proposed by Popov et al. (2004) as a landbridge that separated the Late Eocene Turan Sea from the Tethys and Indian Ocean (Fig. 30). In addition, Middle- to Late Eocene subaerial volcanic eruptions have been described from this region (Asiabanha et al. 2009),

and some of the volcanosedimentary deposits have yielded footprints of terrestrial mammals (Ataabadi & Khazaee 2004). These new data document that new research on continental Eocene sediments in Central Asia is crucial to further understand the Paleogene transcontinental migrations in Eurasia.

Contrary to mammals, the mollusk fauna of Na Duong does not reflect this paleobiogeographic pattern. Most of the recorded genera and/or families of Bivalvia and Gastropoda do not even have fossil or extant representatives in Europe. Like several other families of freshwater fish the Cyprinidae became involved in the faunal turnover that is described as the 'Grande Coupure' in Europe (Böhme 2007). However, the first taxa that entered Europe belong to the Phoxininae and Gobioninae, which both have northern Asian affinities and have never occurred in Southeast Asia. The cyprinid assemblages from Na Duong and Cao Bang (Fig. 1, Böhme et al. 2011) document that, at least at subfamily level, the cyprinid fauna of East Asia remained stable during the last ~37 million years.

In summary, the Eocene fossils from northern Vietnam strongly support a transcontinental migration of Asian mammals during the late Middle and Late Eocene via an island chain consisting of microcontinents and volcanic back-arcs. Some of these mammals (e.g. *Epiaceratherium*) successfully colonized western and central Europe in the course of the Grande Coupure around the Eocene–Oligocene boundary. However, the island chain was selective with regard to the dispersal of freshwater organisms and plants, likely because of climatic and physiogeographic reasons (e.g. drainage pattern, volcanic arcs).

4.4 Paleoclimate during the Late Eocene in northern Vietnam

Paleoclimatic interpretation is based on fossil plant, reptiles, and sedimentology. Dipterocarpaceae, documented from the Na Duong Formation from resin spectroscopy, are regarded as a reliable proxy for tropical to warm-subtropical climates (Böhme et al. 2007; Ghazoul 2012; Shi et al. 2014). They are particularly climate-sensitive, because dipterocarp seed germination usually ceases below 15°C (Tompsett 1998). These data are supported by the northern distribution limit of recent Diperocarpaceae in Eastern Asia (northern Vietnam and southern China) at approximately 24° N (Sam et al. 2004 ; Xiwen et al. 2007). The present-day climate in these regions is characterized by frost-free winter, a mean annual temperature (MAT) above 20°C, and mean January temperatures (CMT) not below 10°C (Weischat & Endlicher 2000).

For fossil crown-group crocodiles, Markwick (1998b) inferred lower temperature limits of >14.2 MAT and >5.5 CMT based on their present-day distribution. These lower limits are based on the recent occurrence of *Alligator sinensis* and thus on single taxon of comparably small body size. The high diversity of fossil crocodiles at Na Duong and their much larger maximum body-size (at least 6 m for *Crocodylus*-type animals) may point to much higher temperatures, which, however, are difficult to quantify (Markwick 1998a, b; Scheyer et al. 2013). The crocodiles recorded from Na Duong may therefore basically support the temperature limits deduced from the dipterocarps.

In a recent paleoclimatic study on the Eocene of China, Wang et al. (2013) used a coexistence approach for palynomorphs. Their database includes four sites from the Late Eocene of southeastern China, which allow for a basic comparison to Na Duong. The temperature limits calculated for the Na Duong Formation (>20°C MAT, >10°C CMT) are significantly higher than the pollen-based estimates from the Bose Basin (14.7–14.9°C MAT, 2.1–5.8°C CMT), and show only minor overlap with ranges derived from southwestern Guangxi, Leishou Peninsula, and the South China Sea (14.3–22.7°C MAT, 3.6–14.3°C CMT). While the estimates for the Bose Basin are certainly too low and in conflict with records of crocodiles (Xin & Ming-zhen 1964), the top end of the temperature intervalls calculated for the other sites in southeastern China at least matches the minumum estimates for Na Duong. With regard to humidity, the sediments from the Na Duong Formation lack any indication for well oxygenated paleosoils or pedogenic carbonate accumulation. These observations clearly indicate per-humid conditions without a dry season. This observation is in accordance with pollen data from Southern China given by Wang et al. (2013).

Acknowledgments

We owe thanks to the following people and organizations that enabled us to carry out this study: The excavations and fossil preparation were financially supported by the Deutsche Forschungsgemeinschaft (DFG; Grant Numbers BO 1550/11-1, 2). Nguyen Viet Hung, Do Duc Quang (all Geology Museum, Hanoi) and Phan Dong Pha (Institute of Geological Sciences, Vietnamese Academy of Science and Technology) greatly helped with local organization and assisted in the field. Ulf Noteboom (Cideon Engineering, Bautzen) also assisted in the field. Regina Ellenbracht, Henrik Stöhr, and Hans Luginsland (all University of Tübingen) carried out the mechanical preparation of the fossils and produced casts. Photographs were taken by Wolfgang Gerber (University of Tübingen). Agnes Fatz (University of Tübingen) produced SEM photographs and assisted with manuscript preparation. The manuscript benefited from careful reviews by Bettina Reichenbacher (Ludwig-Maximilians-University Munich) and Kurt Heissig (Bayerische Staatssammlung für Paläontologie und Geologie, Munich).

5. References

Abel O. 1910. Kritische Untersuchungen über die paläogenen Rhinocerotiden Europas. Abhandlungen der Kaiserlich-Königlichen Geologischen Reichsanstalt 20, 1–52.

Abel O. 1928. *Allognathosuchus*, ein an die cheloniphage Nahrungsweise angepasster Krokodiltypus des nordamerikanischen Eozäns. Paläontologische Zeitschrift 9, 367–374.

Anderson KB, Winans RE, Botto RE. 1992. The nature and fate of natural resins in the geosphere. II. Identification, classification and nomenclature of resinites. Organic Geochemistry 18, 829–841.

Annandale N. 1919. The gastropod fauna of Old Lake Beds in Upper Burma. Records of the Geological Survey of India 50, 209–240.

Annandale N. 1924. The evolution of the shell-sculpture in freshwater snails of the family Viviparidae. Proceedings of the Royal Society of London, Series B, Biological sciences 96, 60–76.

Antoine P-O. 2002. Phylogénie et évolution des Elasmotheriina (Mammalia, Rhinocerotidae). Mémoires du Muséum national d'Historie naturelle 188, 1–359.

Antoine P-O. 2003. Middle Miocene elasmotheriine Rhinocerotidae from China and Mongolia: taxonomic revision and phylogenetic relationships. Zoologica Scripta 32, 95–118.

Antoine P-O, Ducrocq S, Marivaux L, Chaimanee Y, Crochet J-Y, Jaeger J-J, Welcomme J-L. 2003a. Early rhinocerotids (Mammalia: Perissodactyla) from South Asia and a review of the Holarctic Paleogene rhinocerotid record. Canadian Journal of Earth Sciences 40, 365–374.

Antoine P-O, Duranthon F, Welcomme JL. 2003b. *Alicornops* (Mammalia, Rhinocerotidae) dans le Miocène supérieur des Collines Bugti (Balouchistan, Pakistan): implications phylogénétiques. Geodiversitas 25, 575–603.

Antoine P-O, Downing KF, Crochet J-Y, Duranthon F, Flynn LJ, Marivaux L, Métais G, Rajpar AR, Roohi G. 2010. A revision of *Aceratherium blanfordi* Lydekker, 1884 (Mammalia: Rhinocerotidae) from the Early Miocene of Pakistan: postcranials as a key. Zoological Journal of the Linnean Society 160, 139–194.

Antoine P-O, Métais G, Orliac MJ, Peigné S, Rafaÿ S, Solé F, Vianey-Liaud M. 2011. A new late early Oligocene vertebrate fauna from Moissac, SW France. Comptes Rendus Palevol 10, 239–250.

Asiabanha A, Ghasemi H, Meshkin M. 2009. Paleogene continental-arc type volcanism in North Qazvin, North Iran: facies analysis and geochemistry. Neues Jahrbuch für Mineralogie, Abhandlungen 186, 201–214.

Ataabadi MM, Khazaee AR. 2004. New Eocene Mammal and Bird Footprints from Birjand Area, Eastern Iran. Ichnos 11, 363–370.

Baciu C, Hartenberger J-L. 2001. Un exemple de corrélation marin-continental dans le Priabonien de Roumanie. Remarques sur la Grande Coupure. Comptes Rendus de l'Académie des Sciences, Series IIA, Earth and Planetary Science 333, 441–446.

Bănărescu P, Coad BW. 1991. Cyprinids of Eurasia. In: IJ Winfield and JS Nelson (Eds), Cyprinid Fishes – systematic, biology, and exploitation. London, Chapman & Hall, 128–155.

Bandel K, Kowalke T. 1997. Eocene *Melanotarebia* n. g. and its relations among modern Thiaridae (Caenogastropoda: Cerithioidea). Neues Jahrbuch für Geologie und Paläontologie, Monatshefte 11, 683–695.

Becker D. 2009. Earliest record of rhinocerotoids (Mammalia: Perissodactyla) from Switzerland: systematics and biostratigraphy. Swiss Journal of Geosciences 102, 489–504.

Becker D, Antoine P-O, Maridet O. 2013. A new genus of Rhinocerotidae (Mammalia, Perissodactyla) from the Oligocene of Europe. Journal of Systematic Palaeontology 11, 947–972.

Benammi M, Chaimanee Y, Jaeger J-J, Suteethorn V, Ducrocq S. 2001. Eocene Krabi Basin (southern Thailand): Paleontology and magnetostratigraphy. Bulletin of the Geological Society of America 113, 265–273.

Bender F. 1983. Geology of Burma. Berlin & Stuttgart, Gebruder Borntraeger, 260 p.

BiochroM'97. 1997. Synthèses et tableaux de corrélations. In: J-P Aguilar, S Legendre and J Michaux (Eds), Actes du Congrès BiochroM'97. Mém. Trav. E.P.H.E., Inst. Montpellier 21. Montpellier 769–805.

Böhme M. 2001. Die Landsäugerfauna des Unteroligozäns der Leipziger Bucht – Stratigraphie, Genese und Ökologie. Neues Jahrbuch für Geologie und Paläontologie 220, 63–82.

Böhme M. 2007. Revision of the cyprinids from the Early Oligocene of the České Středohoří Mountains and the phylogenetic relationships of *Protothymallus* Laube 1901 (Teleostei, Cyprinidae). Acta Musei Nationalis Pragae B 63, 177–196.

Böhme M, Bruch AA, Selmeier A. 2007. The reconstruction of Early and Middle Miocene climate and vegetation in Southern Germany as determined from the fossil wood flora. Palaeogeography, Palaeoclimatology, Palaeoecology 253, 91–114.

Böhme M. 2010. Ectothermic vertebrates (Actinopterygii, Allocaudata, Urodela, Anura, Crocodylia, Squamata) from the Miocene of Sandelzhausen (Germany, Bavaria) and their implications for environment reconstruction and palaeoclimate. Paläontologische Zeitschrift 84, 3–41.

Böhme M, Prieto J, Schneider S, Hung NV, Quang DD, Tran DN. 2011. The Cenozoic on-shore basins of Northern Vietnam: Biostratigraphy, vertebrate and invertebrate faunas. Journal of Asian Earth Sciences 40, 672–687.

Bosboom RE, Dupont-Nivet G, Houben AJP, Brinkhuis H, Villa G, Mandic O, Stoica M, Zachariasse WJ, Guo Z, Li C, Krijgsman W. 2011. Late Eocene sea retreat from the Tarim Basin (west China) and concomitant Asian paleoenvironmental change. Palaeogeography, Palaeoclimatology, Palaeoecology 299, 385–398.

Bossuyt F, Milinkovitch M. 2001. Amphibians as Indicators of Early Tertiary " Out-of-India " Dispersal of Vertebrates. Science 292, 93–95.

Brochu CA. 2001. Crocodylian snouts in space and time phylogenetic approaches toward adaptive radiation. American Zoologist 41, 564–585.

Brochu CA. 2004. Alligatorine phylogeny and the status of *Allognathosuchus* Mook, 1921. Journal of Vertebrate Paleontology 24, 857–873.

Brochu CA. 2006. Osteology and phylogenetic significance of *Eosuchus minor* (Marsh, 1870) new combination, a longirostrine Crocodylian from the Late Paleocene of North America. Journal of Paleontology 80, 162–186.

Brunet M. 1979. Les grands mammifères chefs de file de l'immigration oligocène et le problème de la limite Eocène–Oligocène en Europe. Fondatión Singer-Polignac, 281 p.

Burnham RJ, Pitman NCA, Johnson KR, Wilf P. 2001. Habitat-related error in estimating temperatures from leaf margins in a humid tropical forest. American Journal of Botany 88, 1096–1102.

Cavender T, Coburn M. 1992. Phylogenetic relationships of North American Cyprinidae. In: R Mayden (Eds), Systematics, Historical Ecology, and North American Freshwater Fishes. California, Standford University Press, 293–327.

Chang M-M, Wang N, Wu F-X. 2010. Discovery of *Cyclurus* (Amiinae, Amiidae, Amiiformes, Pisces) from China. Vertebrata PalAsiatica 48, 85–100.

Chen G, Fang F, Chang M-M. 2005. A new cyprinid closely related to cultrins+xenocyprinins from the mid-Tertiary of South China. Journal of Vertebrate Paleontology 25, 492–501.

Chen YF, Zhang DX. 2005. *Bauhinia larsenii,* a fossil legume from Guangxi, China. Botanical Journal of the Linnean Society 144, 437–440.

Cherniavska S. 1970. Palynomorph zones in some Paleogene coal sediments of Bulgaria. Bulletin of the Geological Institute, Bulgarian Academy of Science, Stratigraphy and Lithology 19, 79–100. (in Bulgarian with English summary).

Chow M. 1957. On some Eocene and Oligocene mammals from Kwangsi and Yunnan. Vertebrata PalAsiatica 1, 263–368.

Chow M. 1958. Some Oligocene mammals from Lunan. Vertebrata PalAsiatica 2, 263–268.

Clark MK. 2011. Early Tibetan Plateau uplift history eludes. Geology 39, 991–992.

Claude J, Zhang JY, Jian-Jun LI, Jin-You MO, Kuang XW, Tong

H. 2012. Geoemydid turtles from the Late Eocene Maoming basin, southern China. Bulletin de la Société géologique de France 183, 641–651.

Clift PD, Long HV, Hinton R, Ellam RM, Hannigan R, Tan MT, Blusztajn J, Duc NA. 2008. Evolving east Asian river systems reconstructed by trace element and Pb and Nd isotope variations in modern and ancient Red River-Song Hong sediments. Geochemistry, Geophysics, Geosystems 9, 10.1029/2007GC001867.

Cotter GdP. 1938. The geology of parts of the Minbu, Myingyan, Pakokku and lower Chindwin districts, Burma. Calcutta, Geological Survey of India, 40, 1–128.

Dai Y-G, Yang J-X. 2003. Phylogeny and zoogeography of the cyprinid hemicultrine group (Cyprinidae: Cultrinae). Zoological Studies 42, 73–92.

Dal Piaz G. 1930. I Mammiferi dell' Oligocene veneto, *Trigonias ombonii*. Memorias dell'Istituto Geologico della R. Università di Padova 9, 2–63.

Dashzeveg DCGR. 1991. Hyracodontids and rhinocerotids (Mammalia, Perissodactyla, Rhinocerotoidea) from the Paleogene of Mongolia. Montpellier, 1–84 p.

Davis GM. 1979. Origin and Eolution of the gastropod family Pomatiopsidae, with emphasis on the Mekong River Triculinae. Monographs of the Academy of Natural Sciences of Philadelphia 20, 1–120.

De Bonis L. 1964. Étude de quelques mammifères du Ludien de la Débruge (Vaucluse). Annales de Palaeontologie 50, 119–154.

Ducrocq S. 1997. The anthracotheriid genus *Bothriogenys* (Mammalia, Artiodactyla) in Africa and Asia during the Paleogene: phylogenetical and paleobiogeographical relationships. Stuttgarter Beiträge zur Naturkunde. Serie B, Geologie und Paläontologie 250, 1–44.

Ducrocq S, Lihoreau F. 2006. The occurrence of bothriodontines (Artiodactyla, Mammalia) in the Paleogene of Asia with special reference to *Elomeryx*: Paleobiogeographical implications. Journal of Asian Earth Sciences 27, 885–891.

Dutta S, Tripathi SM, Mallick M, Mathews RP, Greenwood PF, Rao MR, Summons RE. 2011. Eocene out-of-India dispersal of Asian dipterocarps. Review of Palaeobotany and Palynology 166, 63–68.

Dy ND, Trung PQ, An NQ. 1996. New paleontological data from Cenozoic sediments of the Na Duong depression. Geological Resources 1, 287–296.

Dzanh T. 1996. Chrono-ecological vegetative assemblage and historical development of Neogene and Neogene-Quarternary floras of Vietnam. The Palaeobotanist 45, 430–430.

Englhart S, Jubanski J, Siegert F. 2013. Quantifying Dynamics in Tropical Peat Swamp Forest Biomass with Multi-Temporal LiDAR Datasets. Remote Sensing 5, 2368–2388.

Enkin RJ. 2003. The direction-correction tilt test: an all-purpose tilt/fold test for paleomagnetic studies. Earth and Planetary Science Letters 212, 151–166.

Fejfar O. 1987. A lower Oligocene mammalian fauna from Detan and Dvérce, NW Bohemia, Czechoslovakia. Münchner Geowissenschaftliche Abhandlungen (A) 10, 253–264.

Fejfar O, Kaiser TM. 2005. Insect bone modification and paleoecology of Oligocene mammal-bearing sites in the Doupov Mountains, NW Bohemia. Palaeontologia Electronica 8, 8A.

Feng X, Tang B, Kodrul TM, Jin J. 2013. Winged fruits and associated leaves of *Shorea* (Dipterocarpaceae) from the Late Eocene of South China and their phytogeographic and paleoclimatic implications. American Journal of Botany 100, 574–581.

Fuller M, Haston R, Lin J-l, Richter B, Schmidtke E, Almasco J. 1991. Tertiary paleomagnetism of regions around the South China Sea. Journal of Southeast Asian Earth Sciences 6, 161–184.

Geais G. 1934. Le *Brachyodus borbonicus* des Argiles de St. Henri (près Marseille). Lyon, du Laboratoire de Géologie de la Faculté de Lyon, 54 p.

Geptner AR, Pha P, Petrova VV, Huyen N, Nginh L, Quang N. 2013. Freshwater stromatolites with the cone-in-cone structure from the Neogene lacustrine sediments of Vietnam. Lithology and Mineral Resources 48, 55–64.

Ghazoul J. 2012. The challenge of inferring palaeoclimates from extant plant distributions: An example from *Dipte*

Glaubrecht M, Brinkmann N, Pöppe J. 2009. Diversity and disparity 'down under': Systematics, biogeography and reproductive modes of the 'marsupial' freshwater Thiaridae (Caenogastropoda, Cerithioidea) in Australia. Zoosystematics and Evolution 85, 199–275.

Goloboff P, Farris JS, Nixon KC. 2000. TNT (Tree Analysis using New Technology) (BETA) version 1.1. published by the authors. Tucumán, Argentina.

Goloboff P, Farris JS, Nixon KC. 2008. TNT, a free program for phylogenetic analysis. Cladistics 24, 774–786.

Gradstein FM, Ogg JG, Schmitz M. 2012. The Geologic Time Scale 2012, 2-volume set. Elsevier, 1176 p.

Graf DL, Cummings KS. 2007. Review of the systematics and global diversity of freshwater mussel species (Bivalvia: Unionoida). Journal of Molluscan Studies 73, 291–314.

Greenwood DR. 2005. Leaf form and the reconstruction of past climates. New Phytologist 166, 355–357.

Guérin C. 1980. Les Rhinocéros (Mammalia, Perissodactyla) du Miocène terminal au Pléistocène supérieur en Europe occidentale. Comparaison avec les espèces actuelles. Lyon. Documents des laboratoires de Géologie Lyon 79, 1–421.

Gunawan H, Kobayashi S, Mizuno K, Kono Y. 2012. Peat swamp forest types and their regeneration in Giam Siak Kecil-Bukit Batu Biosphere Reserve, Riau, East Sumatra, Indonesia. Mires and Peat 10, 1–17.

Haeckel JJ. 1843. Abbildungen und Beschreibungen der Fische Syriens: nebst einer neuen Classification und Characteristik sämtlicher Gattungen der Cyprinen. Stuttgart, Schweizerbart'sche Verlagsbuchhandlung, 255 p.

Hall R. 2002. Cenozoic geological and plate tectonic evolution of SE Asia and the SW Pacific: computer-based reconstructions, model and animations. Journal of Asian Earth Sciences 20, 353–431.

Hanson CB. 1989. *Teletaceras radinskyi*, a new primitive rhinocerotid from the late Eocene Clarno Formation, Oregon. In: DR Prothero and RM Schoch (Eds), The Evolution of Perissodactyls. New York, Oxford University Press, 379–398.

Harris N. 2006. The elevation history of the Tibetan Plateau and its implications for the Asian monsoon. Palaeogeography, Palaeoclimatology, Palaeoecology 241, 4–15.

He S, Mayden RL, Wang X, Wang W, Tang KL, Chen W-J, Chen Y. 2008. Molecular phylogenetics of the family Cyprinidae (Actinopterygii: Cypriniformes) as evidenced by sequence variation in the first intron of S7 ribosomal protein-coding gene: Further evidence from a nuclear gene of the systematic chaos in the family. Molecular Phylogenetics and Evolution 46, 818–829.

He X, Shen R, Jin J. 2010. A new species of Nelumbo from South China and its palaeoecological implications. Review of Palaeobotany and Palynology 162, 159–167.

Heissig K. 1969. Die Rhinocerotidae (Mammalia) aus der oberoligozänen Spaltenfüllung von Gaimersheim bei Ingolstadt in Bayern und ihre phylogenetische Stellung. Bayerische Akademie der Wissenschaften Mathematisch Naturwissenschaftliche Klasse Abhandlungen Neue Folge 138, 1–133.

Heissig K. 1979. Die hypothetische Rolle Südosteuropas bei den Säugetierwanderungen im Eozän und Oligozän. Neues Jahrbuch für Geologie und Paläontologie, Monatshefte 1979, 83–96.

Heissig K. 1989. The allaceropine hyracodonts. In: DR Prothero and RM Schoch (Eds), The Evolution of Perissodactyls. Oxford, Oxford University Press, 355–357.

Heissig K. 2003. Origin and early dispersal of the squirrels and their relatives. In: JWF Reumer and W Wessels (Eds.), Distribution and migration of tertiary mammals in Eurasia . A volume in honour of Hans de Bruijn. Deinsea 10, 277–286.

Hellmund M. 1991. Revision der europäischen Species der Gattung *Elomeryx* Marsh 1894 (Anthracotheriidae, Artiodactyla, Mammalia) Palaeontographica Abteilung A A220, 1–101.

Hellmund M. 1992. Schweineartige (Suina, Artidactyla, Mammalia) aus oligo-miozänen Fundstellen Deutschlands, der Schweiz und Frankreichs. II. Revision von *Palaeochoerus* Pomel 1847

und *Propalaeochoerus* Stehlin 1899 (Tayassuidae). Stuttgarter Beiträge zur Naturkunde B 189, 1–75.

Hoang LV, Wu F-Y, Clift PD, Wysocka A, Swierczewska A. 2009. Evaluating the evolution of the Red River system based on in situ U-Pb dating and Hf isotope analysis of zircons. Geochemistry, Geophysics, Geosystems 10, 10.1029/2009GC002819.

Holbrook LT, Lucas SG. 1997. A new genus of rhinocerotoid from the Eocene of Utah and the status of North American "Forstercooperia". Journal of Vertebrate Paleontology 17, 384–396.

Holroyd PA, Tsubamoto T, Egi N, Ciochon RL, Takai M, Tun ST, Sein C, Gunnell GF. 2006. A rhinocerotid perissodactyl from the late middle Eocene Pondaung Formation, Myanmar. Journal of Vertebrate Paleontology 26, 491–494.

Hooker JJ. 2010. The 'Grande Coupure' in the Hampshire Basin, UK: taxonomy and stratigraphy of the mammals on either side of this major Palaeogene faunal turnover. In: JE Whittaker and MB Hart (Eds), Micropalaeontology, sedimentary environments and stratigraphy: a tribute to Dennis Curry (1912–2001). London, The Micropaleontological Society, Special Publications, 147–215.

Hooker JJ. 2012. Paleogene Mammals. In: FM Gradstein, JG Ogg, MD Schmitz and GM Ogg (Eds), The Geologic Time Scale 2012. Elsevier, 878–881.

Hu S, Appel E, Hoffmann V, Schmahl W, Wang S. 1998. Gyromagnetic remanence acquired by greigite (Fe3S4) during static three-axis alternating field demagnetization. Geophysical Journal International 134, 831–842.

Junda W, Huamei L, Zhaoyu Z, Seguin M, Junfa Y, Guomei Z. 1994. Magnetostratigraphy of Tertiary rocks from Maoming Basin, Guangdong Province, China. Chinese Journal of Geochemistry 13, 165–175.

Juranov S. 1992. Stratigraphy of the Eocene series in the Burgas district. Review of the Bulgarian Geological Society 53, 47–59. (in Bulgarian with English summary).

Kawamura T, Hirota M, Aoki H, Morinaga H, Liu Y, Ahn H-S, Zaman H, Yokoyama M, Otofuji Y-I. 2013. Tectonic deformation in the southern part of South China Block: Paleomagnetic study of the Early Cretaceous Xinlong Formation from Shangsi Foredeep Depozone in the Guangxi Province. Journal of Geodynamics 64, 40–53.

Kent DV, Muttoni G. 2008. Equatorial convergence of India and early Cenozoic climate trends. Proceedings of the National Academy of Sciences 105, 16065–16070.

Kirschvink J. 1980. The least-squares line and plane and the analysis of palaeomagnetic data. Geophysical Journal International 62, 699–718.

Köhler F, Glaubrecht M. 2007. Out of Asia and into India: on the molecular phylogeny and biogeography of the endemic freshwater gastropod Paracrostoma Cossmann, 1900 (Caenogastropoda: Pachychilidae). Biological Journal of the Linnean Society 91, 627–651.

Köhler F, Dames C. 2009. Phylogeny and systematics of the Pachychilidae of mainland South-East Asia – novel insights from morphology and mitochondrial DNA (Mollusca, Caenogastropoda, Cerithioidea). Zoological Journal of the Linnean Society 157, 679–699.

Köhler F, Holford M, Do VT, Ho TH. 2009. Exploring a largely unknown fauna: On the diversity of pachychilid freshwater gastropods in Vietnam (Caenogastropoda: Cerithioidea). Molluscan Research 29, 121–146.

Köhler F, Li-Na D, Jun-Xing Y. 2010. A new species of Brotia from Yunnan, China (Caenogastropoda, Pachychilidae). Zoosystematics and Evolution 86, 295–300.

Köhler F, Seddon M, Bogan AE, Tu DV, Sri-Aroon P, Allen D. 2012. The status and distribution of freshwater molluscs of the Indo-Burma region. In: DJ Allen, KG Smith and WRT Darwall (Eds), The status and distribution of freshwater biodiversity in Indo-Burma. Cambridge, Gland, 66–89.

Kolar CS, Chapman DC, Courtenay WR, Jennings DP. 2005. Asian Carps of the Genus *Hypophthalmichthys* (Pisces, Cyprinidae). U.S. Fish and Wildlife Service per Interagency Agreement 94400-3-0128, 1–175.

Kostopoulos D, Koufos G, Christanis K. 2012. On some anthracotheriid (Artiodactyla, Mammalia) remains from northern Greece: comments on the palaeozoogeography and phylogeny of *Elomeryx*. Swiss Journal of Palaeontology 131, 303–315.

Kotzakis T. 1986. Elementi di paleobiogeograpia dei mamiferi terziari dell 'Italia. Hystrix 1, 26–68.

Kowalke T. 2001. Cerithioidea (Caenogastropoda: Cerithiimorpha) of Tethyan coastal swamps and their relations to modern mangal communities. Bulletin of Geosciences 76, 253–271.

Kowalke T. 2004. Evolution of the Pachychilidae Troschel, 1857 (Caenogastropoda, Cerithioidea) – from the Tethys to modern tropical rivers. Zitteliana 44, 41–50.

Li C, Lin Y, Gu Y, Hou L, Wu W, Qui Z. 1985. The Middle Miocene (Aragonian) vertebrate fauna from Xiacaowan, Sihong district, Jiangsu province 1. A brief introduction to the fossil localities and preliminary report on the new material. Vertebrata PalAsiatica 21, 313–327.

Lihoreau F, Ducrocq S. 2007. Family Anthracotheriidae. In: DR Prothero and SE Foss (Eds), The Evolution of Artiodactyls. Maryland, Johns Hopkins University Press, 89–105.

Lihoreau F, Ducrocq S, Antoine P-O, Vianey-Liaud M, Rafaÿ S, Garcia G, Valentin X. 2009. First complete skulls of *Elomeryx crispus* (Gervais, 1849) and of *Protaceratherium albigense* (Roman, 1912) from a new Oligocene locality near Moissac (SW France). Journal of Vertebrate Paleontology 29, 242–253.

Liu H, Chen Y. 2003. Phylogeny of the East Asian cyprinids inferred from sequences of the mitochondrial DNA control region. Canadian Journal of Zoology 81, 1938–1946.

Maddison W, Maddison DR. 2010. Mesquite: a modular system for evolutionary analysis. Version 2.75.

Maher BA, Taylor RM. 1988. Formation of ultrafine-grained magnetite in soils. Nature 336, 368–370.

Mai DH, Walther H. 1978. Die Floren der Haselbacher Serie im Weißelster-Becken (Bezirk Leipzig) DDR. Abhandlung des staatlichen Museums für Mineralogie und Geologie Dresden 28, 1–200.

Markwick PJ. 1998a. Crocodilian diversity in space and time: the role of climate in paleoecology and its implication for understanding K/T extinctions. Paleobiology 24, 470–497.

Markwick PJ. 1998b. Fossil crocodilians as indicators of Late Cretaceous and Cenozoic climates: implications for using palaeontological data in reconstructing palaeoclimate. Palaeogeography, Palaeoclimatology, Palaeoecology 137, 205–271.

Maung M, Htike T, Tsubamoto T, Suzuki H, Sein C, Egi N, Win Z, Maung Thein ZM, Aung AK. 2004. Stratigraphy of the primate-bearing beds of the Eocene Pondaung Formation at Paukkaung area, Myanmar. Anthropological Science 1–5.

Maury-Lechon G, Curtet L. 1998. Biogeography and evolutionary systematics of Dipterocarpaceae. In: S Appanah and JM Turnbull (Eds), A Review of Dipterocarps: Taxonomy, Ecology and Silviculture. Bogor, Indonesia, Center for International Forestry Research, 5–44.

McFadden P, McElhinny M. 1990. Classification of the reversal test in palaeomagnetism. Geophysical Journal International 103, 725–729.

Meng J, McKenna MC. 1998. Faunal turnovers of Palaeogene mammals from the Mongolian Plateau. Nature 394, 364–367.

Meng J, Wang C, Zhao X, Coe R, Li Y, Finn D. 2012. India-Asia collision was at 24° N and 50 Ma: palaeomagnetic proof from southernmost Asia. Scientific Reports 2, 925.

Ménouret B, Guérin C. 2009. *Diceratherium massiliae* nov. sp. des argiles oligocènes de Saint-André et Saint-Henri à Marseille et de Les Milles près d'Aix-en-Provence (SE de la France), premier grand Rhinocerotidae brachypode européen. Geobios 42, 293–327.

Mészáros N, Moisescu V. 1991. Bref apercu des unites lithostratigraphiques du Paléogène dans le Nord-Ouest de la Transylvanie (region de Cluj-Huedin). Bulletin de la Société géologique de France 28, 31–39.

Michel P. 1983. Contribution à l'étude des Rhinocérotidés oligocènes (La Milloque; Thézels; Puy de Vaurs). PhD Thesis, University of Poitiers, 209 p.

Mietto P. 2006. La geologia di Monteviale e le miniere di ligniti. Comune di Monteviale, 125 p.
Mihlbachler MC. 2008. Species taxonomy, phylogeny, and biogeography of the Brontotheriidae (Mammalia: Perissodactyla). Bulletin of the American Museum of Natural History 311, 1–475.
Modell H. 1964. Das natürliche System der Najaden. 3. Archiv für Molluskenkunde 93, 71–126.
Mook CC. 1921. *Allognathosuchus*, a new genus of Eocene crocodilians. Bulletin of the American Museum of Natural History 44, 105–110.
Nelson JS. 1994. Fishes of the world. 3rd ed. New York, John Wiley & Sons, 600 p.
Neubauer TA, Schneider S, Böhme M, Prieto J. 2012. First record of frehswater rissooidean gastropods from the Palaeogene of Southeast Asia. Journal of Molluscan Studies 78, 275–282.
Neumayr M. 1883. Über einige Süsswasserconchylien aus China. Neues Jahrbuch für Geologie und Paläontologie 1883, 21–26.
Niklas KJ. 1995. Size-dependent Allometry of Tree Height, Diameter and Trunk-taper. Annals of Botany 75, 217–227.
Nikolov I. 1967. Neue obereozäne Arten der Gattung *Elomeryx*. Neues Jahrbuch für Geologie und Paläontologie Abhandlungen 128, 205–214.
Nikolov I, Heissig K. 1985. Fossile Säugetiere aus dem Obereozän und Unteroligozän Bulgariens und ihre Bedeutung für die Paläogeographie. Mitteilungen der Bayerischen Staatssammlung für Paläontologie und historische Geologie 25, 61–79.
Nixon KC. 1999–2002. WinClada (BETA) ver. 1.00.08 Ithaca, NY, USA.
Odhner NHJ. 1930. Non-marine mollusca from Pliocene deposits of Kwangxi, China. Palaeontologia Sinica, Series B 6, 7–29.
Pickford M. 2008. The myth of the hippo-like anthracothere: The eternal problem of homology and convergence. Revista Española de Paleontología 23, 31–90.
Popov S, Rögl F, Rozanov AY, Steininger FF, Shcherba IG, Kovac M. 2004. Lithological-palaeogeographic maps of Paratethys. Courier Forschungsinstitut Senckenberg 250, 1–46.
Prothero DR, Guérin C, Manning E. 1989. The history of the Rhinocerotoidea. In: DR Prothero and RM Schoch (Eds), The Evolution of Perissodactyls. New York, Oxford University Press, 322–340.
Prothero DR. 1994. Eocene-Oligocene transition: paradise lost. New York, Columbia University Press, 291 p.
Prothero DR, Heaton TH. 1996. Faunal stability during the Early Oligocene climatic crash. Palaeogeography, Palaeoclimatology, Palaeoecology 127, 257–283.
Prothero DR. 2005. The Evolution of North American rhinoceroses. Cambridge, Cambridge University Press, 218 p.
Pubellier M, Rangin C, Phach PV, Que BC, Hung D-T, Sang CL. 2003. The Cao Bang-Tien Yen Fault: implications on the relationships between the Red River Fault and the South China Coastal Belt. Advances in Natural Sciences 4, 347–361.
Qiu Z, Xie J. 1997. A new species of *Aprotodon* (Perissodactyla, Rhinocerotidae) from Lanzhou Basin, Gansu, China. Vertebrata PalAsiatica 35, 250–267.
Rainboth WJ. 1991. Cyprinids of South East Asia. In: IJ Winfield and JS Nelson (Eds), Cyprinid Fishes – systematic, biology, and exploitation. London, Chapman & Hall, 156–210.
Ramstein G, Fluteau F, Besse J, Joussaume S. 1997. Effect of orogeny, plate motion and land – sea distribution on Eurasian climate change over the past 30 million years. Nature 386, 788–795.
Randall DJ, Cameron JN, Daxboeck C, Smatresk N. 1981. Aspects of bimodal gas exchange in the bowfin,: *Amia calva* L. (Actinopterygii: Amiiformes). Respiration Physiology 43, 339–348.
Raxworthy CJ, Forstner MRJ, Nussbaum RA. 2002. Chameleon radiation by oceanic dispersal. Nature 415, 784–787.
Rincón AF, Bloch JI, Mac Fadden BJ, Jaramillo CA. 2013. First Central American record of Anthracotheriidae (Mammalia, Bothriodontinae) from the early Miocene of Panama. Journal of Vertebrate Paleontology 33, 421–433.
Russell DE, Zhai R. 1987. The Paleogene of Asia mammals and stratigraphy. France, Mémoires du Muséum National d'Histoire Naturelle 488 p.
Rust J, Singh H, Rana RS, McCann T, Singh L, Anderson K, Sarkar N, Nascimbene PC, Stebner F, Thomas JC, Solórzano Kraemer M, Williams CJ, Engel MS, Sahni A, Grimaldi D. 2010. Biogeographic and evolutionary implications of a diverse paleobiota in amber from the early Eocene of India. Proceedings of the National Academy of Sciences 107, 18360–18365.
Rusu A, Brotea D, Melinte MC. 2004. Biostratigraphy of the Bartonian deposites from Gilău area (NW Transylvania, Romania). Acta Palaeontologica Romaniae 4, 441–454.
Sam HV, Nanthavong K, Kessler PJA. 2004. Trees of Laos and Vietnam: a field guide to 100 economically or ecologically important species. Blumea – Biodiversity, Evolution and Biogeography of Plants 49, 201–349.
Scheyer TM, Aguilera OA, Delfino M, Fortier DC, Carlini AA, Sánchez R, Carrillo-Briceño JD, Quiroz L, Sánchez-Villagra MR. 2013. Crocodylian diversity peak and extinction in the late Cenozoic of the northern Neotropics. Nature communications 4, 1907.
Schmidt-Kittler N, Brunet M, Godinot M, Franzen JL, Hooker JJ, Legendre S, Brunet M, Vianey-Liaud M. 1987. European reference levels and correlation tables. Münchner Geowissenschaftliche Abhandlungen A 10, 13–31.
Schneider S, Böhme M, Prieto J. 2013. Unionidae (Bivalvia; Palaeoheterodonta) from the Palaeogene of northern Vietnam: exploring the origins of the modern East Asian freshwater bivalve fauna. Journal of Systematic Palaeontology 11, 337–357.
Schütt H, Besenecker H. 1973. Eine Molluskenfauna aus dem Neogen von Chios (Ägäis). Archiv für Molluskenkunde der Senckenbergischen Naturforschenden Gesellschaft: Organ der Deutschen Malakozoologischen Gesellschaft 103, 1–29.
Schütt H. 1993. Gedanken über die disjunkte Verbreitung einiger Gattungen der großen Süßwassermuscheln Unionacea im europäischen und im südostasiatischen Raum. Club Conchylia Informationen 25, 61–67.
Scott AC. 2000. The Pre-Quaternary history of fire. Palaeogeography, Palaeoclimatology, Palaeoecology 164, 281–329.
Scott AC. 2010. Charcoal recognition, taphonomy and uses in palaeoenvironmental analysis. Palaeogeography, Palaeoclimatology, Palaeoecology 291, 11–39.
Shi G, Jacques FMB, Li H. 2014. Winged fruits of Shorea (Dipterocarpaceae) from the Miocene of Southeast China: Evidence for the northward extension of dipterocarps during the Mid-Miocene Climatic Optimum. Review of Palaeobotany and Palynology 200, 97–107.
Simpson GG. 1930. *Allognathosuchus mooki*, a new crocodile from the Puerco Formation. American Museum Novitates 445, 1–16.
Stehlin HG. 1909. Remarques sur les faunules de mammifères des couches éocènes et oligocènes du Bassin de Paris. Bulletin de la Société géologique de France 9, 488–520.
Strong EE, Gargominy O, Ponder W, Bouchet P. 2008. Global diversity of gastropods (Gastropoda; Mollusca) in freshwater. Hydrobiologia 595, 149–166.
Strong EE, Köhler F. 2009. Morphological and molecular analysis of 'Melania' jacqueti Dautzenberg and Fischer, 1906: from anonymous orphan to critical basal offshoot of the Semisulcospiridae (Gastropoda: Cerithioidea). Zoologica Scripta 38, 483–502.
Strong EE, Colgan DJ, Healy JM, Lydeard C, Ponder WF, Glaubrecht M. 2011. Phylogeny of the gastropod superfamily Cerithioidea using morphology and molecules. Zoological Journal of the Linnean Society 162, 43–89.
Sytchevskaya EK. 1986. Paleogene freshwater fish fauna of the USSR and Mongolia. Trudy joint Soviet-Mongolian Paleontological Expedition 29, 1–157. (in Russian with English summary).
Tanner LG, Martin LD. 1976. New rhinocerotoids from the Oligocene of Nebraska. In: CS Churcher (Eds), Essays in Paleontology in honor of Loris Shano Russell. Ontario, Royal Ontario Museum, Life Sciences Miscellaneous Contributions, 210–219.
Tappert R, Wolfe AP, McKellar RC, Tappert MC, Muehlenbachs K. 2011. Characterizing modern and fossil gymnosperm exudates using micro-Fourier transform infrared spectroscopy. International Journal of Plant Sciences 172, 120–138.
Teilhard de Chardin P. 1926. Description des Mammifères tertiaires

de Chine et de Mongolie. Annales de Paléontologie 15, 1–52.
Thuy DK. 2001. Geology and Mineral Resources Map of Vietnam, Lang Son Sheet, 1:200.000 (F-48-XXIII). Hanoi, Vietnam, Department of Geology and Minerals of Vietnam, Hanoi.
Tompsett PB. 1998. Seed Physiology. In: S Appanah and JM Tornbull (Eds), A review of
Tong H, Zhang J-Y, Li J-J. 2010. *Anosteira maomingensis* (Testudines: Carettochelyidae) from the Late Eocene of Maoming, Guangdong, southern China: new material and re-description. Neues Jahrbuch für Geologie und Paläontologie. Abhandlungen. 256, 279–290.
Tong Y-S. 1989. A review of middle and late Eocene mammalian faunas from China. Acta Palaeontologica Sinica 28, 663–682.
Torrent J, Barrón V, Liu Q. 2006. Magnetic enhancement is linked to and precedes hematite formation in aerobic soil. Geophysical Research Letters 33, L02401.
Torsvik TH, Müller RD, Van der Voo R, Steinberger B, Gaina C. 2008. Global plate motion frames: toward a unified model. Reviews of Geophysics 46, RG3004, doi:10.1029/2007RG000227.
Traiser C, Klotz S, Uhl D, Mosbrugger V. 2005. Environmental signals from leaves – a physiognomic analysis of European vegetation. New Phytologist 166, 465–484.
Trung PQ, Quynh PH, Bat D, An NQ, Khoi DV, Hieu DV, Ngoc N. 2000. New palynological investigation in the Na Duong mine. Oil and Gas Journal (Hanoi) 7, 18–27. (in Vietnamese).
Tsubamoto T, Takai M, Egi N, Shigehara N, Tun ST, Soe AN, Thein T. 2002. The Anthracotheriidae (Mammalia; Artiodactyla) from the Eocene Pondaung Formation (Myanmar) and comments on some other anthracotheres from the Eocene of Asia. Paleontological Research 4, 363–384.
Tsubamoto T, Tsogtbaatar K. 2008. New specimens of anthracotheriid artiodactyls from the upper Eocene Ergilin Dzo Formation of Mongolia. Paleontological Research 12, 371–386.
Tsubamoto T, Z. M. , Maung Thein NE, Nishimura T, Thaung H, Takai M. 2011. A new anthracotheriid artiodactyl from the Eocene Pondaung Formation of Myanmar. Vertebrata PalAsiatica 49, 85–113.
Uhlig U. 1999. Die Rhinocerotoidea (Mammalia) aus der unteroligozänen Spaltenfüllung Möhren 13 bei Treuchtlingen in Bayern. Bayerische Akademie der Wissenschaften Mathematisch Naturwissenschaftliche Klasse Abhandlungen Neue Folge 170, 1–254.
Uhlig U, Böhme M. 2001. Ein neuer Rhinocerotide (Mammalia) aus dem Unteroligozän Mitteleuropas (Espenhain bei Leipzig, NW-Sachsen, Deutschland). Neues Jahrbuch für Geologie und Paläontologie, Abhandlungen 220, 83–92.
Usdowski H-E. 1963. Die Genese der Tutenmergel oder Nagelkalke (cone-in-cone). Beiträge zur Mineralogie und Petrographie 9, 95–110.
Van Valen L. 1966. Deltatheridia, a new order of Mammals. Bulletin of the American Museum of Natural History 132, 1–126.
Vandenberghe N, Hilgen FJ, Speijer RP. 2012. The Paleogene Period. In: FM Gradstein, JG Ogg, MD Schmitz and GM Ogg (Eds), The Geologic Time Scale 2012. Elsevier, 888–922.
Vasiliev I, Franke C, Meeldijk JD, Dekkers MJ, Langereis CG, Krijgsman W. 2008. Putative greigite magnetofossils from the Pliocene epoch. Nature Geoscience 1, 782–786.
Wang C, Zhao X, Liu Z, Lippert PC, Graham SA, Coe RS, Yi H, Zhu L, Liu S, Li Y. 2008. Constraints on the early uplift history of the Tibetan Plateau. Proceedings of the National Academy of Sciences 105, 4987–4992.
Wang Q, Spicer RA, Yang J, Wang YF, Li CS. 2013. The Eocene climate of China, the early elevation of the Tibetian Plateau and the onset of the Asian Monsoon. Global Change Biology 19, 3709–3728.
Wang YJ, Meng XN, Li C. 2007. Major events of Paleogene mammal radiation in China. Geological Journal 42, 415–430.
Watters GT. 2001. The Evolution of the Unionacea in North America, and Its Implications for the Worldwide Fauna. In: G Bauer and K Wächtler (Eds), Ecology and Evolution of the Freshwater Mussels Unionoida. Ecological Studies Springer Berlin Heidelberg, 281–307.
Weischat W, Endlicher W. 2000. Regionale Klimatologie. Teil 2: Die Alte Welt: Europa, Afrika, Asien. Stuttgart, Borntraeger, 625 p.
Wenz W. 1938–1944. Gastropoda. Allgemeiner Teil und Prosobranchia. Handbuch der Paläozoologie. Berlin, Borntraeger, 1639 p.
Wenz W. 1942. Die Mollusken des Pliozäns der rumänischen Erdöl-Gebiete als Leitversteinerungen für die Aufschluss-Arbeiten. Senckenbergiana 24, 1–239.
Whelan NV, Geneva AJ, Graf DL. 2011. Molecular phylogenetic analysis of tropical freshwater mussels (Mollusca: Bivalvia: Unionoida) resolves the position of Coelatura and supports a monophyletic Unionidae. Molecular Phylogenetics and Evolution 61, 504–514.
Wilf P. 1997. When are leaves good thermometers? a new case for leaf margin analysis. Paleobiology 23, 373–390.
Wolfe JA. 1979. Temperature parameters of humid to mesic forests of Eastern Asia and relation to forests of other regions of the Northern hemisphere and Australasia. U.S. Geological Survey Professional Paper 1106, 1–37.
Wunderlin R, Larsen K, Larsen SS. 1987. Reorganization of the Cercideae (Fabaceae Caesalpinioideae). Danske Biologiske skrifter 28, 1–40.
Wysocka A. 2009. Sedimentary environments of the Neogene basins associated with the Cao Bang – Tien Yen Fault, NE Vietnam. Acta Geologica Polonica 59, 45–69.
Xin T, Ming-zhen Z. 1964. The vertebrae-bearing early Tertiary of South China: A review. Vertebrata PalAsiatica 8, 119–133. (in Chinese).
Xiwen L, Jie L, Ashton PS. 2007. Dipterocarpaceae. In: WZ Y., RP H. and HD Y. (Eds), Flora of China. Volume 13. Beijing, St.Louis, Science Press, Beijing, Missouri Botanical Garden Press, St. Louis, 48–54.
Xu Q. 1977. New materials of Bothriodon from Bose Basin of Guangxi. Vertebrata PalAsiatica 15, 203–206. (in Chinese).
Xu Y. 1961. Some Oligocene mammals from Chuching, Yunnan. Vertebrata PalAsiatica 4, 315–329.
Yamada I. 1997. Tropical rainforests of southeast Asia : a forest ecologists view. Hawaii, University of Hawaii Press, 392 p.
Yamakura T, Hagihara A, Sukardjo S, Ogawa H. 1986. Aboveground biomass of tropical rain forest stands in Indonesian Borneo. Vegetatio 68, 71–82.
Yasuno T. 1984. Fossil pharyngeal teeth of the Rhodeinae fish from the Miocene Katabira Formation of the Kani Group, Gifu Prefecture, Japan. Bulletin of the Mizunami Fossil Museum 11, 101–105.
Ying T, Fürsich FT, Schneider S. 2013. Giant Viviparidae (Gastropoda: Architaenioglossa) from the Early Oligocene of the Nanning Basin (Guangxi, SE China). Neues Jahrbuch für Geologie und Paläontologie, Abhandlungen 267, 75–87.
You Y. 1977. Note on the New Genus of Early Tertiary *Rhinocerotidae* from Bose Guangxi. Vertebrata PalAsiatica 15, 46–53. (in Chinese).
Zhang W, Appel E, Fang X, Song C, Cirpka O. 2012. Magnetostratigraphy of deep drilling core SG-1 in the western Qaidam Basin (NE Tibetan Plateau) and its tectonic implications. Quaternary Research 78, 139–148.
Zhuang Z, Tian D, Ma X, Ren X, Jiang X, Xu S. 1988. Cretaceous-lower Tertiary paleomagnetism of the Ya'an-Tianquan section in the Sichuan Basin. Geophysical and Geochemical Exploration 12, 224–227.

APPENDIX 1. Description of dental characters used in the phylogenetic analysis. All characters are treated as unordered. Modified from Lihoreau and Ducrocq (2007) and Rincon et al. (2013).

1- Lower incisors: three (0); from two to three (1); two (2).

2- Upper incisors: three of equal size (0); three with i3 reduced (60% or less) (1); two (2).

3- Lower incisor morphology: not caniniform (0); at least one caniniform (1).

4- Relative dimension of lower incisors: all equal size (0); i2 larger (1); i3 larger (2).

5- Wear on lower canine: distal wear facet caused by the contact with upper C (0); mesial wear facet cause by contact with I3 (1).

6- Upper canine morphology: strong with subcircular cross-section (0); strong and laterally compressed (1); premolariform (2).

7- Lower canine in males: premolariform (0); large (1); evergrowing (2).

8- Lower canine cross-section at cervix: subcircular (0); elliptical with rounded mesial margin and distal keel (1); elliptical with a mesial and distal crest (2); elliptical with a concave buccal margin and a distal keel (3).

9- Accessory cusps on the mesial crest of lower premolars: none (0); only one (1); several (2).

10- Presence of five upper premolars: no (0); yes (1).

11- Distolabial crest on upper premolars: simple (0); with a maximum of two accessory cusps (1); with more than two (2).

12- Accessory cusp on p4: no (0); yes (1).

13- p1 roots: one (0); two (1).

14- Mesial crests on P1–P3: one (0); two (1).

15- Number of P4 roots: three (0); two (1); one (2).

16- Accessory cusp on distolingual margin of P3: one (0); none (1).

17- Upper molar mesostyle; simple (0); V-shaped and invaded by a transversal valley (1); loop-like (2); divided into two (3).

18- Number of postprotocristae: one (0), two (1).

19- Accessory cusp on upper molar mesial cingulum: no (0); yes (1).

20- Number of cristules issued from the metaconule: two (0); three (1).

21- Preprotocristids and prehypocristids on lower molars: do not reach the lingual margin of the tooth (0); reach the lingual margin (1).

22- Hypoconulid on m3: loop-like (0); single cusp (1).

23- Postentocristid on lower molars: does not reach the posthypocristid and leaves the mesio-distal valley open (0); reaches the posthypocristid and closes the long valley (1).

24- Dimension of the lingual and labial cusps: equal (0); different (1). State (1): labial cusps twice as large at their basis as the lingual cusp.

25- Entoconulid on m3: absent (0); present (1).

26- Number of cristids issued to from the hypoconid: three (0); two (1).

27- Position of the preentocristid on lower molars: reaches the hypoconid summit (0); reaches the prehypocrstid (=cristid oblique) (1); reaches the transversal hypocristid (2).

28- Premetacristid on lower molars: present (0); absent (1).

29- Mesial part of looplike hypoconulid: open (0); pinched (1).

30- Entoconid fold on lower molars: absent (0); present (1).

31- Ventral vascular groove on mandible: slightly marked (0); absent (1); strongly marked (2).

32- Morphology of mandibular symphysis cross-section: 'U'-shaped (0); 'V'-shaped (1).

33- Transverse constriction of mandible at Cp1 diastema: no (0); yes (1).

34- Cp1 diastema: absent (0); present (1).

35- p1-p2 diastema: absent (0); present (1).

36- Lateral mandibular tuberosity: absent (0); present (1).

37- Dentary bone fussion at the symphysis: no (0); yes (1).

38- Morphology of the symphysis is sagittal section: elliptic (0); dorsally concave (1); ventrally concave (2).

39- Maximal thickness of the symphysis in sagittal section: in the middle part (0); in the anterior part (1); in the posterior part (2).

40- Number and position of main external mandibular foramina: only one foramen, below the anterior part of the premolar row (0); two foramina, one below the anterior part of the premolar row, the other below its posterior part (1); one foramen, below the posterior part of the premolar row (2).

41- Tuberosity on the dorsal border of the mandible at c–p1 diastema: no (0); yes (1).

42- Palatine depression between the canines: no (0); yes (1).

43- Canine fossa: short (0); long (1).

44- Aperture of the main palatine foramen: between M3 and P3; between P2 and P1 (1); between P1 and C.

45- Morphology of the frontonasal suture: V-shaped (0); rounded or straight (1).

(46) Lachrymal extension: separated from the nasal by the frontal (0); in contact with the nasal (1).

(47) Supraorbital foramina on the frontal: one (0); several (1).

(48) Facial crest: horizontal (0); oblique (1).

(49) Anterior border of premaxillary in lateral view: concave (0); convex (1).

(50) Postglenoid foramen position: posterior to the styloid process of the tympanic bulla (0); anterior to the styloid process of the tympanic bulla (1).

(51) Opening of internal choanes: at M3 (0); behind M3 (1).

APPENDIX 2. Character-taxon matrix used in the phylogenetic analyses of Anthracotheriidae. See Appendix 1 for character descriptions.

S. krabiense	000?? 00?00 00000 00000 00000 00000 00000 00000 000?0 0?00?0
A. magnum	00000 01000 0000? 00111 00001 00000 00001 11001 0000? ???0?0
A. ulnifer	00001 10100 00000 10101 00000 00000 00111 00100 00000 000000
B. fraasi	00??0 20200 0000? 11001 00100 00000 00010 00120 00?00 ?000?1
B. aequatorialis	22120 20200 0001? 11000 00100 11100 00010 01120 00020 000001
B. onoideus	22120 20200 0001? 11000 00100 11100 00010 01120 00020 ??0001
A. americanus	00010 20200 00000 12100 00100 11010 00111 01120 00000 0000?0
B. velaunus	00010 20200 00000 12101 00100 11010 00111 01120 000?0 000000
E. crispus	00000 01300 01000 12101 00110 11010 00011 00210 00000 000001
E. armatus	00000 01300 00000 12101 00110 11010 00011 00210 00000 000001
E. borbonicus	00000 01310 01000 12100 00110 11010 00011 00210 0000? ?000??
A. acridens	00010 01300 0000? 12000 00110 11010 00011 00210 00001 ?1?001
A. zelteni	10000 01310 1101? 12100 00010 11010 00010 00211 00?11 ?1?0?1
S. palaeindicus	0?000 ?1310 11110 12100 10010 11010 00010 00211 1???? 11????
H. blandfordi	??0?? ?132? ?11?? ?2200 10010 11010 00010 00210 1???? 11????
M. dissimilis	00000 02310 11110 13000 11010 11111 20010 00202 00111 111011
L. petrocchii	11000 01321 21111 12000 11010 11111 10010 00211 01121 111111
Bk. orientalis	0000? 0?000 00?00 12101 00100 00010 00010 00220 0?0?0 ???0??
Bk. palaeopontica	0?00? ??00? ?000? ????? 00100 00010 00000 00?20 0???? ??????